Escola de Camins
Escola Tècnica Superior d'Enginyeria de Camins, Canals i Ports
UPC BARCELONATECH

TREBALL FINAL DE MÀSTER

Simulation of cantilever construction of cable-stayed bridges taking creep into account

Treball realitzat per:
Josep Farré Checa

Dirigit per:
José Turmo Coderque
Gonzalo Ramos Schneider
Jose Antonio Lozano-Galant

Màster en:
Enginyeria de Camins, Canals i Ports

Barcelona, 22 de setembre de 2017

Departament d'Enginyeria Civil i Ambiental

Acknowledgements

Firstly I would like to thank my supervisors José Turmo, Gonzalo Ramos and Jose Antonio Lozano for giving me the opportunity to carry out this thesis. All the dedication and great enthusiasm they put in this investigation allowed me to learn and increase my knowledge in the interesting field of cable-stayed bridges.

I am indebted to the Spanish Ministry of Economy and Competitiveness and the FEDER funds for the funding provided through the research project BIA2013-47290-R, directed by José Turmo. I am also indebted to the Spanish Ministry of Education, Culture and Sports for the scholarship "Iniciación a la Investigación" provided for the 2015-2016 academic year in order to develop this investigation.

I want to express my gratitude to the professor Raid Karoumi in KTH for his advice and inspiring ideas. Furthermore I thank José Romo from FECHOR, José Antonio Llombart from EIPSA and Ramón Sánchez de León from AIA for the information provided which is very valuable due to their experience in the design and construction of cable-stayed bridges.

As this is the last step of my studies I would like to thank my friends, especially Ricard Caus and Miquel Ferré who have been studying with me since the beginning and with whom I share my passion for civil engineering. I also want to mention all my friends I have met this year in Stockholm, in particular people from Tyresö KTH Accommodation who have been like a family for me this last year.

Finally I want to say thanks to my parents Josep M. and Encarna, and all my family for all the support. Without them this thesis would not have been carried out.

Barcelona, September 2017

Josep Farré Checa

Abstract

In the design of cable-stayed bridges, the construction analysis is very important since the worst stresses are usually reached during the construction process. In addition, if the bridge is made of concrete, the effects of time dependent phenomena have great importance. Some commercial software are able to simulate the construction process, but one of their main drawbacks is that they simulate in a backward approach where creep is difficult to analyze.

In this thesis two new criteria to define the Objective Service Stage (OSS) are presented which take the constructive process into account. Tensioning operations are very expensive, so the main goal is to define the pretension forces in the stays such that only one pretension operation is necessary in each stay.

Furthermore, an algorithm has been developed to simulate the construction process of cable-stayed bridges erected by cantilever method. This algorithm includes the creep effects into the structure. The Dischinger simplification, which is explained in this document, has been improved in order to better take into account the loading time and the age of the concrete in every stage. The creep simulation of the algorithm has been validated with some patch tests.

The developed algorithm has been implemented in a full scale FEM model adapted from the Giribaile Dam project developed in 1990. In this study case, the new OSS criteria are implemented. Moreover, the axial forces in the stays, the bending moments, and the displacements are analyzed during the construction process and a comparison is carried out between two cases: with and without taking creep into account. With the first new OSS criterion, the Objective Service Stage is achieved without taking the creep into account. However the creep effects, which are of huge importance in concrete bridges built by cantilever method, require the definition of an OSS which considers time dependent phenomena, which has been defined in this thesis (second criterion).

Keywords: Cable-stayed bridges, Cantilever method, Objective Service Stage, CIP concrete, Creep, Dischinger hypothesis, Forward analysis.

Resumen

En el diseño de puentes atirantados el análisis del proceso constructivo es muy importante ya que los esfuerzos críticos en la estructura se producen normalmente durante la construcción. Además, si el puente es de hormigón, los efectos que dependen del tiempo tienen gran importancia. Algunos programas de cálculo comerciales pueden simular el proceso constructivo, pero uno de sus mayores inconvenientes es que simulan el proceso en el sentido contrario al de la construcción, por lo que la fluencia es difícil de analizar.

Esta tesis presenta dos nuevos criterios para definir el Estado de Servicio Objetivo (OSS) considerando el proceso constructivo. Las operaciones de tesado son muy caras. Por esta razón es aconsejable definir unas fuerzas de tesado en los cables con las cuales solo sea necesario una sola operación de tesado en cada cable.

También se ha desarrollado un algoritmo para simular el proceso constructivo de puentes atirantados construidos por voladizos sucesivos. Este algoritmo incluye los efectos de la fluencia en la estructura. La simplifación de Dischinger, la cual es explicada en este documento, se ha mejorado. De esta forma se tiene mejor en cuenta la edad del hormigón y el tiempo de carga en las distintas etapas. La simulación de la fluencia ha sido validada con algunos patch tests.

El algoritmo desarrollado se ha implementado en un modelo de elementos finitos adaptado del proyecto de la presa de Giribaile desarollado en 1990. En el estudio de este caso se han implementado los dos nuevo criterios de OSS. Además se ha analizado las fuerzas en los cables, los momentos y los desplazamientos durante la construcción. También se ha comparado los resultados de dos casos: considerando y sin considerar los efectos de la fluencia. Con el primer nuevo criterio de OSS se llega al Estado de Servicio Objectivo si no se considera la fluencia. Sin embargo, los efectos de la fluencia, los cuales son muy importantes en puentes de hormigón construidos por voladizos sucesivos, hacen necesario que se defina un OSS en el que se considere los efectos dependientes del tiempo, el cual se ha desarrollado en esta tesis (segundo criterio).

Keywords: Puentes atirantados, Voladizos sucesivos, Estado Objetivo de Servicio, Hormigón in situ, Fluencia, Hipótesis de Dischinger, Análisis hacia adelante.

General Index

List of Figures

List of Tables

Chapter 1

Introduction and objectives

1.1 Background

Over the last decades the construction of cable-stayed bridges has been increased mainly due to the development of the erection techniques, the high-strength steel decks, orthotropic decks and the computer technology. A part from their aesthetic appeal, one of the main advantages of this bridge system is that they can overcome large spans. Their spans are in the range from 200 m to 1100 m but there are already designs for cable stayed bridges with main spans up to 1800 m [8].

The cable-stayed bridges are complex structures due to they are highly statically indeterminate, the active forces and their evolutionary constructive process. It is important to do a complete simulation of the erection process to guarantee that the limit states are not exceeded during the construction. Modelling the constructive process is even more difficult in concrete bridges as the time dependent phenomena are taken into account. Obtaining the Objective Service Stage at a certain age is difficult and for this reason additional tensioning operations are carried out.

In order to minimize these operations some algorithms are implemented in structural software to simulate the constructive process. However they have some drawbacks. They are designed only for some commercial software and they can not be used in other stiffness method programs. They simulate the constructive process in a backward approach. For this reason the deviations in the tensioning process and the time dependent phenomena are difficult to model.

The constructive process of this type of bridges have been studied by many authors. Some studies present the backward approach in the cantilever erection method. Some other papers a forward approach for the cantilever method and the temporary support method. A forward direct approach taking into account the time dependent phenomena has been studied for the temporary supports erection method but not for cantilever erection method.

The Objective Service Stage (OSS) is defined as the target geometry or/and stress state to be achieved at a certain time. Some methods to define the OSS have been

found in the literature but non of them consider the type of construction process. Furthermore, in case of cast-in-place concrete bridges, the OSS can only be achieved at one target time, T_t, due to the time dependent phenomena. Some studies have been carried out to study the effects of these phenomena in cable-stayed bridges. However, a definition of the OSS taking into account the time dependent phenomena for cantilever erection method has not been found in the literature.

1.2 Objectives and limitations

The aim of this investigation is to develop an algorithm which permits to simulate the constructive process taking into account the time dependent phenomena in cable-stayed bridges built with cantilever erection method. For this type of erection process two new criteria to define the Objective Service Stage are presented.

The objectives of this study are defined:

1. Simulation of the cantilever erection method taking into account the time dependent phenomena in cable-stayed bridges.
2. Study of the effects of creep in the different stages during the erection process.
3. Definition of the procedures to achieve the Objective Service Stage in cable-stayed bridges not taking creep into account.
4. Definition of the procedures to achieve the Objective Service Stage at one target time taking creep into account.
5. Comparison between two cases: considering and not considering creep effects when the Objective Service Stage is defined not taking creep into account. The achievement of the Objective Service Stage with the first new method is checked in both cases.
6. Validation of the software and application in a full scale FEM model.

Given the objectives of this investigation only static analysis is carried out. The models used are in two dimensions since the transversal loads are not important for the purposes stated above. Bernoulli beam theory has been used so shear deformation is not considered. Due to the dimensions of the bridge analyzed in the study case the sagging effect in cables is not simulated. More details of the limitations in the modelling analysis are given in chapter 3.

The investigation is focused in cast-in-place concrete bridges since the creep has a great importance in this type of bridges.

1.3 Methodology

To carry out the investigation the structural behaviour of the cable-stayed bridge have been studied, in particular, the response of the cables. For this investigation the study of the erection process has a great importance too. It is important to know the typical dimensions of the different elements of the bridge such as the length of the concrete girder segments, know the weight of the derricks and formworks or how is tensioning process implemented in the cantilever erection method.

To do the simulation of the construction process a Fortran FEM code has been used. A previous Fortran FEM code, developed previously by the professors Estradera, J.M.; Chio, Gustavo and Lozano, J.A, has been modified to be able to simulate the cantilever constructive process in cable-stayed bridges. Furthermore, the effects of creep in different stages have been implemented. To validate the algorithm some patch tests have been realized.

The achievement of the OSS has been tested in a full scale model adapted from a previous model used in Carrillo L. Thesis [7]. Then the developed algorithm has been used in this model to simulate the constructive process considering and not considering creep. The new methods to define the OSS have been tested.

Chapter 2

State of the art

2.1 Cable-stayed bridges

The cable-stayed bridges is one of the typologies more used in those bridges which have spans of more than 200 m [7]. The first modern cable-stayed bridge was the Strömsund Bridge in Sweden, designed by Dischinger, and finished in 1955. Two important findings made possible to build the modern cable-stayed bridges. The discovery, made by Dischinger [9], of the softening effect of cable sag in long cables and the development of jointless superstructures where all parts act together as one structural unit [10]. Since that moment the erection techniques have been developed and improved as well as the computation tools and numerical analysis models [4].

Figure 2.1: Strömsund bridge.

This typology tends to be used more than other typologies in bridges with main spans from 150 m to 1000 m due to the fact that they have many advantages. First of all the bending moments are greatly reduced by the load transfer of the stay cables. By installing the stay cables with their predetermined precise lengths, the support conditions for a beam rigidly supported at the cable anchor points can be

achieved and thus the moments from permanent loads are minimized [8].

Secondly, these structures are stable during construction if some erection techniques such as the free cantilevering method are applied. The fact that temporary supports are not necessary makes these bridges suitable to overcome obstacles such as rivers.

As regards the length of the main span, for spans between 150 m and 1100 m cable-stayed bridges are preferable for economic reasons. Straight bridges tend to be very expensive with spans of more than 100 m as the edge of the girder has to be very high and a great amount of concrete or steel is needed. Leonhardt and Zellner [11], after studying different bridge systems, concluded that cable-stayed bridges offers technically and economically superior solutions for large-span bridges.

Another advantage is that they are stiffer than suspension bridges. Suspension bridges are generally not suitable for high railway loads. The eigenfrequencies of cable stayed bridges are significantly higher than those of suspension bridges [8]. As stated Aschrafi, M. [12] the cable-stayed bridge with fan-type cables is superior to the suspension bridge both technically and economically and with regards the aerodynamic stability. However, for very long spans huge compressions appear in the girder due to the forces induced by the stays. Thus the deck needs to have more stiffness and the cost increase if we compare with suspension bridges.

2.1.1 Types

For the vast majority of cable supported bridges the structural system can be divided into four main components:

- The stiffening girder with the bridge deck.
- The cable system supporting the stiffening girder.
- The towers (or pylons) supporting the cable system.
- The anchor blocks (or anchor piers) supporting the cable system vertically and horizontally, or only vertically, at the extreme ends.

The cable-stayed system contains straight cables connecting the stiffening girder to the pylons [1].

Depending on how the cables are disposed in the system there are some typologies: pure fan system (figure 2.2), harp system (figure 2.3) and modified fan system (figure 2.4). In the pure fan system the cables are anchored all in the top of the pylon. In the harp system the stays are located parallel to each other. According to Podolny, W. and Scalzi, J.B. [3] the stays are more effective in the pure fan system as the oblique angle with respect to the girder is minor than in other typologies. Thus the axial force is minor and less steel is needed. The main drawback of the pure fan

system is the difficulty to install all the cables at the head of the pylon.

The modified fan system is an intermediate typology between the previous two. It combines the resistance advantages of the pure fan system and the constructive advantages of the harp system. For this reason the designers tend to use this typology in the recent cable-stayed bridges.

Figure 2.2: Pure fan system [1].

Figure 2.3: Harp system [1]

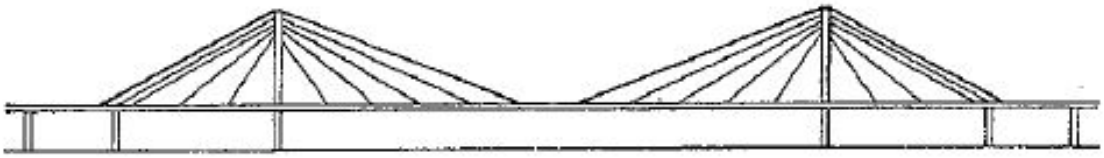

Figure 2.4: Modified fan system [1].

As regards the number of spans there are several typologies too. The most common is the three-span bridge (figures 2.2, 2.3, 2.4) with a large main span flanked by two smaller side spans [1]. The length of the small spans should not be greater than 0.4 times the length of the main span in order to avoid too big positive bending moments in the small span [2]. In case this condition is not fulfiled the main span is too flexible and don't compensate the horizontal forces generated by the stays which support the side spans.

There are also symmetrical and asymmetrical two-span bridges and multi-span cable supported bridges. The new criteria of the OSS proposed in this investigation is applied in the three-span bridges but can also be used in multi-span bridges.

Another differentiation concerns the materials used in the deck. The deck can be made of steel, prefabricated concrete or CIP (cast in place) concrete and composite steel-concrete. According to Schlaich [13] concrete decks are the most economical

solution for spans up to 350 m as the axial forces in the deck, from the horizontal components of the cable forces, can be used as a cost-free prestress. For the CIP concrete is very important to take into account the time dependent phenomena such as creep or shrinkage. In figure 2.5 an example of a concrete section can be seen.

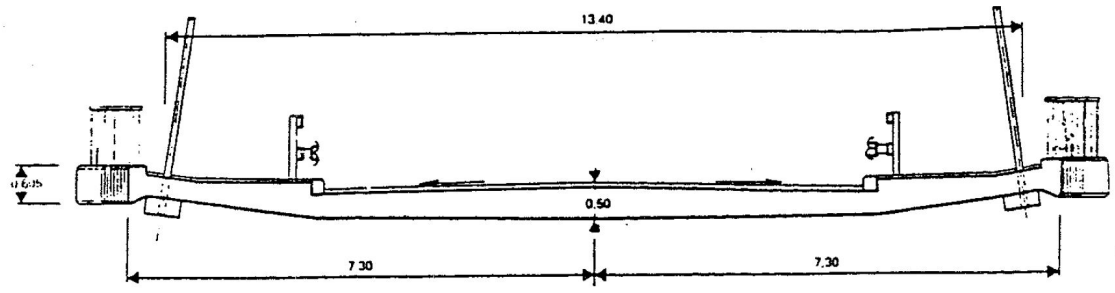

Figure 2.5: Concrete deck section of Dala river Bridge in Switzerland [2].

In bridges with longer span length the concrete decks become too heavy and the steel decks are not an alternative since they are too expensive. Therefore composite steel-concrete decks are used. Over the last 50 years the composite steel-concrete cable-stayed bridges have been also developed as it can be considered the most efficient and competitive solution with spans up to 600 m [4].

For spans above 600 m the steel decks are necessary despite of its elevate cost of the material. The low weight of the deck makes this solution suitable when the load is determinant such as in the case of long span bridges. An example of a steel closed section can be seen in figure 2.6.

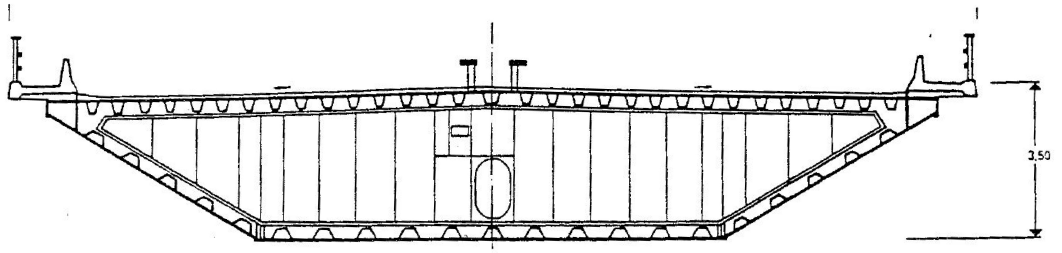

Figure 2.6: Steel deck section of Faro Bridge in Denmark [2].

Over the last years the decks are tending to be more slender and flexible. As we reduce the stiffness of the deck the deformations produced by the permanent loads are higher and the time dependent phenomena effects have more importance as the differed deformation increase.

2.1.2 Design

The overall design of modern cable-stayed bridges have been studied by many authors [1, 8, 2, 3]. The resistance of this type of bridges is given by two different resistant mechanisms which are combined to give the overall resistance of the structure. The first one is the stay system and the second one the bending resistance of the deck. The deck behavior is similar as the behavior of a continuous beam but considering elastic supports in the stay locations. The deck is also subjected to high compression stresses due to the horizontal components of the cable forces. All the forces taken by the stays are transfered to the pylons which have to support almost all the loads and thus they are subjected to high compression stresses too.

The efficiency of the stay system depends on many factors such as the location of the different stay cables, the angle in which the cables are located in the deck, the stiffness of the pylon and the deck, the number of planes used or the utilization of anchorage cables.

The number of stay cables are chosen in such a way that for each stay only one cable is required so that the anchorages become simpler. The cable capacity is up to 20 MN and the distances between anchorages at the beam can be from 5 to 15 m in concrete bridges and between 5 and 25 m in steel decks. The advantages of using this small distances are several. Firstly the size of the stay cables can be smaller which are easily to fabricate. Secondly the bending moments are reduced wich permits the design of thinner decks. Thirdly the small distance permit a better control of the bending moments during the construction process. In order to reduce the construction period, long beam section equal to the cable distance can be used.

The stays can be located just in one plane or in two planes. If only one plane is used the girder must have a closed section to have torsion strength to resist the eccentric loads. Using two planes makes possible to use open sections as the stays can resist the eccentric loads.

As regards the connection between the pylon and the deck there are several options. One of the most used option consists in having the deck supported by the cables and there is only an horizontal link between the pylon and the deck.

Another alternative is to support the deck into a girder that connect the two parts of the pylon. According to Carrillo, L. [7] this alternative has disadvantages because of the high stresses that are produced at that point. In this part the vertical displacement is totally restricted whereas in the stay anchorages the restraints can be considered as elastic supports which don't generate those high stresses.

Another option is to link all the movements of the deck with the pylon. This alternative is not commonly used as it stiffens the deck and the efficiency of the stay system is lower. This configuration is used during the constructive process while the deck is not properly connected to the stay system.

For the design is also important to take into account the geometrical nonlinearities which are the cable sagging, the beam-column effect and the large displacement effect. These effects have been studied by several authors [1, 3, 2, 5, 4].

Cables

The technology and design of stay cables have been studied by many authors [1],[3], [8]. The basic element for all cables is steel wire which has approximately four times larger tensile strength than the ordinary steel and twice the high-strength structural steel. The modulus of elasticity is slightly smaller. It is assumed that the bending stiffness of the stays is zero.

The cable-stayed bridges can be supported by mainly four different types of cables.

- Parallel-bar cables.
- Parallel-wire cables.
- Stranded cables.
- Locked-coil cables.

Parallel-bar cables (figure 2.7) are formed of steel bars, parallel to each other in metal ducts, kept in position by polyethylene spacers. Due to transport issues the bar lengths are limited and couplers have to be used thus the fatigue strength is reduced. Since mild steel is used, it is needed larger sections than when wire steel is used.

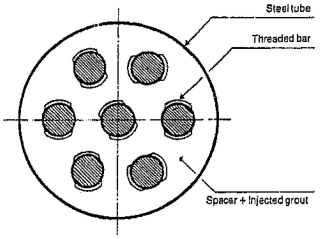

Figure 2.7: Parallel bars [3].

Parallel-wire cables (figure 2.8) are formed of a large number of wires disposed in a parallel way which are twisted by a steel rope that keeps them in place. To give an adequate corrosion protection the wires are surrounded by a polyethylene tube filed with corrosion inhibitor. Their fatigue strength is satisfactory because of their good mechanical properties [3]. The main drawback of this stay cable is that the polyethylene tube the corrosion inhibitor and the steel rope increases the equivalent density and the steel rope makes the outer diameter too large.

Stranded cables (figure 2.9) consists in a bundle of between 18 and 90 strands which can have a maximum tensile strength of 2400 Tn. Every stay has two anchorages

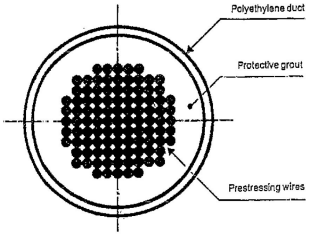

Figure 2.8: Parallel wires [3].

and in one of them is possible to apply a tensile force. Nowadays this is the typology most used for its better fatigue strength beyond the other types. Furthermore they are very cheap because of its mass production. The technical progress as regards the effective protection against corrosion has increased the durability of this type of cable.

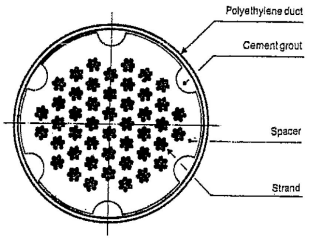

Figure 2.9: Stranded cable [3].

In the Locked-coll cables (figure 2.10) the wires are arranged in successive layers around a central core which consists of circular, parallel wires. This type of cable has some advantages. They are flexible and they have high density which makes their connections smaller and lighter. In addition only few outer layers have to be galvanized wince the rest of the section is filled-up with red lead which provides an acceptable resistance at a very low cost [14].

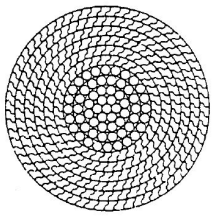

Figure 2.10: Locked-coll cable [2].

To establish the cross sectional areas of the cables, as a first iteration, it has to be verified that the stress produced by the permanent loads is less than the maximum admissible stress σ_{adm} which is defined as:

$$\sigma_{adm} < 0.45 f_u \tag{2.1.1}$$

Where:

f_u: ultimate stress of the steel.

When the permanent stress has values greater than 50% of the ultimate stress the relaxation accelerates significantly.

As regards the fatigue strength the stay should resist variations of stresses around 200 MPa for $2 \cdot 10^6$ cycles according to Setra [15].

$$\Delta\sigma_{adm} < 200MPa \tag{2.1.2}$$

Geometrical nonlinearities in cables can appear due to the cable sagging effect. This effect is produced by the selfweight of the cable and it depends of the length and the prestress of the cable. To model the sagging effect the Ernst's Modulus [2, 5] can be used. It consists in a reduced elasticity modulus E_{eq} which is calculated taking into account the modulus of elasticity (E), the sectional area (A), the cable weight per unit length (w), the projected length of the cable (L) and the tensile force in the cable (T). The reduced elasticity modulus in different conditions can be seen in figure 2.11.

$$E_{eq} = \frac{E}{1 + \frac{(wL)^2 AE}{12T^3}} \tag{2.1.3}$$

Objective Service Stage

The Objective Service Stage (OSS) is defined as the target geometry or/and stress state to be achieved at a certain time considering a target load. The OSS is related with the definition of the stay forces to be introduced in the tensioning process and there are many criteria to calculate these forces.

The OSS can be defined by the Rigidly Continuous Beam Criterion ([16], [17], [3]). The forces in the stays are obtained by projecting the support reactions of an equivalent continuous beam rigidly supported by the stays. Then the prestressing cable forces are obtained solving a system of equations. More details are given in section 4.1.

There are other methods such as the Minimal Bending Energy Criterion [18] which is based on the minimization of the bending energy of the structure. The Zero Displacement Criterion [19] where the tensioning stay forces are those which produces zero displacement at some points of the structure including the pylon. As a result we obtain the desired geometry. The Unit Load Method [10] allows the definition of a desired-moment distribution in the final structure under dead load. The method computes the tensioning forces of the stays in order to achieve a predetermined

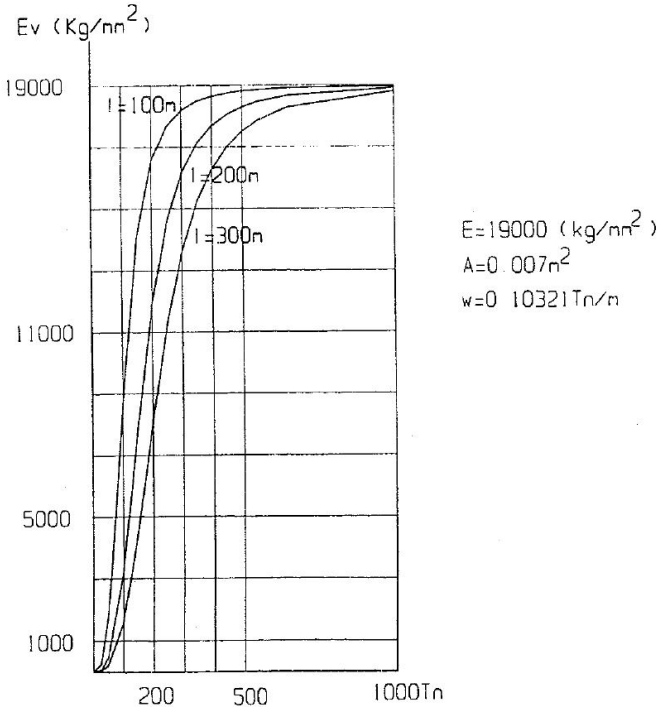

Figure 2.11: Elasticity modulus with respect to the tensile force and the projected length [2].

moment distribution. Another example is the Optimization Method [20, 21] where the tensioning forces of the stays are defined according to objective functions. This functions concern the structural efficiency or economy. All the solutions are based on obtaining the tensional forces to introduce in the cables to achieve the OSS but not considering the constructive process.

Some softwares permit to calculate the OSS by using optimization techniques. This is the case of the software MIDASoft [22]. There is a function called "ULF-Unknown Load Factor" which allows to calculate the pretension cable forces by imposing some conditions made by the designer. Some of the conditions which can be applied are zero displacements at some points of the structure or a specific force can be imposed at some elements of the structure. Nevertheless this method doesn't allow to take into account conditions considered in previous stages, only in the final stage. Thus, the constructive process doesn't take part in the definition of the OSS.

In concrete bridges the OSS can only be achieved at a time T_t due to the time dependent phenomena. Some studies have been carried out to study the effects of these phenomena in cable-stayed bridges [23, 24, 25, 26]. This effects have been considered to define the OSS for bridges built by the temporary supports method [27]. However, a definition of the OSS taking into account the time dependent phenomena and considering the constructive process for cantilever erection method has not been found in the literature.

2.1.3 Construction methods

The erection of cable-stayed bridges is equally as important as their final stage. The final stresses and deformations of the completed structure are completely dependent of the previous stages and the construction method chosen. Some authors [28, 14] stated the erection process is essential for designing the different elements as the critical stresses are reached during the construction most of the times.

There are mainly four constructions methods:

- The cantilever erection method.
- The temporary supports method.
- Incremental launching.
- Rotation method.

The cantilever method consists in building the structure from the pylons adding the different elements of the girder one by one. After adding the section of the girder the cable stays are installed in it and are connected to the pylon in each erection stage. The elements are added in a symmetric way with respect to the pylon in order to make the structure stable during the erection. This method is useful as it permits the construction in places where it is difficult to access. It makes possible to overcome obstacles such as wide rivers, lakes or closed valleys. Another great advantage is that during the construction the intermediate systems are stable by themselves. Furthermore the no necessity of using temporary supports reduces the cost of the structure and the construction time. Examples of bridges erected with this method are the Normandie Bridge (1995) in France or the Ting Kau Bridge (1998) in China (figure 2.12).

The temporary supports methods consists in building the girder above a falsework or temporary supporting towers. After the deck is erected the cables are installed and the temporary supports removed once the structure is stable and the CIP concrete (cast in place) has enough strength. This method typically is used for short and middle span length bridges where the ground can carry a falsework and there is no traffic or obstacles such a river. It is not suitable for locations where it is difficult to access. The cost of construction is smaller since conventional construction techniques can be used. An example of a bridge erected with this method is the Rokto Bridge (1976) in Japan.

In the incremental launching the structure is erected on land at one abutment and is launched from one pylon to the next. Some temporary towers can be added to provide additional support. One of the advantages is that the fact of casting the girder on land permits an accurate concrete control. The main drawbacks are the necessity of special bearings at the supports, straight decks and the cost can be elevated since specialized contractors and jacking systems are required. An example of a bridge erected with this method is the Millau Bridge (2004) in France (figure 2.13).

Figure 2.12: Cantilever method in Ting Kau Bridge.

The last method is the rotation method where the structure is built above temporary supports. Then the girder is lifted after giving tension to the cables and the structure is rotated to its final position. The most important limitation is the space needed at the abutment to build the structure. An example of a bridge erected with this method is the Ben-Ahin Bridge (1987) in Belgium.

If we consider the tensioning process to classify the construction methods there would be mainly only two methods. The last two methods can be considered as temporary supports methods as they have the same tensioning process.

In the temporary support methods (temporary supports, incremental launching, rotation) in order to not exceed the stresses limits during construction the stay forces are adjusted in two stages. In the first stage normally a force between 70% and 85% of the forces of the OSS is applied to the cables. However, in the cantilever method the 100% of the force is applied at the first stage and another stage to adjust the stays is not needed.

Cantilever erection method

As this investigation focuses in the cantilever erection method some more details about this construction technology are presented below.

The cantilever method proposed by Gimsing [1] is shown in figures 2.14 and 2.15. If we look the figure 2.14 at the first stage the pylons are erected. At stage 2 the

Figure 2.13: Incremental launching applied in Millau Bridge.

free cantilevering starts and the firsts sections of the girder are added with cranes (the cranes are used only when the girder elements are made of precast concrete or steel). Then the stays are installed and tensioned. The following sections are installed symmetrically to make stable the structure. The sections are added one by one till the bridge is closed at midspan and additional loads such as wearing surface or railings are applied.

In this method the stability depends on the fixity of the superstructure to the pylon piers but also on the connexion of the girder to the pylon. As soon as the new girder elements are in place the joints have to be closed in order to transmit the forces to the rest structure. As a result, the new elements can carry the cranes or the formworks for the next elements to be installed.

At figure 2.15 cantilever method and temporary supports method are combined. The main span is erected by free cantilivering. First of all the girder of the side spans is erected followed by the erection of the pylons. The girder of the side spans is built above temporary supports. Then the procedure is the same as the double-sided free cantilivering but only on one side of the pylon. After the completion of half of the main span, the other half is carried out. Finally the bridge is closed at midspan.

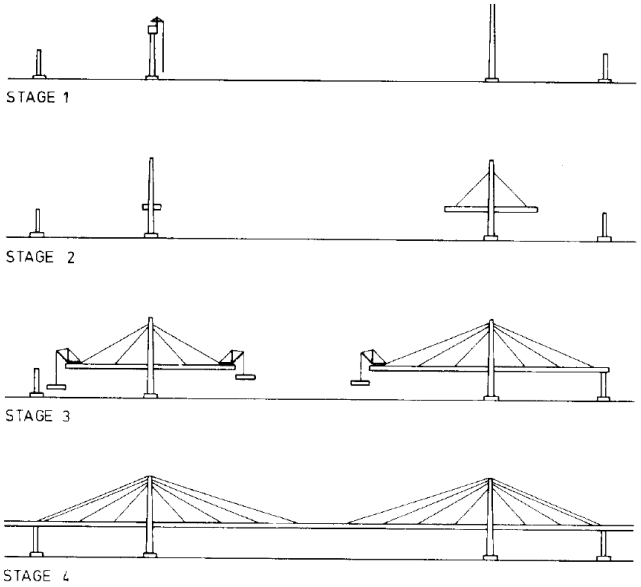

Figure 2.14: Doble-sided free cantilevering construction process [1].

Type of girder

This constructive process can have variations depending on the material and the type of section used for the girder. The girder can be made of concrete elements (cast in place or precast concrete), steel elements or composite elements.

For girders made of steel the boxes are installed using joined welds while the concrete segments are usually joined using epoxy resin.

The concrete girder elements can be made of CIP concrete (cast in place) or precast concrete. The CIP concrete has the advantage that no heavy precast elements have to be transported and lifted. Moreover there are less chances to have cracks since it allows the overlapping of the reinforcement. One disadvantage is that CIP construction requires about one to two weeks for each new beam section, whereas precast elements permit a construction progress of one to two elements per week according to Svensson [8].

It has become very common these recent years to use composite sections where the slab is made concrete, as it has low cost, and the rest of the girder made of steel. According to Gimsing [1] the main advantage of using steel is that the cantilevering from one anchor point to the next can be made by light steel permitting the cable being installed before the concrete slab is added. A typical composite section is showed in figure 2.16.

The time dependent phenomena effects can be neglected for the steel and precast concrete girders but not for CIP concrete bridges.

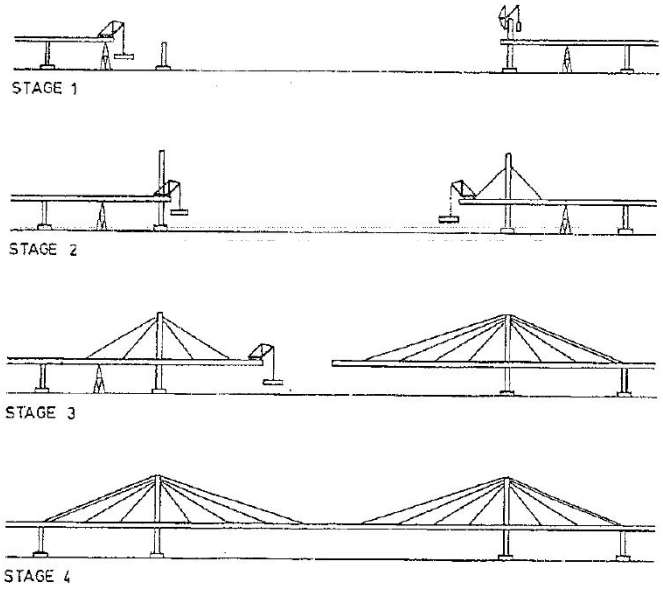

Figure 2.15: One-sided free cantilevering construction process [1].

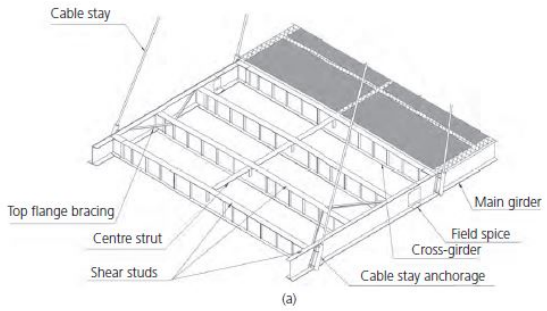

Figure 2.16: Typical composite cable-stayed deck structure. [4].

The procedure to install the new segments depends on the material used. For pre-fabricated elements cranes usually are used. The new segments are transported by trucks or boats depending the situation of the structure and then they are lifted by the cranes to the final location. For cast in place concrete segments formworks and derrick cranes are required (figure 2.17). The weight of these auxiliary elements is different in every bridge. It depends mostly on the length of the segments. It is usually between 40% and 60% of the girder element weight according to some project executors. There is not an exactly relation since the auxiliary elements are reused in the construction of bridges which have different characteristics. In table 2.1 the weight of auxiliary elements used in some projects is given in relation to the weight of the deck element.

Figure 2.17: Derrick crane and formworks.

Table 2.1: Relation between weight of the auxiliary elements and weight of concrete element in some projects.

Project	Auxiliary elements Weight (kN)	Segment weight (kN)	Wauxiliary/Wsegment
Guiniguada Bridge	787	2280.170	0.35
Ubera Bridge	550	886.500	0.62
Pisuerga Bridge	500	1120.230	0.45
Ebro Bridge	600	1524.630	0.39
Trapagarán Bridge	1250	3428.740	0.36
Teror Bridge	945	1736.400	0.54
Tenoya Bridge	950	1960.000	0.48
Botijas Bridge	844	1838.000	0.46
Cimarrón Bridge	650	1473.030	0.44

2.2 Construction Analysis

Due to the increasing of the slenderness of the new modern bridges it is very important to check that the stresses are not too high during the construction until the structure is finished under dead load. For this reason many algorithms have been developed to simulate the different erection methods.

Backward approach

Some studies present the backward approach in the cantilever erection method [29, 14, 28, 5] and for the temporary supports method [30]. In this approach the final stage is defined considering dead and life loads. Once the OSS is modeled the structure is disassembled stage by stage in the opposite time direction of the real construction.

The calculations are less time-consuming than in the forward approach to converge because they start from a structurally correct solution (final stage). It is better to implement this in commercial software because optimization of time is required. The main drawback of backward algorithms is that time dependent phenomena are very complicated to simulate since the simulation doesn't follow the real time direction

of the construction, thus, these effects can only be approximated. Moreover this method is not appropriate to take into account deviations in the tensioning process. To overcome this problems in concrete bridges a forward approach has been studied.

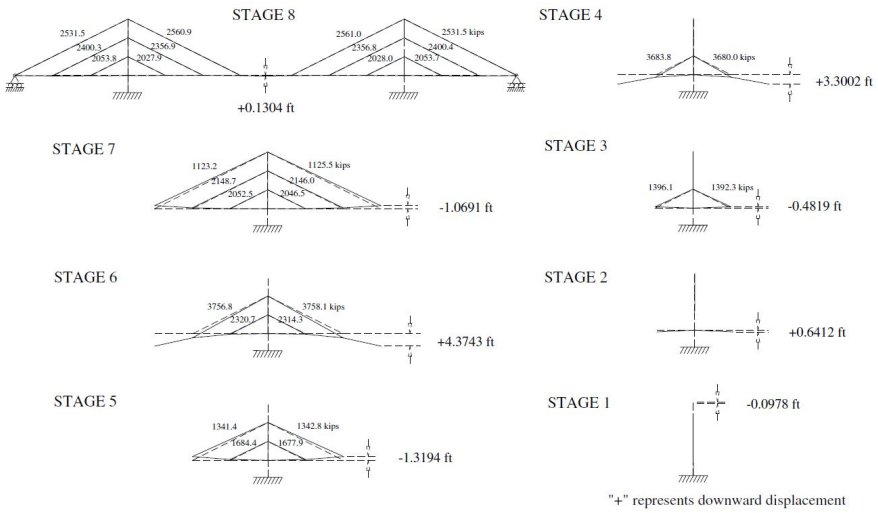

Figure 2.18: Backward approach for double cantilever method proposed by Wang et al. [5].

Forward approach

Other papers have considered a forward approach for the cantilever method [5] and for the temporary supports method [31]. It simulates the erection process in the time direction of the real construction.

The creep and shrinkage effects can be easily computed as it follows the real time direction. Differences of temperatures between reality and the structural analysis don't need separate models to be calculated. Another advantage is that the calculation of the stresses in the mono-strands when the strand by strand prestressing technique is used don't need separate models. The main drawback of the forward algorithm is being time-consuming.

Both algorithms presented as far can be very useful to solve determined problems. These methods have been analyzed by Pipinato et al. [32] and it is proved that they can be used successfully for both one-sided and double-sided free cantilevering construction methods. As Carrillo, L. [7] states, the backward algorithm can be used to obtain the tensile forces of the stays and the forward algorithm to simulate more easily the time-dependent phenomena and to do a control during the real construction of the bridge.

Other algorithms

A direct algorithm is presented by Lozano J.A. et al. [33]. It introduces the un-

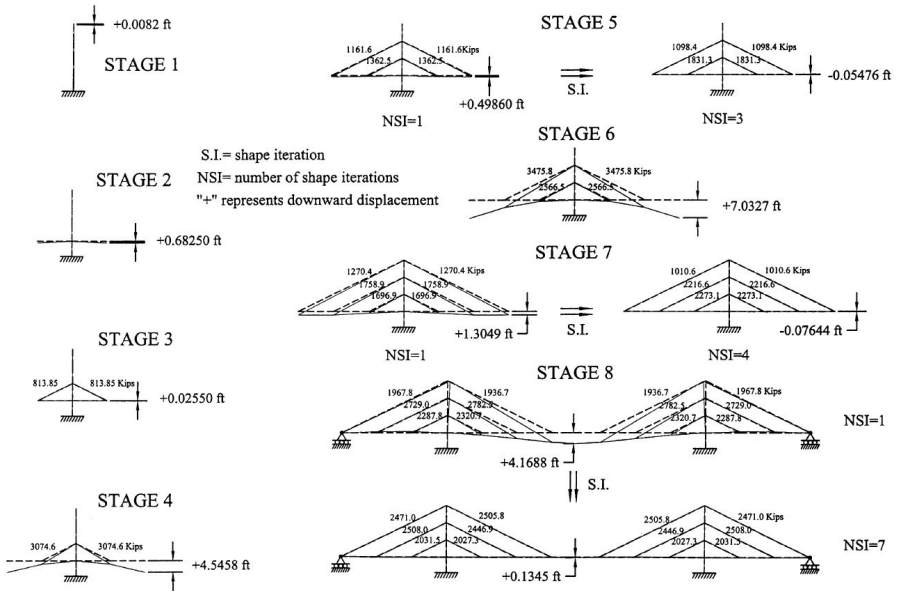

Figure 2.19: Forward approach for double cantilever method proposed by Wang et al. [5].

stressed length of the stays concept into the modeling of the construction process of cable-stayed bridges. The algorithm requires less information than the backward and forward algorithm. Any construction stage can be analyzed with an independent Finite Element Model and information of the previous or the following stages are not needed. As the superposition principle is not applied it is less time consuming but the time dependent phenomena can not be easily simulated. It can be applied in any structural analysis software. The algorithm can be suitable for steel bridges but not for concrete.

A forward direct approach taking into account the time dependent phenomena has been studied for the temporary supports erection method [27] but not for cantilever erection method. The forward approach of this algorithm facilitates the simulation of the time dependent phenomena. The superposition of stages principles is applied to simulate changes during construction in the structural system, loads or boundary conditions. The stay forces are simulated by imposed strains on the stays. It is called direct algorithm since the simulation of the last tensioning operations is based on the unstressed length concept to avoid the requirement of an overall iterative process as it is required in the forward algorithm.

As regards the creep effects, Schlaich [13] stated that for pure concrete decks the creep effects due to bending do not to be considered if dead load configuration with continuous beam criterion is considered. This is because the sum of the negative and positive moments are zero so the variation of moments due to the creep is eliminated. The initial moment distribution doesn't change so the moment creep is not considered. In this method only the creep of the axial forces is considered. This simple method has been used for several cable-stayed bridges with pure concrete decks and for the designing of Ting Kau Bridge in Hong Kong which has a composite deck

with precast slabs.

Unstressed length of the stays concept

This concept is explained in detail by Lozano et al. [33, 26, 27]. To sum up, the main ideas of the concept are explained below.

The unstressed or neutral length of the cable, L_{0n}, is the length of a prefabricated cable when it is not loaded and it is measured when the cable rest horizontally. This parameter is intrinsic of the cable which it means that it doesn't depend of the loads and the conditions of the structure.

L_n is the length of the cable in the FEM model. The cable of length L_{0n} in order to achieve the correct position on site needs to be stressed. Then the stressed length, L_{Sn} is achieved. The relation between the different length is presented in Equation 2.20. The unstressed or neutral length can be obtained from the stressed length as it shows Equation 2.2.2.

$$\epsilon_n = \frac{\Delta L_n}{L_{0n}} = \frac{L_{Sn} - L_{0n}}{L_{0n}} \tag{2.2.1}$$

$$L_{0_n} = L_{S_n} - \frac{N_n}{E_n A_n} L_{S_n} \tag{2.2.2}$$

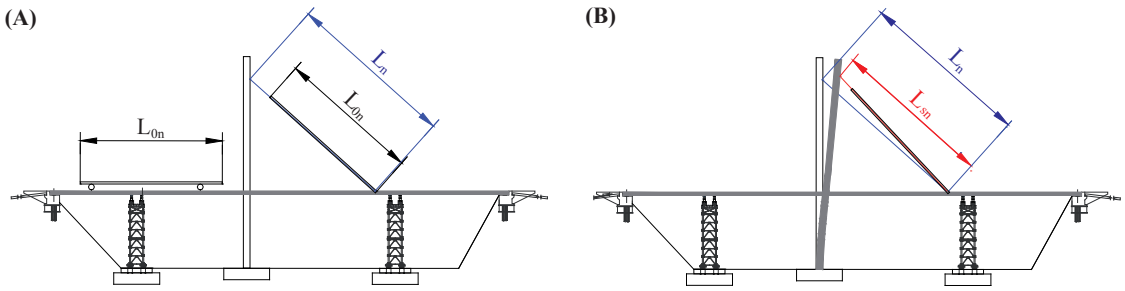

Figure 2.20: Definition of the different cable length: L_{0n}, L_n, L_{Sn}. [6]

The concept is used in a direct simulation. It can be assumed that extending a cable of length L_{0n} with a given stress gives the same result than shortening a cable of length L_n. The relation is shown in Equation 2.2.3. The shortening is modeled by an imposed strain to the cable. In the direct algorithm the imposed strain of the OSS, ϵ_n^{OSS}, can be obtained with the methods explained in Section 2.1.2.

$$L_{Sn} = L_{0n}\left(1 + \frac{N_n}{E_n A_n}\right) = L_n\left(1 - \epsilon_n^{OSS} + \frac{N_n}{E_n A_n}\right) \tag{2.2.3}$$

The main advantage of this concept is that it can be used in a direct approach where superposition of stages are not required to simulate the construction process.

Chapter 3

Modeling analysis aspects

Cable-stayed bridges are structures difficult to simulate with simplified analysis due to their high hyperstaticity, the evolutionary constructive process, the active forces introduced in the stays and the high deformability of the partials structures during the construction.

In order to simulate the erection process a Fortran FEM code has been used. This code has been developed previously by the professors Estradera, J.M.; Chio, Gustavo and Lozano, J.A.

The examples analyzed to validate the software are FE models in 2D. In this investigation only a static analysis is carried out due to the complexity of the time dependent phenomena effects. In future investigation it could be advisable to include a dynamic analysis. These type of bridges are very sensitive to the dynamics loads induced by wind or traffic. Furthermore over the last years the dynamic load effects have increased as the result of the increasing vehicle speed and the lighter and more slender bridge designs.

Superposition principle is considered since cable-stayed bridges are designed in order that the stresses remain in the elastic range. The superposition of stages is used to simulate changes during construction in the structural system, loads (including shrinkage and creep effects) or boundary conditions. Euler-Bernoulli beam theory is used, thus the deformation due to shear forces is neglected.

The stay forces are simulated by imposed strains on the stays. Calculating the stresses in the mono-strands when the strand by strand prestressing technique is used do not need separate models [27].

It is considered a forward and direct approach. The forward approach, as it is in the real direction of the construction, facilitates the simulation of the time dependent phenomena.

The algorithm can also consider the effect of the shrinkage, creep or the difference of the temperature between the moment that the cable is located and the time

considered for the OSS (Objective Service Stage). To calculate the total strain the superposition principle is used. For the computation of the creep the Dischinger's hypothesis, used to simplify the numerical procedure, is improved. This improvement is explained in this section.

Stress relaxation which is the loss of stress under constant strain is not considered. Since the stresses in cables are limited to 45% of the ultimate strength, f_u the stress relaxation can be neglected. According to Cluley, N. C. and Shepherd R. [34] relaxation is negligibly small for $\sigma_p/f_y < 0.55$, being σ_p the prestress force and f_y the yield strength of steel.

As follows, the implementation in the algorithm of time dependent phenomena is explained.

3.1 Creep

Concrete is a material which has deflections along time. Shrinkage is the deformation of the concrete with respect to time without applying any load whereas creep depends on the load applied. This phenomena are related with the response of the different materials of the concrete with the interior pressure and the hydraulic equilibrium between concrete and the exterior.

In those bridges whose construction method involves concrete used at different ages, time dependent phenomena take importance. This is the case of cable-stayed bridges erected by the cantilever method.

Creep and shrinkage interfere in the following points:

- Variations of deflection as the cantilever grows.
- Stress redistribution. In hyperestatic structures such as cable-stayed bridges the reactions are redistributed due to the creep and shrinkage and thus the stresses change.

These effects changes the target stress state to be achieved in service. The Objective State Service (OSS) can only be obtained at certain time.

For cable-stayed bridges erected with cantilever method the redistribution of stresses is higher than when other constructive techniques are used. This is because the deck elements contain concrete of different ages, the loading is done at different times and the boundary conditions change during the construction. However, when the temporary supports method is used the concrete is placed at the same time. This fact reduce redistribution of stresses and the creep and shrinkage rotation is more or less proportional to the elastic rotation according to Manterola [2].

The total strain in concrete is:

$$\epsilon(t) = \epsilon_E(t) + \epsilon_{cs}(t) + \epsilon_c(t) + \epsilon_T(t) \tag{3.1.1}$$

Where:

$\epsilon_E(t)$: Instantaneous elastic strain.
$\epsilon_{cs}(t)$: Shrinkage strain.
$\epsilon_c(t)$: Creep strain.
$\epsilon_T(t)$: Thermal strain.

The instantaneous elastic strain and the thermal strain can be calculated directly from the mechanical and geometric properties of the structure. However, the shrinkage and creep strain vary throughout time and they depend on the ambient humidity, the concrete strength and the basic element dimensions.

The creep strain, $\epsilon_c(t)$ is defined in Eurocode 2 (EN 1992-1-1:2004) and is related to the creep coefficient, $\phi(t, t_0)$, the constant stress,σ_0 and the Young modulus,E. The first hypothesis is that the creep deformation is proportional to the constant stress.

$$\epsilon_c(t, t_0) = \phi(t, t_0)\frac{\sigma_0}{E} \tag{3.1.2}$$

Then the total strain, which consists on the elastic strain and the creep strain, is:

$$\epsilon(t, t_0) = \sigma_0 \left[\frac{1}{E_C(t_0)} + \frac{\phi(t, t_0)}{E_c}\right] \tag{3.1.3}$$

The linearity of the deformation is considered valid if σ_0 is not higher than 45% of the characteristic concrete resistance. If it is higher creep non-linearity appears and the creep deformations accelerates.

Another hypothesis considered is the superposition principle. The creep strains produced by different loads at different ages can be summed. The variation of strain during one interval of time is obtained by the following expression:

$$\begin{aligned}\Delta\epsilon(\Delta t_j) = \frac{\sigma_0}{E_{c(t_0)}} + \frac{\sigma_0}{E_{c,28}}\phi(t_j, t_0) + \sum_{i=1}^{j-1}\left[\frac{\Delta\sigma_i}{E_C(t_i)} + \frac{\sigma_i}{E_{c,28}}\phi(t_j, t_i)\right] + \frac{\Delta\sigma_j}{E_C(t_j)} \\ + \frac{\sigma_j}{E_{c,28}}\phi(t_j, t_j) - \frac{\sigma_0}{E_{c(t_0)}} - \frac{\sigma_0}{E_{c,28}}\phi(t_{j-1}, t_0) - \sum_{i=1}^{j-1}\left[\frac{\Delta\sigma_i}{E_C(t_i)} - \frac{\sigma_i}{E_{c,28}}\phi(t_{j-1}, t_i)\right] + \frac{\Delta\sigma_j}{E_C(t_j)} \\ - \frac{\sigma_j}{E_{c,28}}\phi(t_{j-1}, t_j)\end{aligned} \tag{3.1.4}$$

Creep coefficient

The creep coefficient is calculated from:

$$\phi(t, t_0) = \phi_0 \beta_c(t, t_0) \tag{3.1.5}$$

Where ϕ_0 is the notional creep coefficient and $\beta_c(t, t_0)$ is a coefficient to describe the development of creep with time after loading.

The notional creep coefficient (3.1.6) is estimated from ϕ_{HR}, $\beta(f_{cm})$ and $\beta(t_0)$. ϕ_{HR} is a factor to allow for the effect of relative humidity on the notional creep coefficient. $\beta(f_{cm})$ is a factor to allow for the effect of concrete strength on the notional creep coefficient. $\beta(t_0)$ is a factor to allow for the effect of concrete age at loading on the notional creep coefficient.

$$\phi_0 = \phi_{HR} \beta(f_{cm}) \beta(t_0) \tag{3.1.6}$$

$\beta_c(t, t_0)$ is defined in equation (3.1.7) and it depends of the age of concrete in days, t the age of concrete at loading in days, t_0 and a coefficient depending on the relative humidity (RH) and notional member size (h_0).

$$\beta_c(t, t_0) = \left[\frac{t - t_0}{\beta_H + t - t_0} \right]^{0.3} \tag{3.1.7}$$

More details of how to calculate the creep coefficient are given in ANNEX B of Eurocode 2.

3.1.1 Dischinger hypothesis

For the creep analysis the Dischinger hypothesis is usually considered which consists in a simplification of the creep law.

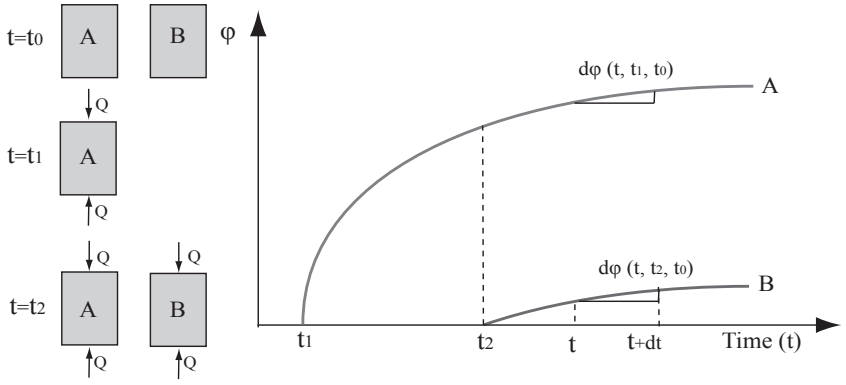

Figure 3.1: Dischinger's Hypothesis [6]

Dischinger states that the creep coefficient only depends on the time of evaluation and the concrete age but not the loading age which is used in the general method.

As we can see in figure 3.1 the variation of the creep coefficient in concrete specimen A is the same as in B since their concrete age is the same. So according to Dischinger:

$$d\phi(t, t_1, t_0) = d\phi(t, t_2, t_0) = d\phi(t, t_0) \tag{3.1.8}$$

Equation 3.1.4 is simplified and reduced to:

$$d\epsilon = \frac{\sigma_0}{E} d\phi + \frac{\sigma}{E} d\phi + \frac{d\sigma_0}{E} \tag{3.1.9}$$

3.1.2 Simulation of creep

To simulate the creep effects the procedure described by Lozano et al. [26] has been used. From a previous model of the structure the axial forces and bending moments are calculated in every element i. In each element the average of the axial forces, $\overline{N_{i,E}}$, and the average of the bending moment, $\overline{M_{i,E}}$, are computed as it can be seen in figures 3.2 and 3.3. To do the average the values of the edge of the element are taken. Regarding the bending moment this approximation is valid when the length of the element is small.

Then the axial strain, $\epsilon_{i,E}$, and the curvature, $\chi_{i,E}$, of the element are obtained from the approximation of the axial and bending forces using the corresponding elastic modulus, E_i, area, A_i, and inertia, I_i, of the element.

$$\overline{N_{i,E}} = \frac{N_i + N_{i+1}}{2} \tag{3.1.10}$$

$$\epsilon_{i,E} = \frac{\overline{N_{i,E}}}{E_i A_i} \tag{3.1.11}$$

$$\overline{M_{i,E}} = \frac{M_i + M_{i+1}}{2} \tag{3.1.12}$$

$$\chi_{i,E} = \frac{\overline{M_{i,E}}}{E_i I_i} \tag{3.1.13}$$

In order to obtain the strain and curvature produced by the creep during one interval (t_j, t_{j+1}) the strain and curvatures obtained are multiplied by the increment of the creep factor, $d\phi(t, t_0)$, which is obtained considering the loading time.

$$\Delta\phi(t, t_0) = \phi(t_{j+1}, t_0) - \phi(t_j, t_0) \tag{3.1.14}$$

$$\Delta\epsilon_i = \Delta\phi(t, t_0)\epsilon_{i,E} \tag{3.1.15}$$

$$\Delta\chi_i = \Delta\phi(t, t_0)\chi_{i,E} \tag{3.1.16}$$

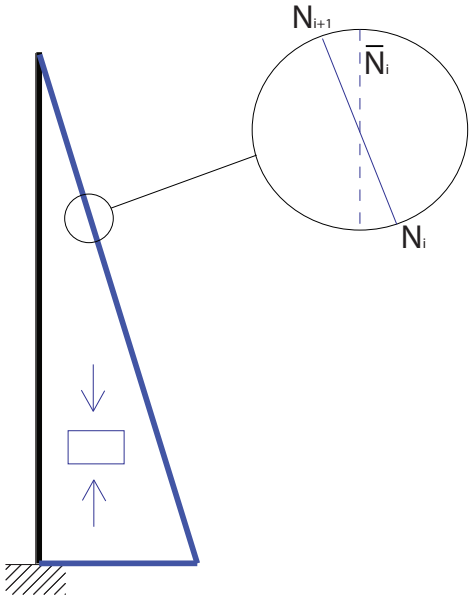

Figure 3.2: Element average axial forces. Column under self weight.

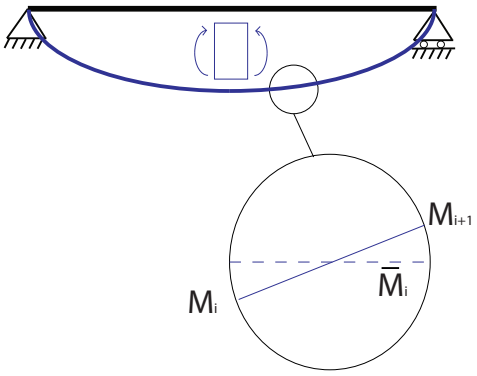

Figure 3.3: Element average bending moment. Beam under self weight.

The curvatures and strains are introduced as imposed loads to the different elements in the FEM model. As a result the stresses ($\Delta N_{i,creep}$, $\Delta M_{i,creep}$) produced by the creep during the interval are obtained and they are added to the elastic stresses ($N_{i,E}, M_{i,E}$). With the new stresses the procedure explained in equations 3.1.10 to 3.1.16 is done for the next intervals until the time required is reached.

The increment of time in every interval is smaller at the first days and it is increased throughout the time in order to reduce the computational cost. The increments of time chosen are the following:

- $\Delta t = 1$ when t<180.
- $\Delta t = 2$ when 180≤t<360.
- $\Delta t = 5$ when 360≤t<730.

- $\Delta t = 14$ when 730≤t<1850.
- $\Delta t = 28$ when 1850≤t<3670.
- $\Delta t = 365$ when t>3670.

3.1.3 Creep in different stages

Some authors have studied time dependent phenomena effects during the construction process [23, 35, 26]. In this thesis superposition principle and an improvement of Dischinger simplifications are used to develop the algorithm.

To show how the algorithm simulates the creep in different stages a simple structure made of concrete is analyzed. Three stages are considered as it can be seen in figure 3.4. At the first stage the pylon is erected and self weight, $SW1$, is considered. At the second stage a beam is supported by the pylon and self weight, $SW2$, is considered. At the third stage two supports at both edges of the beam are located and an additional distributed load, $q1$, along the beam is considered.

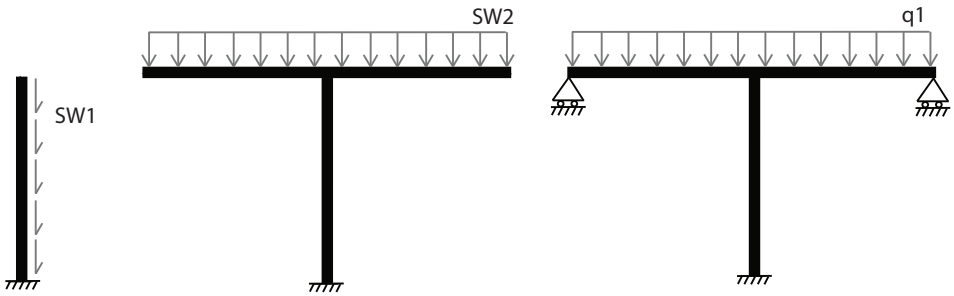

Figure 3.4: Stages of a simple structure.

First of all the static stresses are calculated in the first stage (figure 3.5: Stage 1: t_1). From the stresses obtained in the pylon the axial strains of every element of the pylon, $\epsilon_E^{i,1}$, are obtained. These strains are introduced in an auxiliary FEM model multiplied by the variation of creep coefficient $\Delta\phi(t, t_0)$. To calculate $d\phi(t, t_0)$ for the elements added in the first stage, $t_{0,1}$, is used. This procedure is carried out until the final time of the first stage, $t_{f,1}$, is reached.

At the second stage (figure 3.5 Stage 1 t_1) new elements, which define the beam above the pylon, are added and a new load, $SW1$, is considered. The elastic stresses are calculated and new strains, $\epsilon_E^{i,2}$, and curvatures, $\chi_E^{i,2}$, are obtained. Then new increment of strains and curvatures due to the creep are calculated. For the elements in the pylon the stresses of the first and second stage are taken into account so two sets of strains and curvatures are obtained. For the elements added at the second stage only the creep effects of this stage are considered. The procedure is carried

out until the final time of the first stage, $t_{f,2}$, is reached.

At the last stage of this example (figure 3.5 Stage 1 t_1) the elastic strains, $\epsilon_E^{i,2}$, and curvatures, $\chi_E^{i,2}$, are calculated after changing the boundary conditions and adding another uniformly distributed load along the beam. In the pylon three sets of increment of strains and curvatures due to the creep will be added taking into account the three stages. For the elements in the beam only the creep effects of the last two stages are considered.

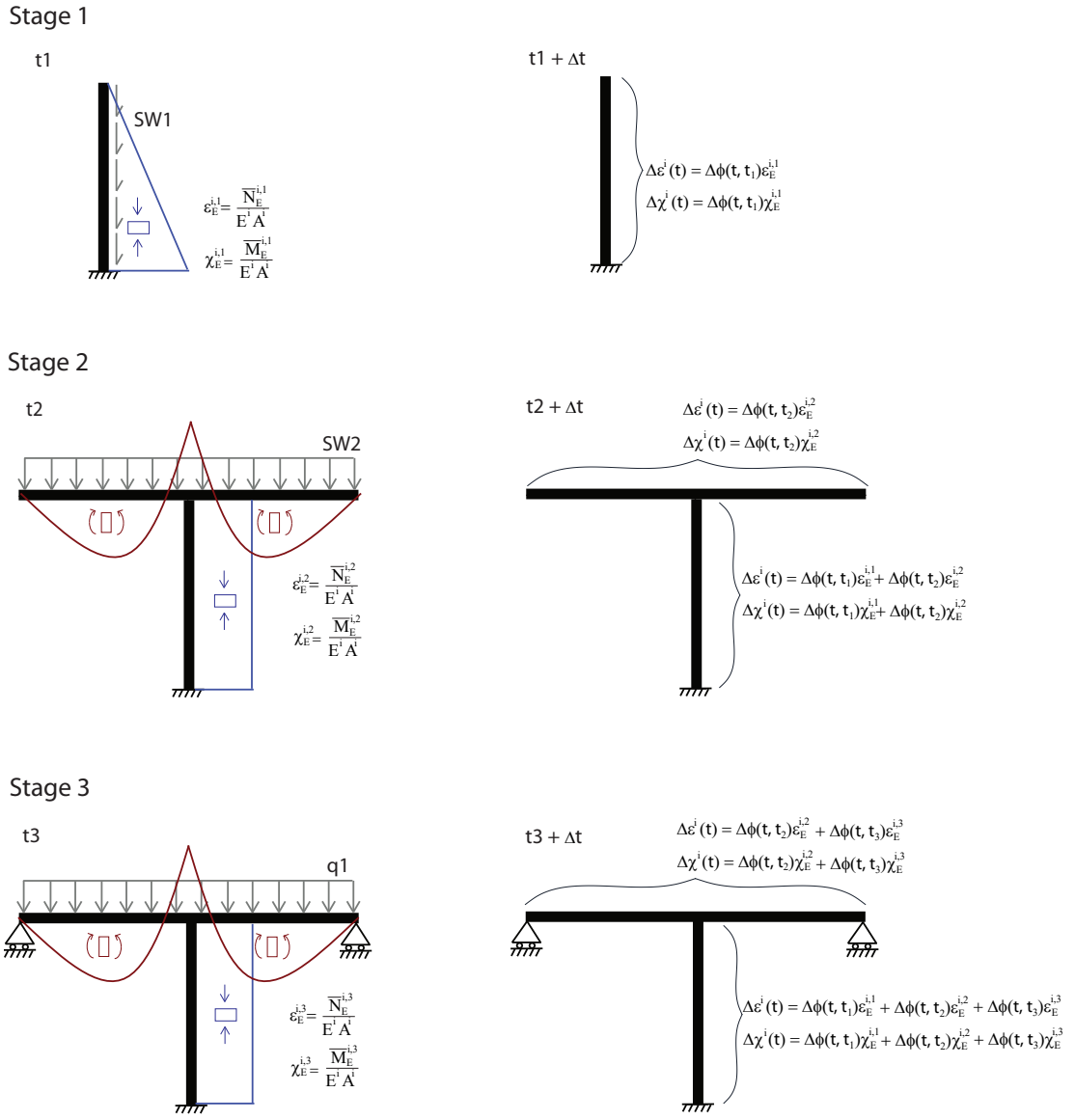

Figure 3.5: Procedure to add the effects of the creep into the structure.

In figure 3.5 the strains and curvatures obtained in every stage are shown. At the left column the elastic strain and curvature are obtained. At the right column it can be seen how the deformations due to the creep are obtained for every element

depending on what time they have been added to the FEM model.

Loading time

In this algorithm the Dischinger hypothesis has been improved taking into account the time of loading in every stage. Every element will have several creep laws, as many as times a load is added, instead of having only one as Dischinger simplification states.

For example in the pylon the increments due to the creep would be what it shows equations considering Dischinger simplification and only one creep law. The loading time considered in three sets of increment is the concrete age in stage 1.

$$\Delta\epsilon_i(t) = \Delta\phi(t,t_1)\epsilon_E^{i,1} + \Delta\phi(t,t_1)\epsilon_E^{i,2} + \Delta\phi(t,t_1)\epsilon_E^{i,3} \tag{3.1.17}$$

$$\Delta\chi_i = \Delta\phi(t,t_1)\chi_E^{i,1} + \Delta\phi(t,t_1)\chi_E^{i,2} + \Delta\phi(t,t_1)\chi_E^{i,3} \tag{3.1.18}$$

However, if several creep laws are used the age of concrete is considered to compute the creep coefficient every time a new load is added.

$$\Delta\epsilon_i(t) = \Delta\phi(t,t_1)\epsilon_E^{i,1} + \Delta\phi(t,t_2)\epsilon_E^{i,2} + \Delta\phi(t,t_3)\epsilon_E^{i,3} \tag{3.1.19}$$

$$\Delta\chi_i = \Delta\phi(t,t_1)\chi_E^{i,1} + \Delta\phi(t,t_2)\chi_E^{i,2} + \Delta\phi(t,t_3)\chi_E^{i,3} \tag{3.1.20}$$

3.2 Validation of the developed software

In order to validate the software and check if the creep effects are well simulated some patch tests can be performed. They consist in evaluate simple structures with different load and boundary conditions cases. Some of the obtained results from the software are compared to the analytical ones.

The following patch tests have been carried out to validate the software:

1. Axial loading of a pylon.
2. Axial loading of a pylon with change in boundary conditions.
3. Axial loading of a pylon in different ages.
4. Distributed load in a cantilever beam.
5. Distributed load in a cantilever beam with change in boundary conditions.
6. Distributed load in a cantilever beam. Load implemented in different ages.
7. System of two materials axial loaded.
8. System of one beam supported by one stay in the middle.

a) Steel stay.
b) Pretensioned stay.
c) Concrete stay.

9. Beam built by the union of two cantilever beams.

All the results of the validation carried out can be seen in Appendix B.

Chapter 4

Tensioning process

4.1 OSS without time dependent phenomena

In section 2 the different methods used to get the OSS without taking time dependent phenomena into account have been presented. All of them are based on obtaining the active forces of the cables to achieve the OSS and they do not consider the type of constructive process. As follows, another criterion is presented adding some other conditions to achieve the OSS.

The new criterion proposed in this thesis takes the constructive process of cantilever cable-stayed bridges into account. It has to be stated that this method can be applied to two-span bridges, three-span bridges with a large main span flanked by two smaller side spans or multi-span bridges built by cantilever erection method.

Some of the conditions of this new criterion to achieve the OSS are based in the Continuous Beam Criterion which do not consider the constructive process. One of the conditions added consists in achieving zero bending moment at the middle point of the main span when the completion stage is reached, $M_{midspan} = 0$. This condition is not applied in two-span bridges. Another condition to define the pretension of the cables is to consider reaction equal to zero in the side supports at the stage when they are installed, $R = 0$. To achieve this objective a displacement in the bearings, d_L and d_R, and a curvature, χ have to be introduced in the FEM model.

The main advantage of defining this conditions is that only one tensioning operation is needed to achieve the Objective Service Stage. Adding this conditions and applying the unstressed length of the stays concept an overall iterative process is not needed. The other criteria found in the literature, including the developed software tools, don't take into account the erection process of the structure.

In case that anchorage cables are used some other conditions have to be added such as consider that the horizontal component of the anchorage cable has to be equal to the horizontal force of the cable at the other side which supports the main span. As a result the displacement in top of the pylon at the end of the construction has to be close to zero.

In the Rigidly Continuous Beam Criterion the behaviour of a cable-stayed bridge is assumed to be like a fictitious continuous beam where the stays are substituted by bearings. The stay forces, N^{OSS}, are defined by projecting into the stays direction the vertical reaction of the supports of the equivalent continuous beam. The forces in the stays are obtained from the expression 4.1.1.

$$N^{OSS} = \frac{R}{sin(\alpha)} \tag{4.1.1}$$

Then a system of equations have to be solved where the unknowns are the imposed deformations in the stays and the restraints are the stay forces obtained from the equivalent continuous beam.

$$N^{OSS} = N_P + N_A = N_P + [IM]\epsilon^{OSS} \tag{4.1.2}$$

$$\epsilon^{OSS} = [IM]^{-1}(N^{OSS} - N_P) \tag{4.1.3}$$

Where:

ϵ^{OSS}: Imposed strain in the OSS.

$[IM]$: Influence matrix that shows the increments of axial forces in all the stay cables when an unitary strain is introduced in each stay.

N_P: Passive forces of the stays.

N_A: Active forces of the stays.

Some other conditions are added. Equations 4.1.4 and 4.1.5 have to be fulfilled at the state 1 in figure 4.1. The condition of equation 4.1.6 is fulfilled at state 2 and the equation 4.1.7 and 4.1.8, which come from the continuous beam criterion, are fulfilled at the final stage.

$$\sum N_i sen(\alpha_i) = g_1 L \tag{4.1.4}$$

$$R = 0 \tag{4.1.5}$$

$$M = 0 \tag{4.1.6}$$

$$N_i^1 + N_i^2 = \frac{R_j}{cos(\alpha_i)tg(\alpha_j)} \tag{4.1.7}$$

$$N_i^1 + N_i^2 = \frac{R_i}{sen(\alpha_i)} \tag{4.1.8}$$

For the simple case, which is shown in figure 4.1 the system to be solved is presented in expression 4.1.9.

$$
\begin{aligned}
N_1(\epsilon_1^1,\epsilon_2^1,\epsilon_3^1,\epsilon_4^1,\delta_1)sen(\alpha_1) + N_2(\epsilon_1^1,\epsilon_2^1,\epsilon_3^1,\epsilon_4^1,\delta_1)sen(\alpha_2) & \\
+N_3(\epsilon_1^1,\epsilon_2^1,\epsilon_3^1,\epsilon_4^1,\delta_1)sen(\alpha_3) + N_4(\epsilon_1^1,\epsilon_2^1,\epsilon_3^1,\epsilon_4^1,\delta_1)sen(\alpha_4) &= g_1 L - \sum(N_i(g1)) \\
R_1^1(\epsilon_1^1,\epsilon_2^1,\epsilon_3^1,\epsilon_4^1,\delta_1) &= 0 - R(g_1) \\
N_1^1(\epsilon_1^1,\epsilon_2^1,\epsilon_3^1,\epsilon_4^1,\delta_1) + N_1^2(\epsilon_1^2) &= \frac{R_4}{cos(\alpha_1)\tan(\alpha_4)} - N_1(g1,g2) \\
N_2^1(\epsilon_1^1,\epsilon_2^1,\epsilon_3^1,\epsilon_4^1,\delta_1) + N_2^2(\epsilon_1^2) &= \frac{R_2}{sen(\alpha_2)} - N_2(g1,g2) \\
N_3^1(\epsilon_1^1,\epsilon_2^1,\epsilon_3^1,\epsilon_4^1,\delta_1) + N_3^2(\epsilon_1^2) &= \frac{R_3}{sen(\alpha_3)} - N_3(g1,g2) \\
N_4^1(\epsilon_1^1,\epsilon_2^1,\epsilon_3^1,\epsilon_4^1,\delta_1) + N_4^2(\epsilon_1^2) &= \frac{R_4}{sen(\alpha_4)} - N_4(g1,g2)
\end{aligned}
\tag{4.1.9}
$$

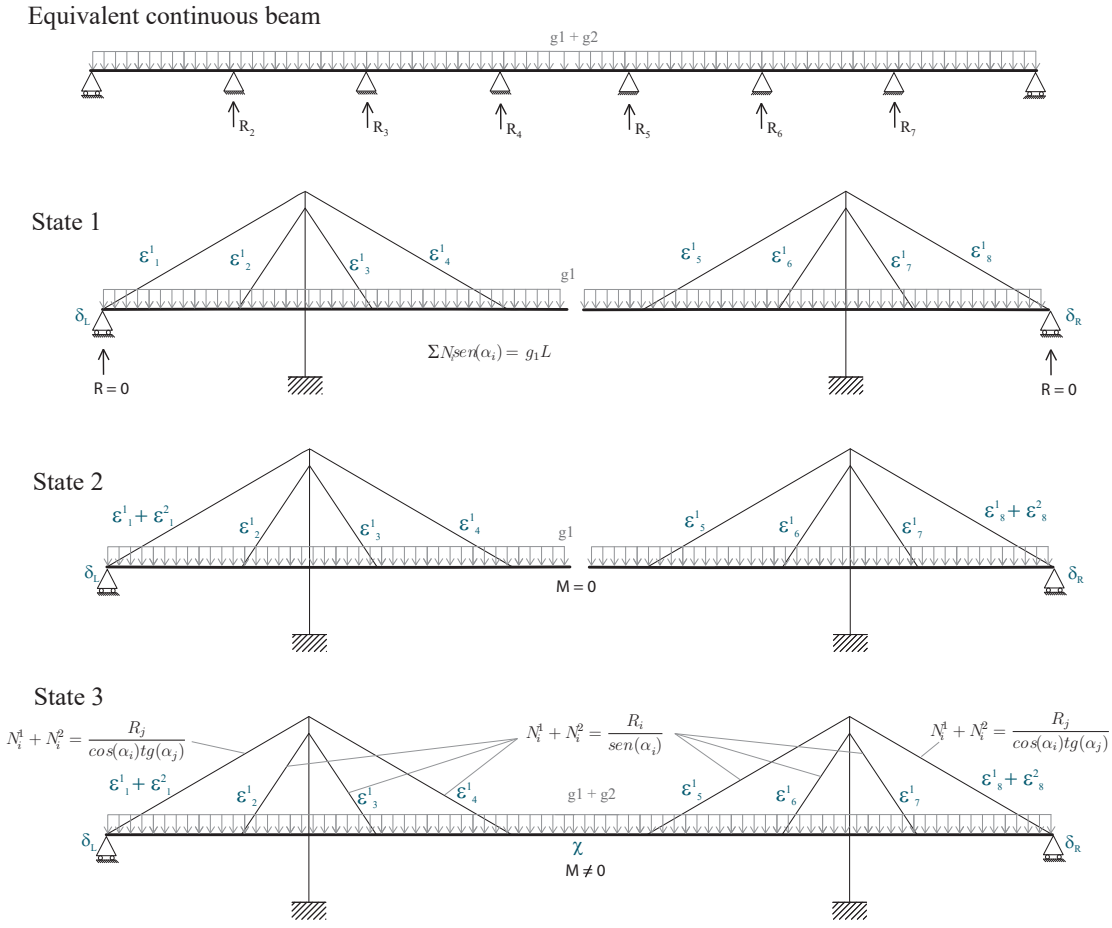

Figure 4.1: Conditions to define the OSS in different states during construction.

4.2 Simulation of the constructive process

The Fortran code developed permits to analyze the creep effects when the elements of the structure are placed at different times. To do it the algorithm takes into account the concrete age and the load in every stage.

Input data

The algorithm needs the following input data:

- Number of stages.
- Geometric and mechanical characteristics of every stage m.
- Imposed strains in the stays in case we analyze construction process of cable-stayed bridges.
- Initial ($t_{i,m}$) and final ($t_{f,m}$) time of every stage m.
- Age of concrete ($t_{0,m}$) of the new elements considered in the FEM model in every stage, m.
- Increments of time.

Output data

- Accumulated stresses and increments of stresses at the final time of every stage.
- Accumulated deformations and increments of deformations at the final time of every stage.
- Accumulated reactions and increments of reactions at the final time of every stage.

Flow chart

In figure 4.3 the flow chart of the algorithm is presented. The flow chart of the creep calculation has been presented separately in figure 4.4.

The simulation of the constructive process is summarized as follows: (1) The input data is introduced. (2) If at the current stage there is not a change of the type of link between the pylon and the deck the analysis goes on. (3) An independent FEM model is analyzed introducing the OSS deformations to obtain the stresses at the current stage (direct approach) not taking into account time dependent phenomena. (4) Another FEM model is analyzed only considering the loads added at this stage (superposition principle and forward approach). The deformations to add at the cables are those which permit to achieve the state obtained in the direct analysis of the current stage. To obtain the deformations the procedure is explained as follows. (5) An influence matrix of the cables added at the stage is created. It includes the effect

in other cables when one cable is pretensioned. (6) The deformations are obtained by solving the system $N^{k,i} = [IM]\epsilon^{k,i}$ where $N^{k,i}$ are the axial forces of the cables obtained from the direct approach, [IM] is the influence matrix and $\epsilon^{k,i}$ are the deformations that are needed. (7) Then the deformations obtained are introduced in an auxiliary model which is summed to the previous one calculated. (8) By considering the forward approach and superposition principle the time dependent phenomena effects can be calculated. The flow chart of the creep analysis is explained in the next paragraph. (9) The analysis is carried out until the last stage is reached. (10) If there is a change of the link between the deck and the pylon another procedure is carried out. To simulate the change of the conditions an auxiliary model is created where some forces are added depending which relative movement is restricted or not. For example if the vertical movement is not restricted after a certain stage the axial force in the pylon should be continuous. Thus two forces of equal magnitude but opposite direction are added in the pylon and the deck to achieve continuity. This procedure is shown in figure 4.2. (11) The stresses and deformations of the auxiliary model are added to the previous stages (superposition principle).

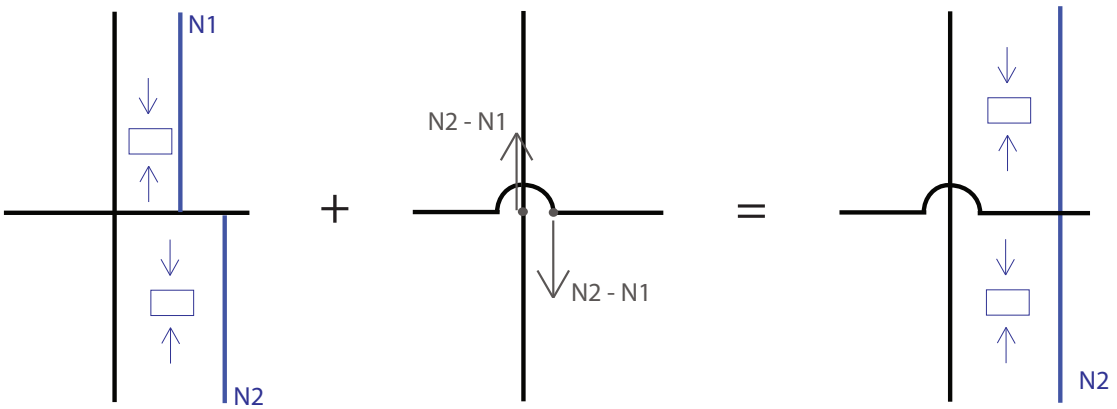

Figure 4.2: Example of simulation when the type of link is changed.

The flow chart of the creep analysis in figure 4.4 is summarized as follows: (12) Creep computation until the final time of the stage is reached. The effects of the creep are calculated taking into account the loads of the actual and previous stages (13). (14,15,16) Depending on which stage the elements were added to the FEM model and the time the load is applied, different times are used to define the loading time and the age of the concrete of the different elements. (17) The imposed strains and curvatures are calculated considering the actual and the previous stages. (18) Then the different strains and curvatures obtained are summed and added to an auxiliary model (19) to obtain additional stresses which are added to the previous stage (20) (superposition principle). Finally the same procedure is carried out for the next interval of time.

More details of the analysis of creep is given in section 3.1.

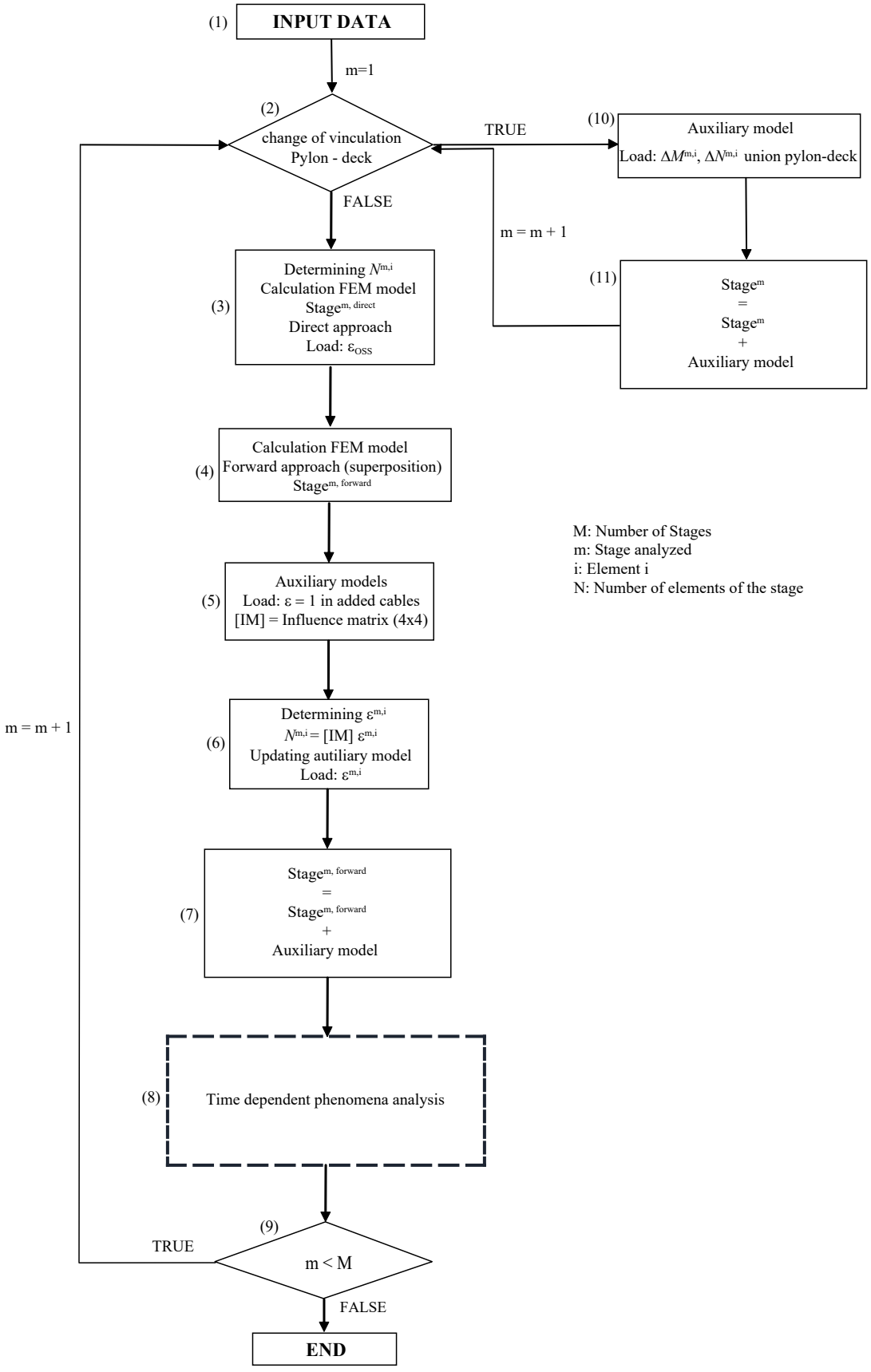

Figure 4.3: Flow chart of the constructive process.

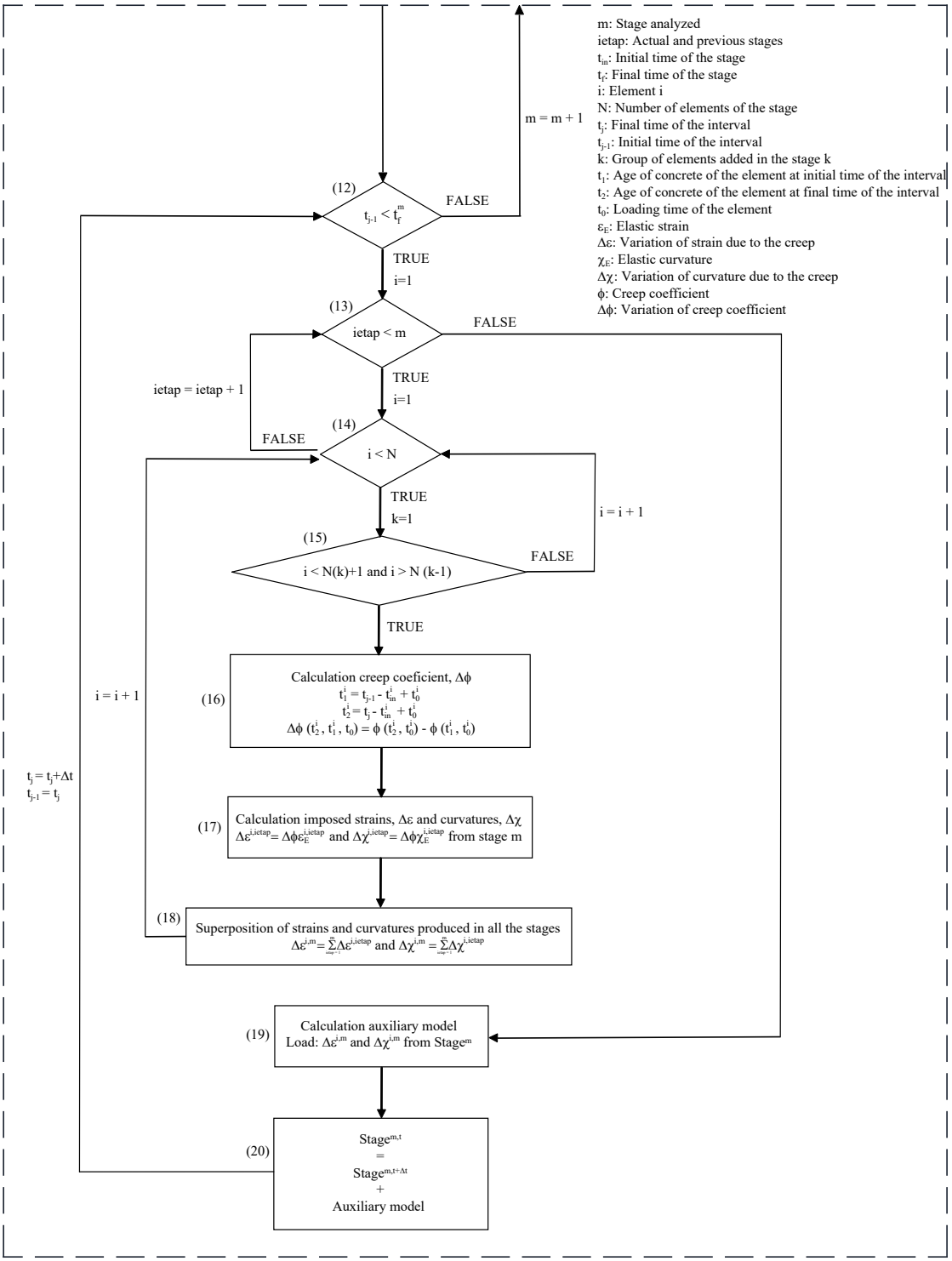

Figure 4.4: Flow chart of creep calculation in different stages.

4.3 OSS with time dependent phenomena

In this section two methods are presented in order to reach the Objective Service Stage at a certain time, t_T, taking creep into account. The constructive process and the creep are considered to define the tensioning process.

Method 1

The first method consists in an iterative process which is shown in equations 4.3.1 and 4.3.2. Using a first approximation of imposed deformations in each cable at the moment they are installed, the cable forces are obtained at time t_T as presented in figure 4.5. Once it is computed another set of imposed deformations using the equations presented below are applied. The process is carried out until the error is lower than a certain tolerance.

$$\{\epsilon^{i+1}\} = \{\epsilon^{i}\} + \left\{\frac{\Delta N^{i,t_T}}{EA}\right\} \tag{4.3.1}$$

$$\{\Delta N^{i,t_T}\} = \{N^{OSS}\} - \{N^{i,t_T}\} \tag{4.3.2}$$

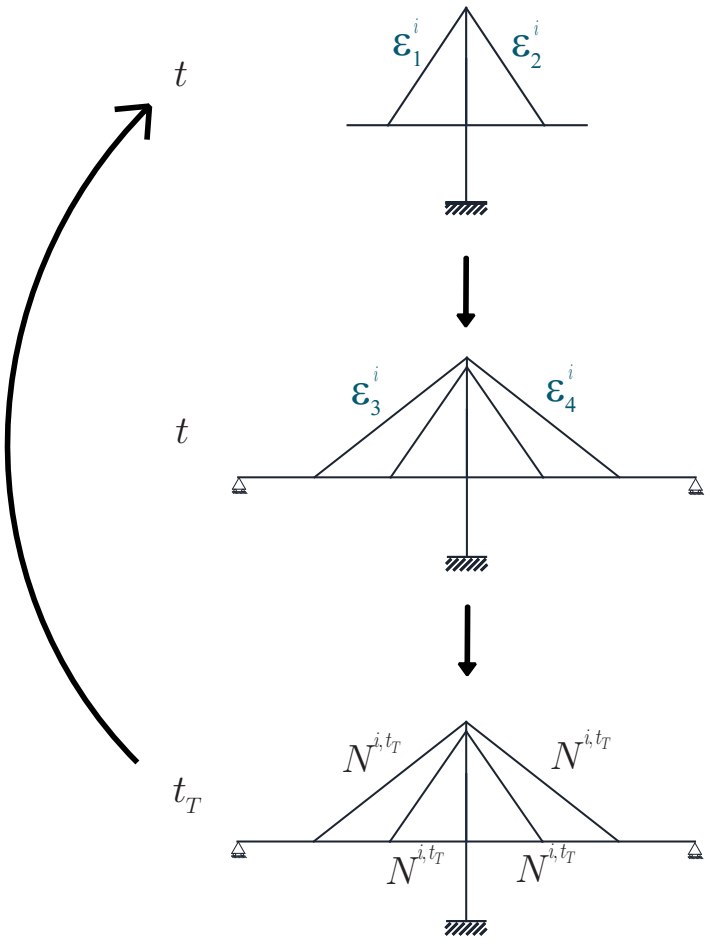

Figure 4.5: Method 1. Iterations

The error can be computed as it is stated in equation 4.3.3. The criterion is that the sum of the relative errors in all stay forces have to be equal or lower than the tolerance.

$$\sum_{I=1}^{N} \frac{N_j^{OSS} - N_j^{i,t_T}}{N_j^{OSS}} \leq Tolerance \tag{4.3.3}$$

To define the OSS forces the Rigidly Continuous Beam Criterion is used. It means that the bridge at time t_T is assumed to have the same bending moment distribution as the equivalent fictitious continuous beam where the stays are substituted by bearings. For the anchorage cables the horizontal component of the anchorage cable has to be equal to the horizontal force of the cable at the other side which supports the main span.

The imposed deformations obtained without taking the creep into account can be used as a first approximation in the iterative process. The method has been explained previously in section 4.1.

Method 2

A direct method to achieve the OSS is presented in equation 4.3.4. As stated in section 4.1 the stay forces have two components: passive and active forces. The active forces can be decomposed in a product of an influence matrix, $\{\Delta N^{t_T}\}$, and a vector of imposed deformations, $\{\epsilon^t\}$.

$\{N^{OSS,t_T}\}$ contains the OSS cable forces which are calculated with the same criteria as in method 1. $\{N^{g,t_T}\}$ is a vector which contains the stay forces due to the permanent loads after applying the time-dependent phenomena until time t_T. $[\Delta N^{t_T}]$ is the influence matrix of increments of stay forces, when an unitary strain is introduced in each stay, during the construction process and applying the time dependent phenomena until time t_T is reached. $\{\epsilon^t\}$ represents the strains to be introduced in each stay at the time they are installed. The strains simulate the pretension forces.

$$\{N^{OSS,t_T}\} = \{N^{g,t_T}\} + [\Delta N^{t_T}]\{\epsilon^t\} \tag{4.3.4}$$

Equation 4.3.4 is developed in equation 4.3.5. The subindices in vectors $\{N^{OSS,t_T}\}$, $\{N^{g,t_T}\}$ say the number stay which corresponds the force. The subindex in the vector $\{\epsilon^t\}$ say in which stay is applied the imposed deformation. The superindex in vector $\{N^{OSS,t_T}\}$ means that the force of the OSS is reached at time t_T. The superindex in vector $\{N^{g,t_T}\}$ means that the force is obtained due to the permanent loads, g, at time t_T.

The influence matrix $[\Delta N^{t_T}]$ gathers the variation of cable forces until t_T is reached when an unitary deformation is applied in each cable when it is installed. The constructive process and the creep effects are simulated. The procedure is shown in figure 4.6. The subindex $\epsilon_N^{t_N}, N$ indicates in which cable and the time the unitary deformation is applied. The number, N, next to it, shows the cable where the vari-

ation of force is obtained at time t_T.

$$\begin{Bmatrix} N_1^{OSS,t_T} \\ N_2^{OSS,t_T} \\ \vdots \\ N_N^{OSS,t_T} \end{Bmatrix} = \begin{Bmatrix} N_1^{g,t_T} \\ N_2^{g,t_T} \\ \vdots \\ N_N^{g,t_T} \end{Bmatrix} + \begin{bmatrix} \Delta N^{t_T}_{\varepsilon_1^{t_1},1} & \Delta N^{t_T}_{\varepsilon_2^{t_2},1} & \dots & \Delta N^{t_T}_{\varepsilon_N^{t_N},1} \\ \Delta N^{t_T}_{\varepsilon_1^{t_1},2} & \Delta N^{t_T}_{\varepsilon_2^{t_2},2} & \dots & \Delta N^{t_T}_{\varepsilon_N^{t_N},2} \\ \dots & \dots & \dots & \dots \\ \Delta N^{t_T}_{\epsilon_1^{t_1},N} & \Delta N^{t_T}_{\epsilon_2^{t_2},N} & \dots & \Delta N^{t_T}_{\epsilon_N^{t_N},N} \end{bmatrix} \begin{Bmatrix} \varepsilon_1^{t_1} \\ \varepsilon_2^{t_2} \\ \vdots \\ \varepsilon_N^{t_N} \end{Bmatrix} \tag{4.3.5}$$

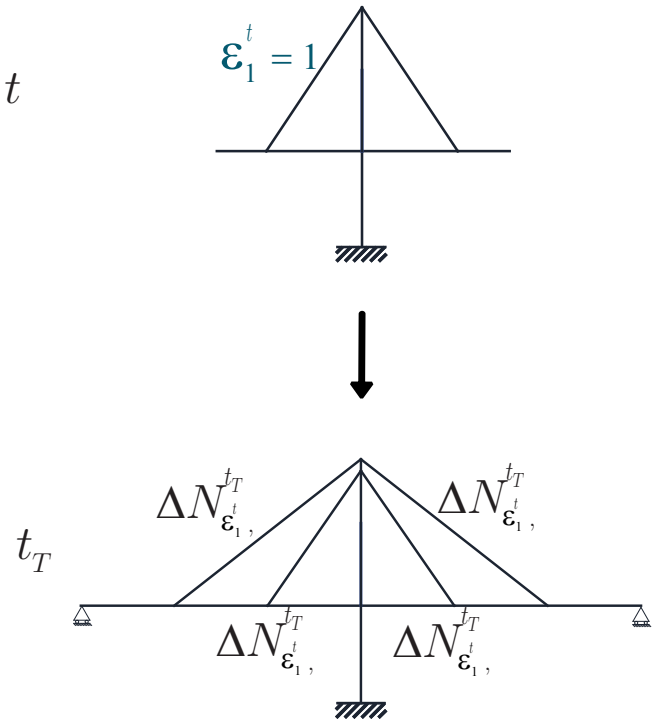

Figure 4.6: Obtaining of the influence matrix.

The system stated in equation 4.3.5 has to be solved where $\{\epsilon^t\}$ is the vector of unknowns. The vector is obtained using the inverse of the influence matrix and solving equation 4.3.6.

$$\{\varepsilon^t\} = [\Delta N^{t_T}]^{-1}(\{N^{OSS,t_T}\} - \{N^{g,t_T}\}) \tag{4.3.6}$$

Chapter 5

Application to a full scale FEM model

The new OSS criteria and the algorithm to take into account the time dependent phenomena effects have been implemented in two different structures.

The results of the definition of the new OSS are presented for this cases. Then the deformations, which simulate the pretension in cables, are applied in the simulation of the constructive process to check if the OSS is achieved taking and not taking into account the time dependent phenomena.

The response of the structure during the constructive is analyzed and the differences between considering creep effects in concrete are studied.

5.1 Characteristics

The full scale model consists in a three span symmetric cable-stayed bridge adapted from one model used in Carrillo Thesis [7]. That model was taken from a bridge project for a 2 lanes road that belongs to the Giribaile Dam project developed in 1990 by the Ministry of Public Works of Spain. The original structure consisted in a two span bridge (91 m + 85 m) with a central pylon.

The main span has a length of 182 m while the side spans are 55 m long as it can be seen in figure 5.1. The stay cables are located every 10 m in the deck having a central girder element of 12 m. A modified fan system is used regarding the location of the cables in the pylon. The shortest cable is situated in the pylon at 28.75 m from the girder and the longest one at 39.9 m. The separation of the cables in the pylon varies between 1.25 m and 1.65 m.

The stays are located in two planes. A total number of 36 cables are used in each plane where 10 of these stay cables are anchorage cables.

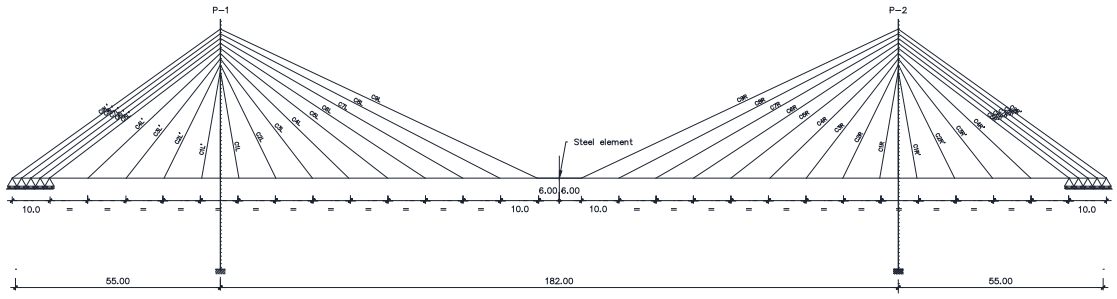

Figure 5.1: Longitudinal scheme of the full scale model (units in m).

The girder is made of cast in place concrete having the cross section showed in figure 5.2 with 13.8 m of width and 0.9 m of edge height at the sides and 1.05 at the center. There is also 11 lightening blocks of 0.65 m of diameter.

The pylons have a variable H section with 64 m of height in total and 42.5 m of height with respect to the deck.

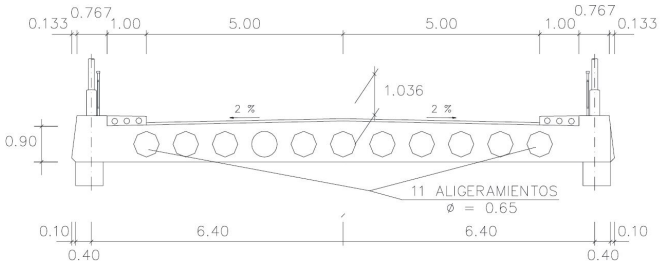

Figure 5.2: Concrete girder section of the full scale model [7].

The relative vertical and horizontal displacements and the relative rotation between the pylon and the girder are restricted during the construction process. However, in service the relative vertical movement and rotation are permitted.

For the end of the side spans and for the anchorage stays the horizontal displacement and the rotation are permitted and only the vertical displacement is restricted.

It is also important to state that in the midspan the girder elements after the cantilever process are joined with a steel element. This element has not axial stiffness and it has the same bending stiffness as the girder. Since it is a steel element the time dependent phenomena effects do not take place.

The sagging effect is not considered in this structure as the cables length is short.

The permanent loads applied consist in the selfweight, g_1, and the non structural dead load, g_2, which are gathered in table 5.1.

Table 5.1: Dead loads implemented in the FEM model

Load	**Value** (kN/m)
g_1	250
g_2	25

Details of the characteristics of the structure introduced in the software are given in Appendix A.

5.2 Constructive process

As follows the constructive process for the full scale FEM model is described. In figure 5.4 some of the stages are represented considering superposition of stages principle:

- First of all the two pylons of the bridge are erected and the first deck elements are built using a falsework. Once the concrete has enough resistance two pairs of cables are installed and pretensioned. This is considered as the first stage in the simulation.
- At stage 2 the derrick cranes and formworks are positioned which are modeled as a punctual force and an applied moment as it can be seen in figure 5.3. In figure 5.4 the derrick cranes are represented with forces in color blue and the forces produced by the fresh concrete, in grey.

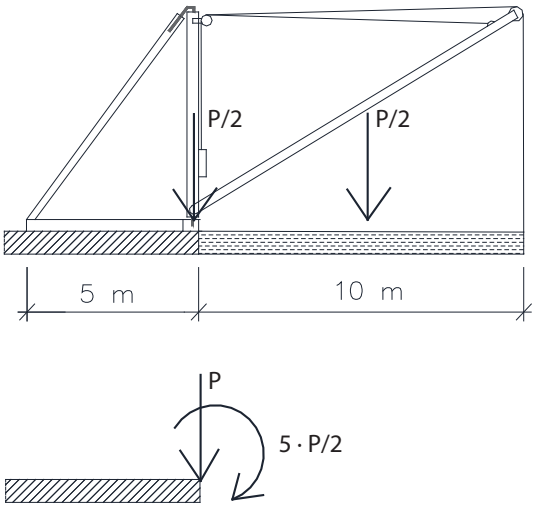

Figure 5.3: Forces representing the derrick cranes.

Table 5.2: Forces that simulate the derrick cranes and the weight of the fresh concrete.

Load	**P** (kN)	**M** (kNm)
New segment concrete	2500	6250
Derrick crane	1250	3125

The weight of the derrick cranes have been considered as 50% of the total weight of the concrete segments. This value is extracted from the recommendations given in section 2.1.3 and in table 2.1.

- At stage 3, once the concrete has enough resistance, the new segments are added to the model and two more pair of cables are installed and pretensioned. The forces representing the fresh concrete are deleted by applying forces in the opposite direction of the ones in the previous stage.
- At stage 4 the derrick cranes are moved to the new location and new loads are added to simulate the fresh concrete used to erect the following deck elements. For the next stages the same procedure explained in stage 3 and 4 is carried out until stage 10.
- At stage 10 the link between the deck and the pylon is changed. The relative vertical movement and the rotation between the two parts are set free and only the horizontal movement remains restricted. Then the structure is connected to the support and the anchorage cable is stressed again (stage 11).
- At the next stages the same procedure explained before is carried out in the main span whereas in the side spans the anchorage cables are installed.
- At stage 19 the last elements of the deck are added and the derrick cranes are removed from the FEM model.
- Finally at stage 20 the steel midspan element is installed and the dead load g_2 is applied in the model.

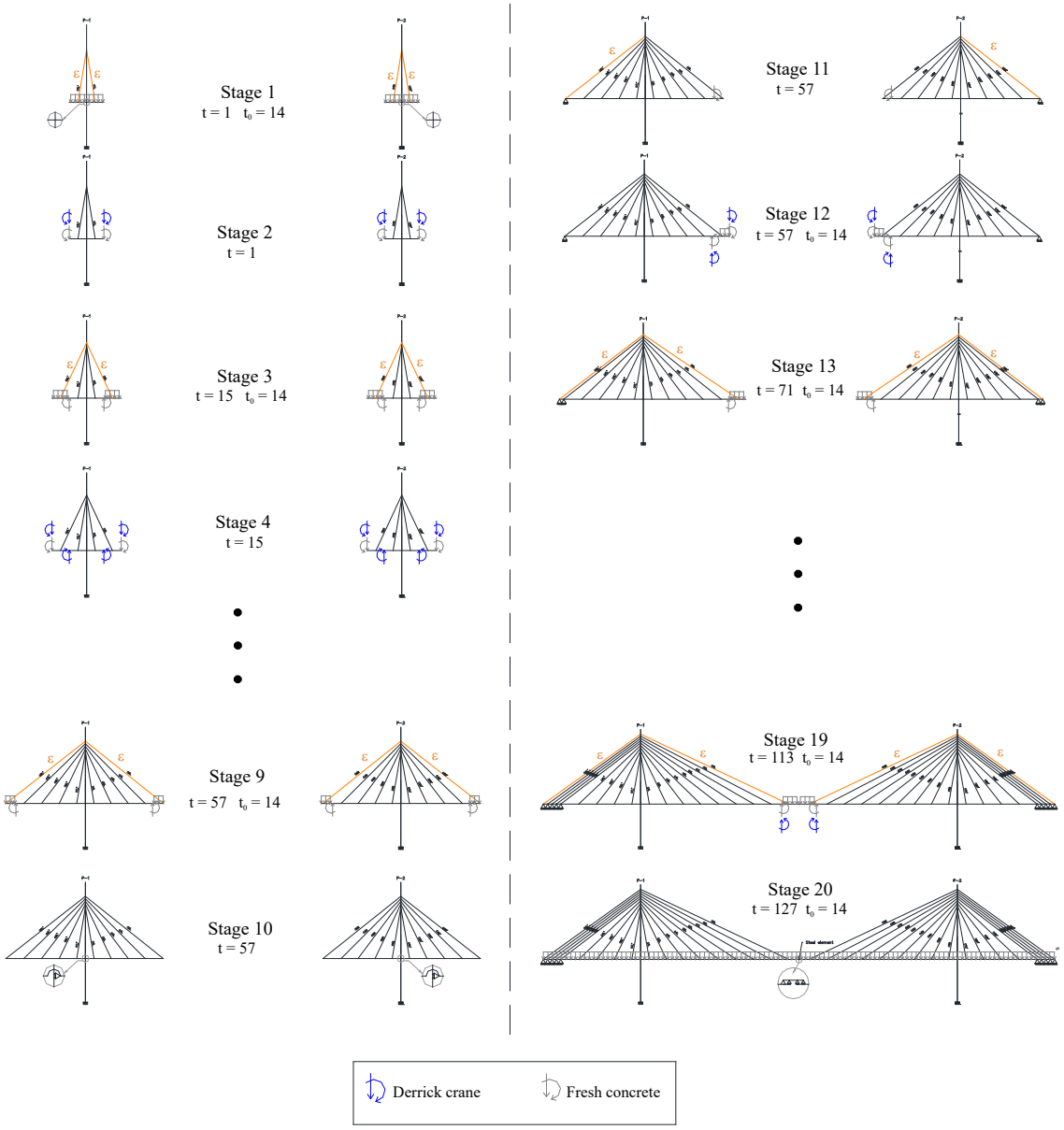

Figure 5.4: Constructive process of the full scale FEM model.

5.3 Definition of the OSS (not creep)

To define the Objective Service Stage the procedure explained in section 4.1 is applied in the full scale FEM model. In this structure the conditions are applied in three states as it can be seen in figure 5.5. The first one is when side spans reach the supports and 10 cables are installed in each pylon.

The second one is at the end of the construction of the structure when the the two parts of the main span are joined with a steel element. Then the conditions derived from the continuous beam criterion are applied in the third state when the load g_2 is applied.

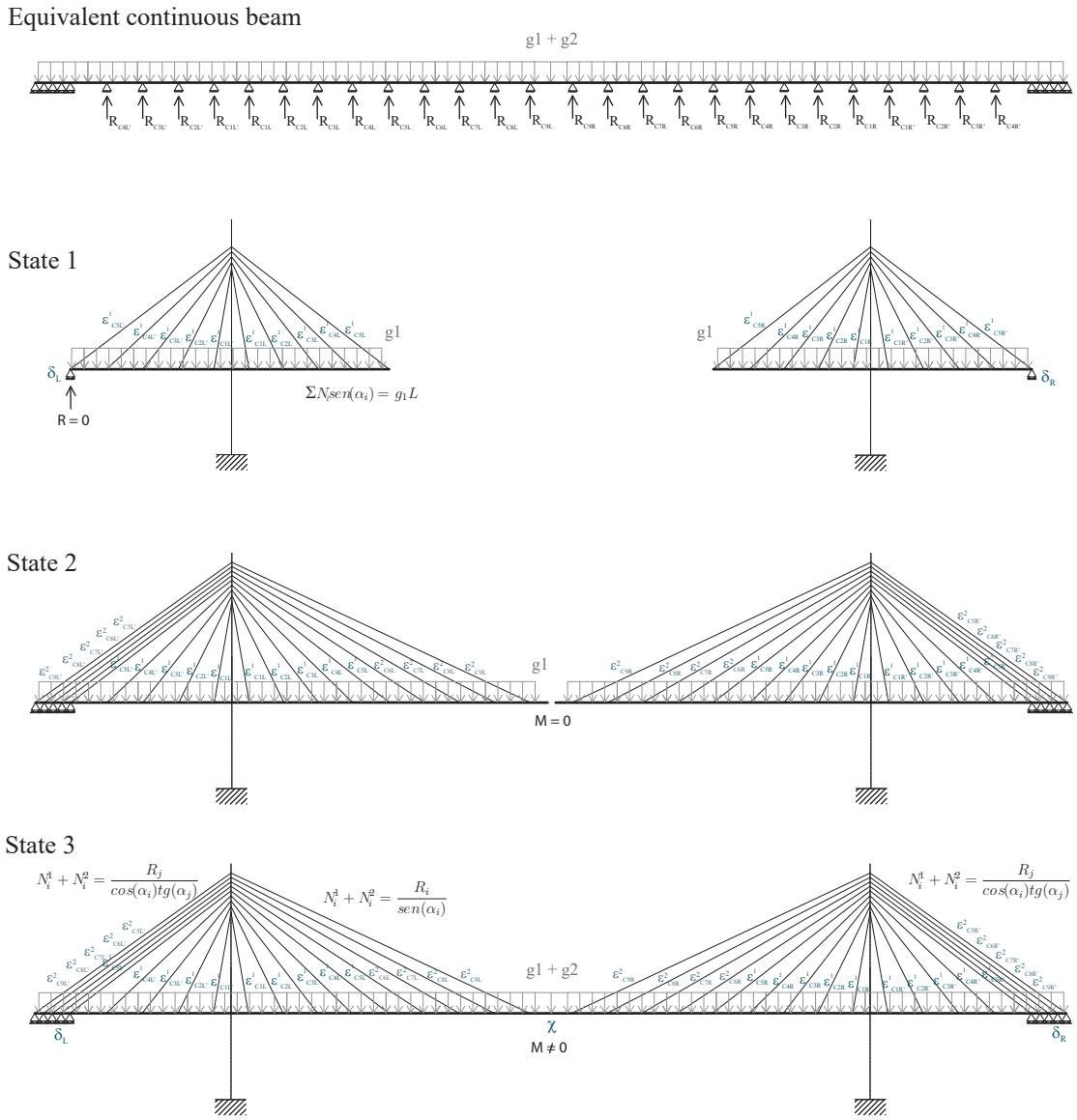

Figure 5.5: Conditions and unknowns do define the Objective Service Stage.

5.4 Results

Objective Service Stage

Considering the conditions defined in the previous chapter to achieve the OSS the following deformations, displacements and curvature are obtained in order to be introduced in the FEM model.

Table 5.3: Imposed strains, curvature and displacements to define the OSS.

Unknowns	Value
$\epsilon_{CL9'}$	-0.003490156
$\epsilon_{CL8'}$	-0.002196448
$\epsilon_{CL7'}$	-0.002521731
$\epsilon_{CL6'}$	-0.002262757
$\epsilon^1_{CL5'}$	-0.001429372
$\epsilon^2_{CL5'}$	-0.000691253
$\epsilon_{CL4'}$	-0.002114775
$\epsilon_{CL3'}$	-0.002134962
$\epsilon_{CL2'}$	-0.002317887
$\epsilon_{CL1'}$	-0.003213759
ϵ_{CL1}	-0.003473044
ϵ_{CL2}	-0.002918332
ϵ_{CL3}	-0.002873425
ϵ_{CL4}	-0.002816828
ϵ_{CL5}	-0.002834663
ϵ_{CL6}	-0.002822878
ϵ_{CL7}	-0.002959507
ϵ_{CL8}	-0.002588434
ϵ_{CL9}	-0.003694295
d_L	1.94023E-06 m
χ	0.011076787 $\frac{1}{m}$

All the deformations are negative, thus pretension is needed in all the cables. All the values of the predeformations are close to the value $\epsilon = -0.003$, which is generally a typical value for cable-stayed bridges according to SETRA [15].

The deformations obtained previously are applied in the simulation of the constructive process, which is automatized in the developed algorithm. Some results are presented showing maximum and minimum values reached during construction. Furthermore there is a comparison between taking and not taking into account the creep effects.

Bending moments in the deck

Figures 5.6 and 5.7 show the maximum and minimum values of the bending moment in the deck that are reached during the construction process. It can also be seen the moments at the final stage. In figure 5.6 the creep is not taking into account whereas in figure 5.7 it is. Finally in figure 5.8 the effect of the creep along time can be seen. The end of construction and the situation in 1000 days and 10000 days is showed. Furthermore, the differences between considering and not considering the creep are represented.

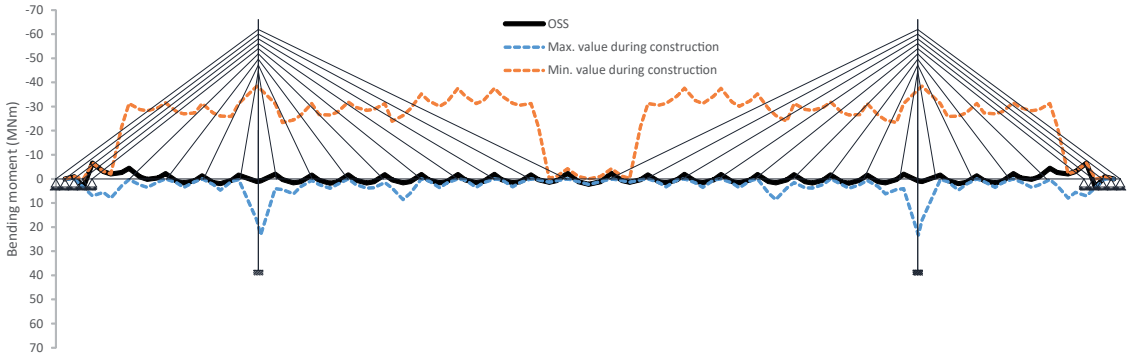

Figure 5.6: Bending moments in the deck not taking the creep into account.

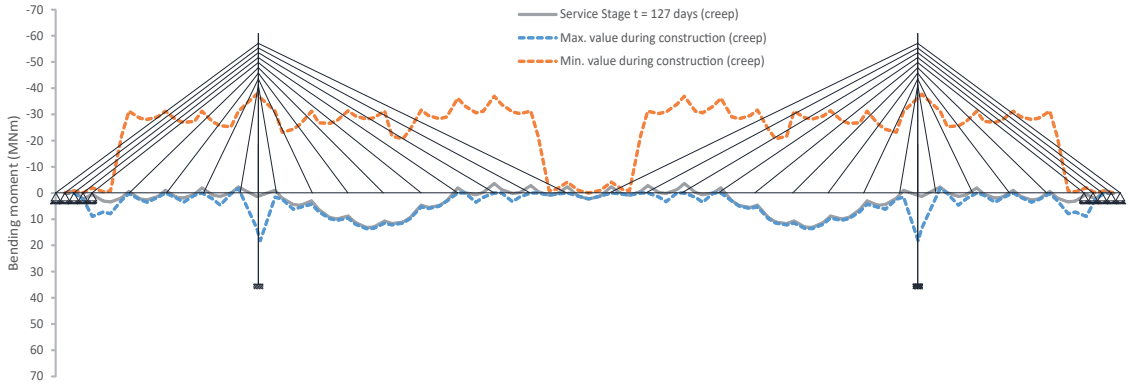

Figure 5.7: Bending moments in the deck taking the creep into account during construction.

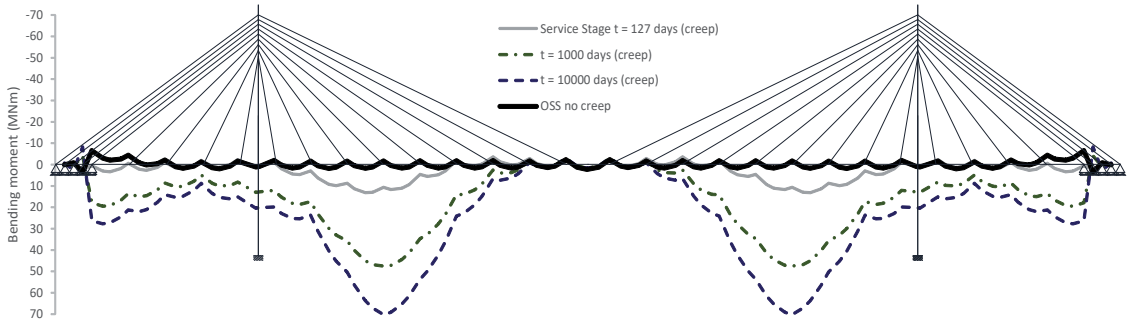

Figure 5.8: Comparison of bending moments in the deck taking and not taking the creep into account.

From the results of the bending moments some conclusions can be stated:

- When creep is not computed the OSS defined in terms of bending moments is achieved whereas when the creep is considered the final stage does not correspond with the OSS.
- The bending moments at time = 10000 days are much bigger than not considering creep. The creep has a great importance in CIP concrete bridges, specially in cable-stayed bridges built by cantilever method. Using this construction method the new segments of concrete are loaded at early ages due to the derrick cranes that are used to install the following segments.
- During the construction the maximum (positive) and minimum moments (negative moments) reached are similar for both cases (creep and not creep). The final stage has bending moments inferior than the bending moments obtained during the construction process.
- The minimum moments (negative) are reached when the derrick cranes, carrying the fresh concrete and the formworks, are installed. The load of the derrick cranes acts only in one segment so in every stage there is a peak of bending moment in that section. The simulation of the weight of the derrick crane is explained in section 5.2.
- The maximum (positive) moment of the deck is located at the the union between the deck and the pylon at the stage before the link between the two parts is changed.

Axial forces in the stays

Figure 5.9 shows the stay forces not taking creep into account at the final stage and during construction. Figure 5.10 shows the stay forces taking creep into account. The response in 1000 days and 10000 days is also represented. Moreover in figure 5.11 there is a comparison of both cases at time 10000 days. The evolution of the

axial forces in three cables is shown in figures 5.12 and 5.13.

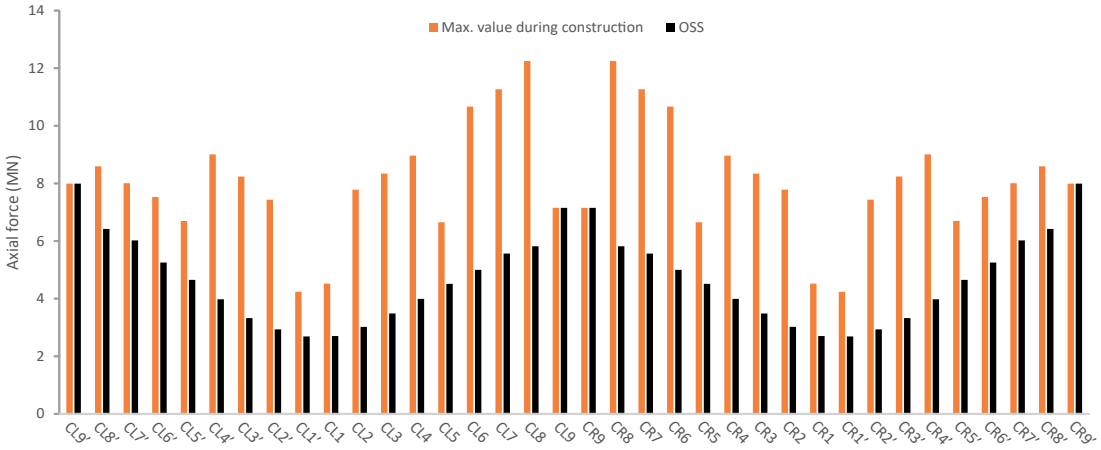

Figure 5.9: Stay forces not taking the creep into account.

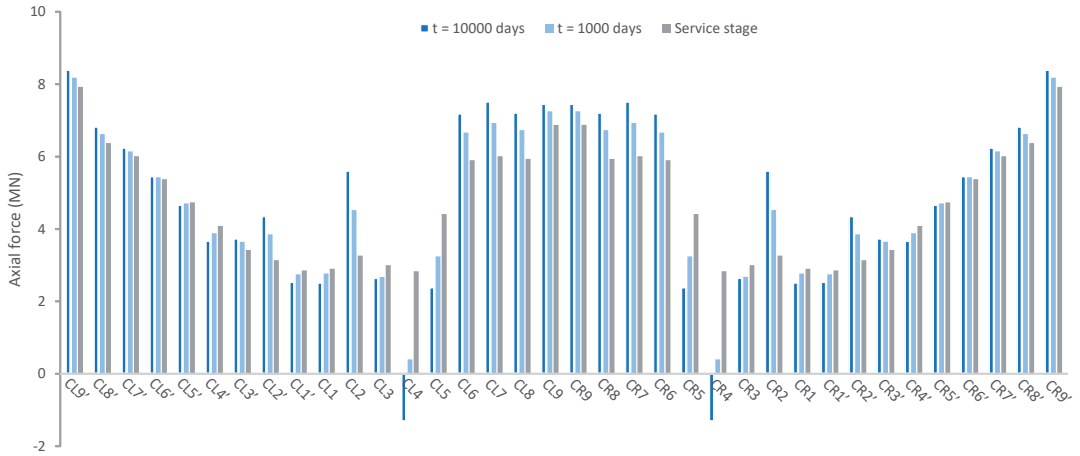

Figure 5.10: Stay forces taking the creep into account.

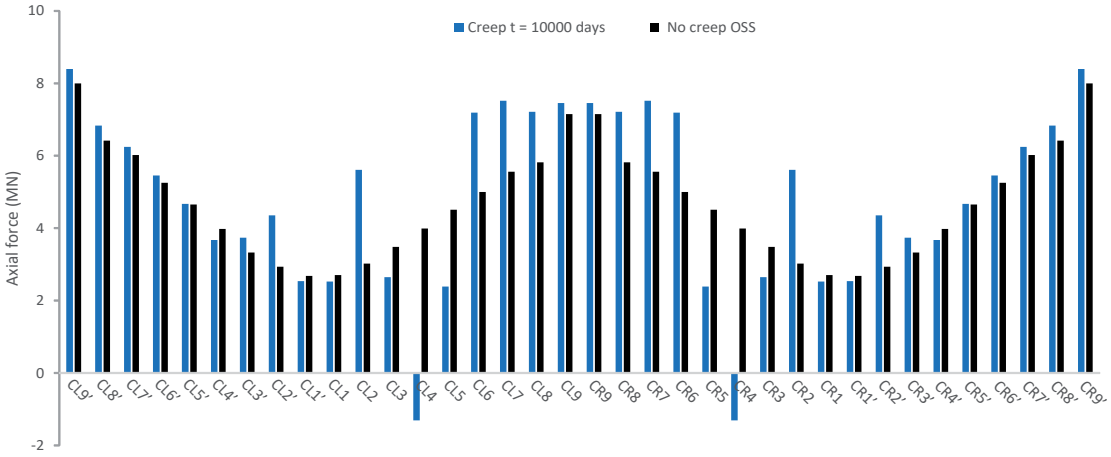

Figure 5.11: Comparison of the stay forces taking and not taking the creep into account.

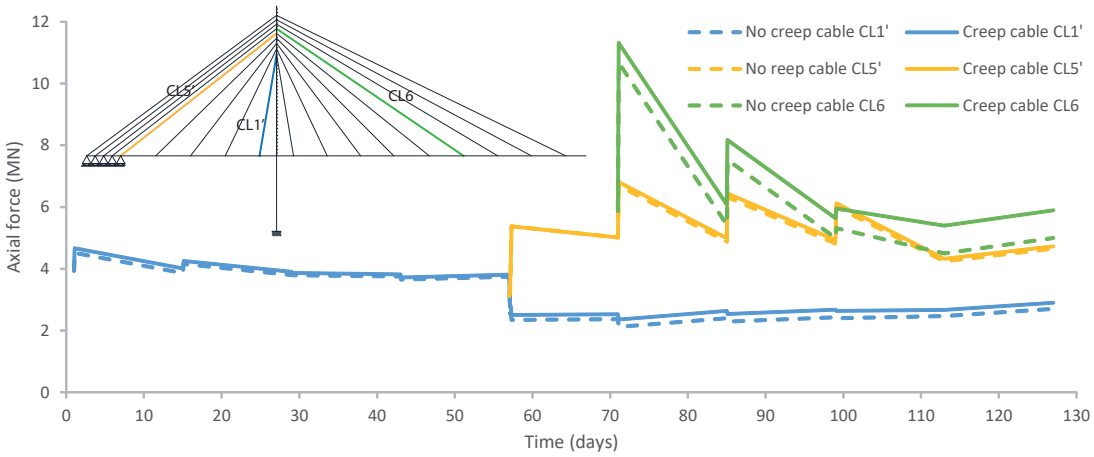

Figure 5.12: Evolution of the axial forces in three cables considering and not considering creep during construction.

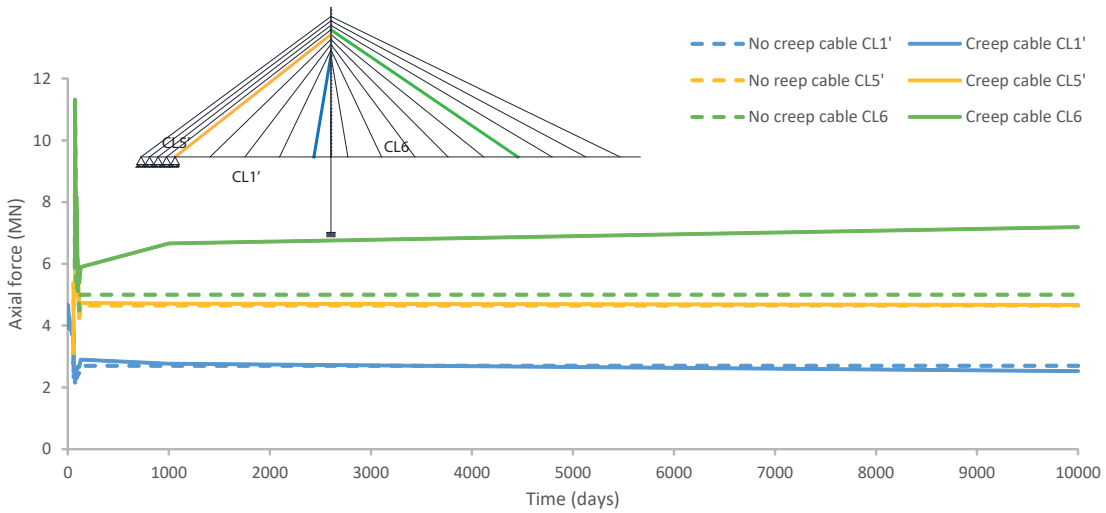

Figure 5.13: Evolution of the axial forces in three cables considering and not considering creep along time.

From the results of the stay forces some conclusions can be stated:

- When creep is not computed the OSS defined in terms of axial forces is achieved whereas when the creep is considered the final stage does not correspond with the OSS.
- The axial forces in the cables during construction are greater than in the final stage. The major differences are produced near the midspan when the derrick cranes are installing the last segments. The smaller differences are produced near the pylons and the side supports.
- It can be observed that the axial forces grow as we get further from the pylons. This is because the inclination of the cables. As a certain vertical reaction is needed to satisfy the OSS conditions, due to the larger inclination and less efficiency of this cables the force needed is greater.
- From figure 5.10 and 5.11 it is observed that the behaviour of the cables along time depends of the position. The axial force along time due to the creep increase in those cables situated in midspan and lesser in the cables situated at the side spans. At 10000 days after the construction there is the case of two cables which would be in compression under permanent loads. Since the cable elements have been modelled as truss elements compression appears, which is not possible in cables. In reality the cable loses its functionality and the forces are redistributed to the rest of the structure. In a commercial software the cable elements should be modelled as elements which can not be in compression.
- If creep is not considered all the cables remain in tension. To have all the cables in tension is one of the main reasons of the necessity of defining a new OSS taking into account time dependent phenomena.

Bending moments in the pylon

As follows the behaviour of the left pylon is studied. It is assumed that the behaviour is the same as the right pylon since the structure is symmetric. Figure 5.14 shows the bending moment of the pylon not taking creep into account at the final stage and during construction. The same is showed in figure 5.15 but considering creep. Finally in figure 5.16 there is a comparison at time 10000 days taking and not taking creep into accound.

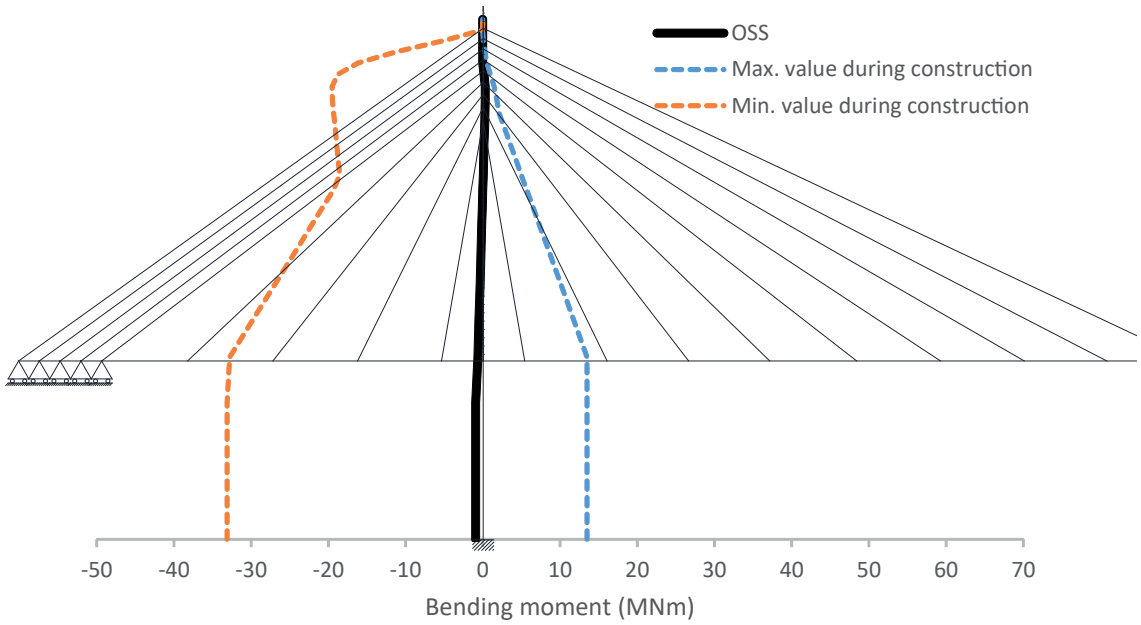

Figure 5.14: Bending moments in the pylon not taking the creep into account.

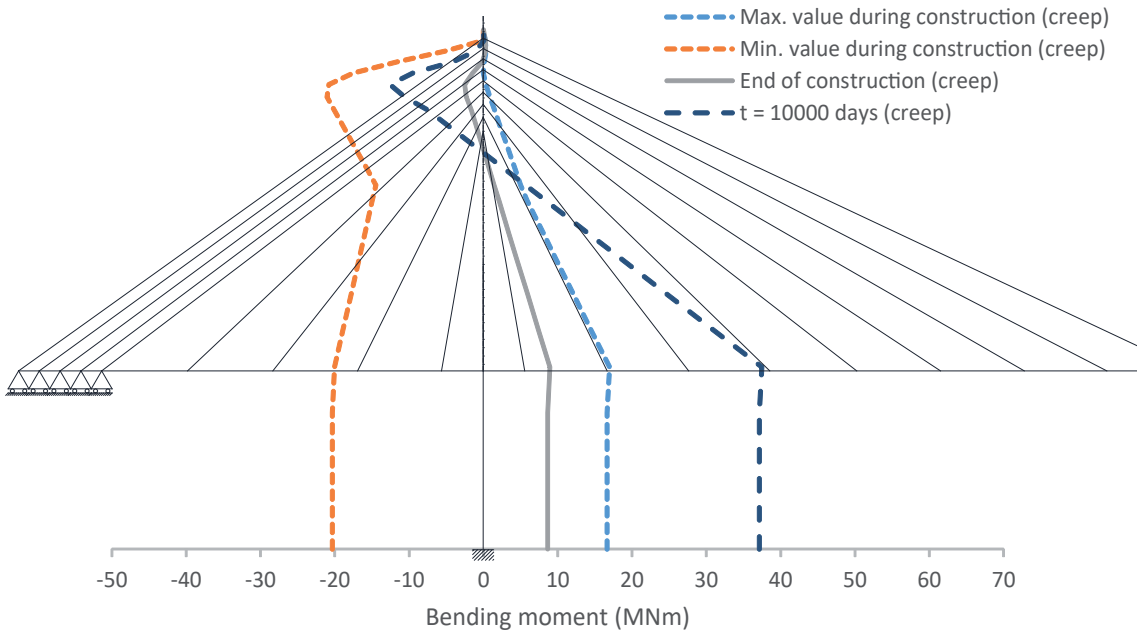

Figure 5.15: Bending moments in the pylon taking the creep into account.

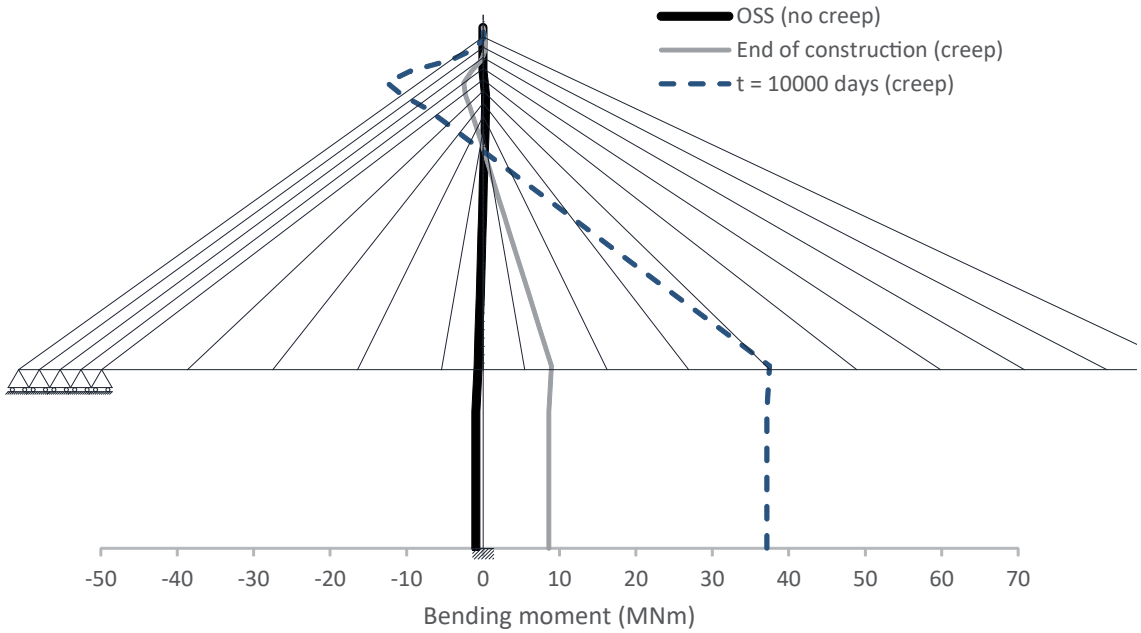

Figure 5.16: Comparison of bending moments in the pylon taking and not taking the creep into account.

From the results of the bending moments in the pylon some conclusions can be stated:

- When creep is not computed the OSS defined is achieved whereas when the creep is considered the final stage does not correspond with the OSS.

- From figure 5.14 it can be seen that the OSS is achieved because the bending moment of the pylon is close to zero at the final stage. The maximum moments are achieved during the construction due to the asymmetric geometry of the bridge while the different elements are installed.
- If creep is considered the maximum bending moment is reached during service. The bending moment after 10000 days is greater than the maximum during construction.
- The creep is an important issue during construction. As we can see in figure 5.16 the OSS is not achieved when creep is considered even at the end of the construction.

Displacements

The displacements in the deck and the pylon have also been studied. Figure 5.17 show the displacements in the deck. The displacements of the left pylon are showed in figure 5.18 and in figure 5.19. The maximum displacements during cosntruction and the final displacements after 10000 days have been analyzed taking and not taking the creep into account.

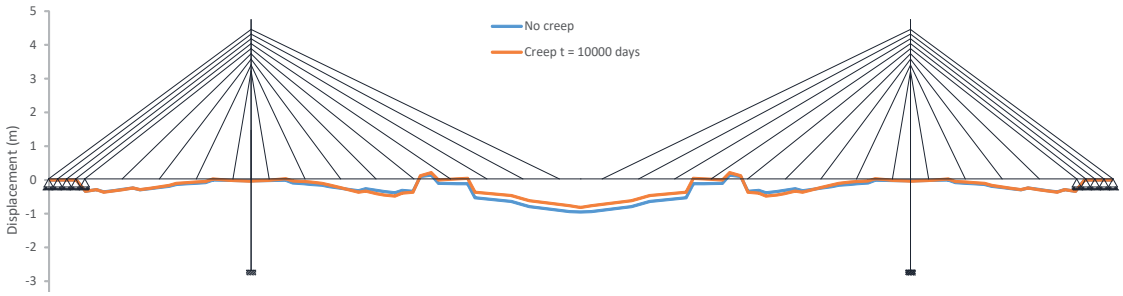

Figure 5.17: Displacements in the deck .

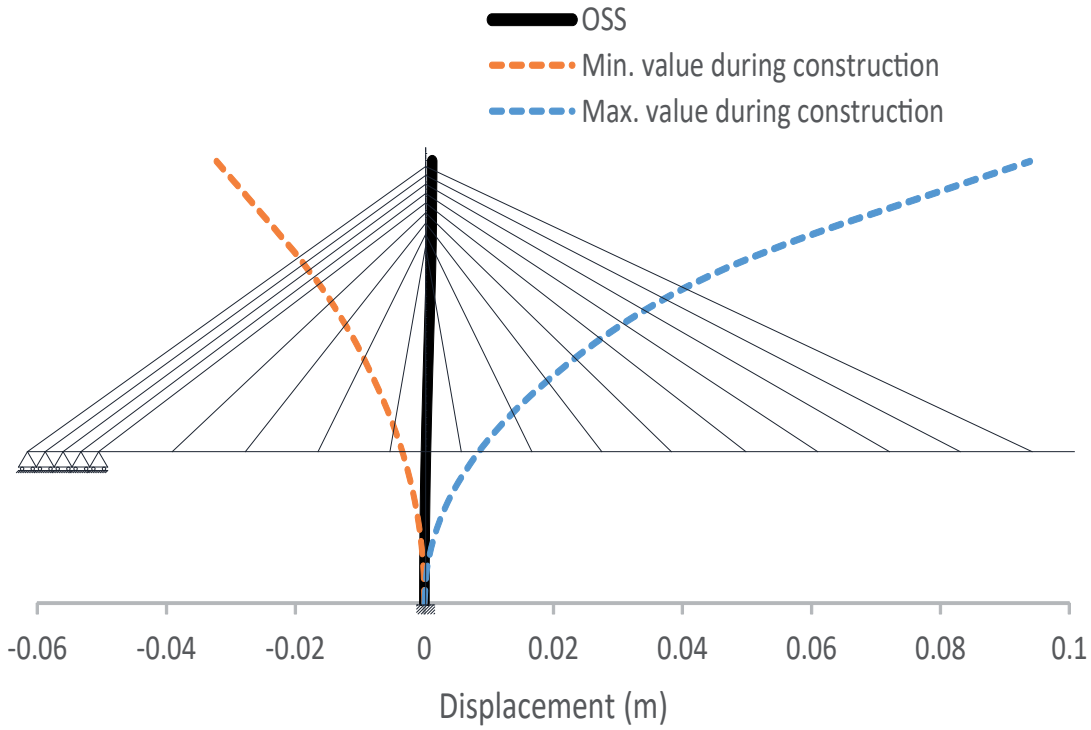

Figure 5.18: Displacements in the pylon not taking the creep into account.

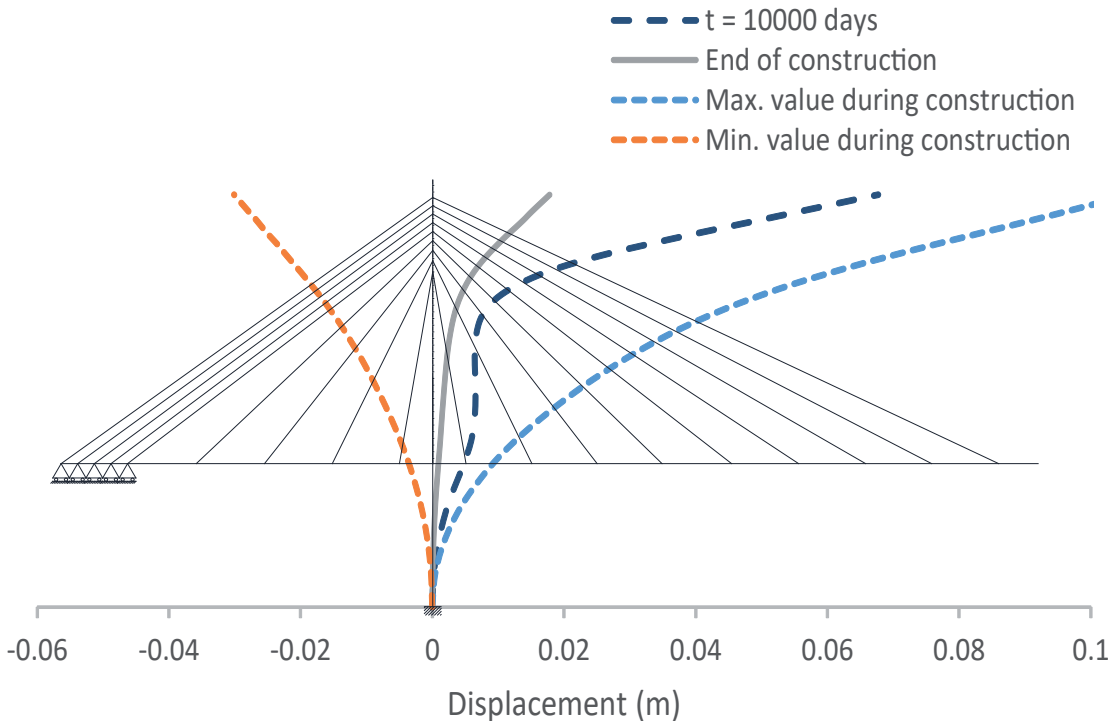

Figure 5.19: Displacements in the pylon taking the creep into account.

From the results of the displacements in the pylon and the deck some conclusions can be stated:

- The deformation of the deck changes when creep is considered. In some parts the deflection increases whereas in other parts it decreases.
- The displacement at the top of the pylon is almost zero when creep is not considered. Thus in this case the OSS is achieved.
- When the creep is considered the OSS is not achieved neither in the end of construction nor after 10000 days.
- The maximum displacements in both cases are maximum during construction. The magnitude of the displacements are very similar if we compare creep case and case without creep.

5.5 Addition of creep effects into the OSS

The two methods explained in section 4.3 have been used in the Full scale FEM model. Using method 1 the solution doesn't converge and the tolerance is never reached for t=10000 days. Using method 2 the OSS is achieved for any time is considered. The results of the OSS using this last method are presented as follows.

Figures 5.20 and 5.21 show the maximum and minimum bending moments when the OSS is considered at 1000 days and 10000 days. Table 5.4 and 5.5 show the imposed deformations to simulate the cable pretension needed to achieve the OSS.

Table 5.4: Imposed strains, curvature and displacements to define the OSS at 1000 days taking creep into account.

Unknowns	**Value**
$\epsilon_{CL9'}$	-0.00417076
$\epsilon_{CL8'}$	-0.003028413
$\epsilon_{CL7'}$	-0.003584821
$\epsilon_{CL6'}$	-0.002862064
$\epsilon_{CL5'}$	-0.005803647
$\epsilon_{CL4'}$	-0.006275327
$\epsilon_{CL3'}$	-0.000987528
$\epsilon_{CL2'}$	0.002822134
$\epsilon_{CL1'}$	-0.010622865
ϵ_{CL1}	-0.012668212
ϵ_{CL2}	0.002094359
ϵ_{CL3}	0.000263863
ϵ_{CL4}	-0.004564257
ϵ_{CL5}	-0.002854083
ϵ_{CL6}	0.000361604
ϵ_{CL7}	-0.003596138
ϵ_{CL8}	-0.00427291
ϵ_{CL9}	-0.005846693

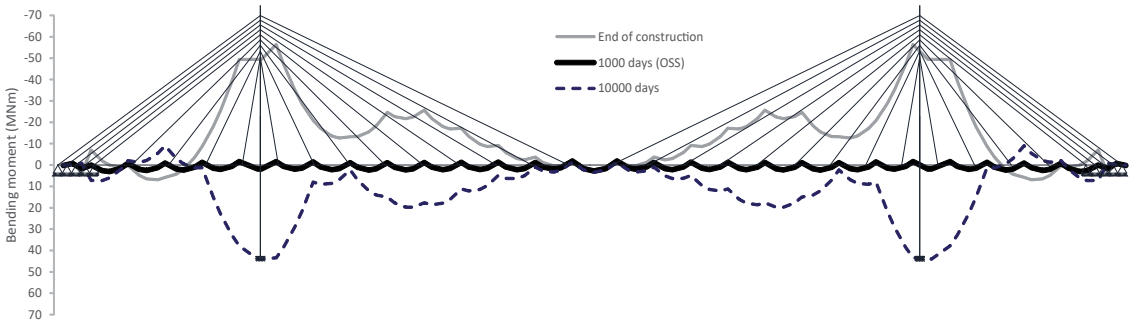

Figure 5.20: Bending moments at the deck. OSS achieved in 1000 days.

Table 5.5: Imposed strains, curvature and displacements to define the OSS at 10000 days taking creep into account.

Unknowns	**Value**
$\epsilon_{CL9'}$	-0.00427688
$\epsilon_{CL8'}$	-0.00319819
$\epsilon_{CL7'}$	-0.00384191
$\epsilon_{CL6'}$	-0.00326587
$\epsilon_{CL5'}$	-0.00689558
$\epsilon_{CL4'}$	-0.00734925
$\epsilon_{CL3'}$	0.00304189
$\epsilon_{CL2'}$	0.01135504
$\epsilon_{CL1'}$	-0.01420603
ϵ_{CL1}	-0.01612295
ϵ_{CL2}	0.01169332
ϵ_{CL3}	0.00389857
ϵ_{CL4}	-0.00585366
ϵ_{CL5}	-0.00185879
ϵ_{CL6}	0.00319817
ϵ_{CL7}	-0.00127618
ϵ_{CL8}	-0.00282698
ϵ_{CL9}	-0.00520745

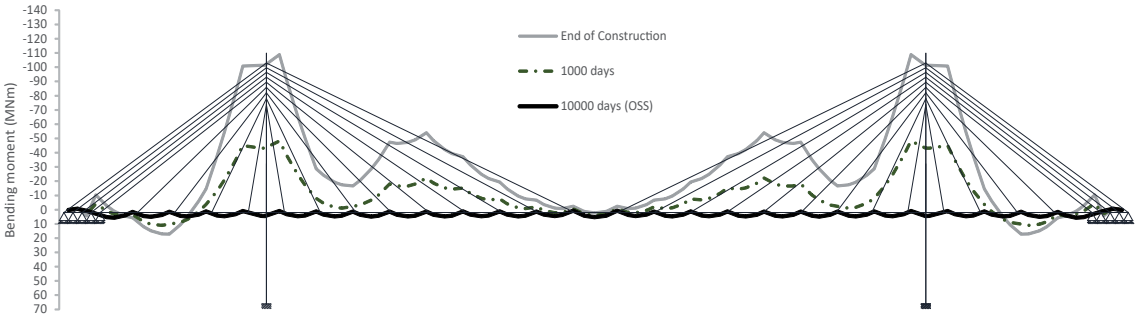

Figure 5.21: Bending moments at the deck. OSS achieved in 10000 days.

The bending moments at the end of construction are extremely high specially when OSS is considered at 10000 days. In addition the imposed deformations, some of them positive, needed to achieve the OSS put some cables in compression during the constructive process and at the end of the construction as it can be seen in figures 5.22 and 5.23. As the cables can not be in compression, this elements would loose their functionality.

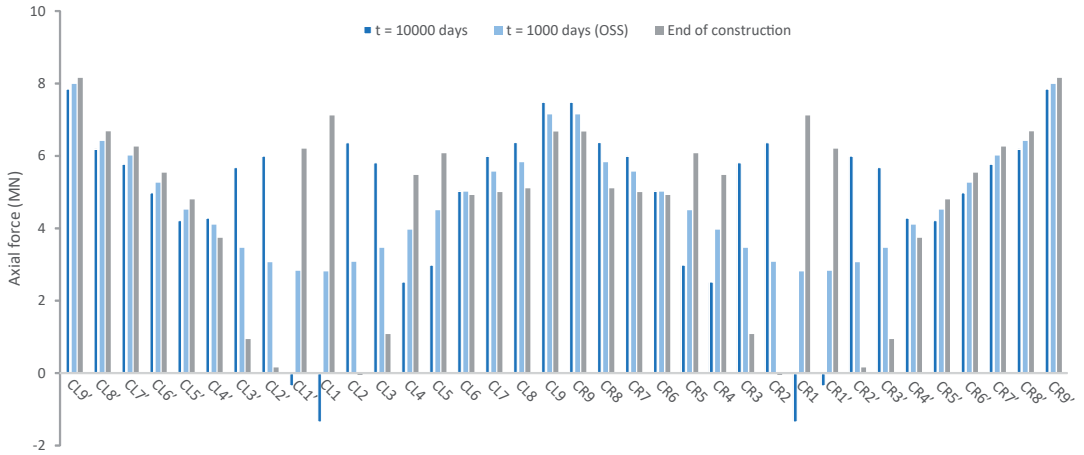

Figure 5.22: Stay forces. OSS achieved in 1000 days.

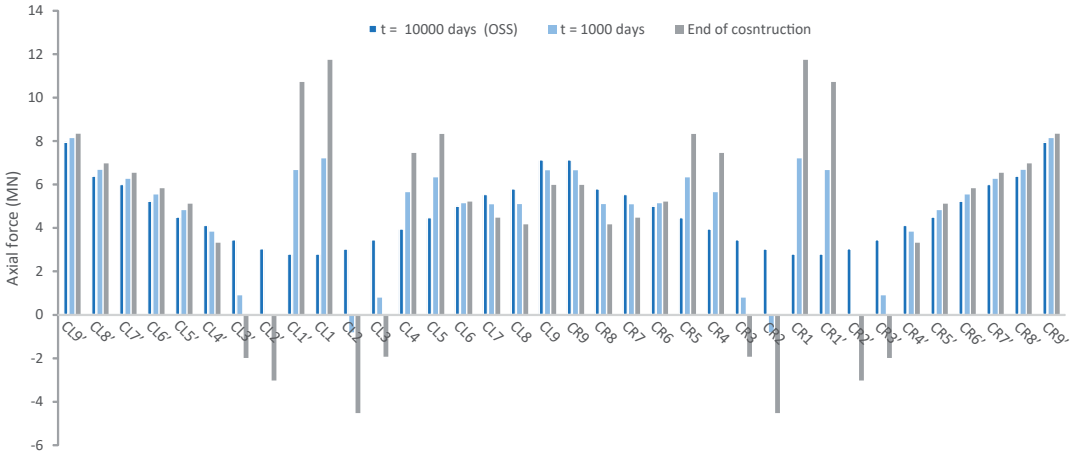

Figure 5.23: Stay forces. OSS achieved in 10000 days.

For this structure built by cantilever method the OSS can not be achieved at 1000 days and 10000 days with only one pretension operation as some cables would not be in tension during early ages. Since the cable elements have been modelled as truss elements compression appears, which is not possible in cables. In reality the cable loses its functionality and the forces are redistributed to the rest of the structure. It can be observed that the cables closer to the pylon suffer a huge variation of axial force along time whereas the cables located further from the pylon have little force differences.

Due to the impossibility to achieve the OSS with only one pretension operation, another structure has been tested from the original model to implement the method to define the OSS at 10000 days taking creep into account. In this another model the link between the deck and the pylon is changed. All the relative movements are restricted. To increase the efficiency of the stay system the cables next to the pylon are removed.

In table 5.6 the imposed deformations are gathered. Figure 5.24 shows the maximum and minimum bending moments during the construction, at the end of construction and at 10000 days. In addition figures 5.25 and 5.26 show the axial forces, figure 5.27 shows the bending moments at the pylon and figure shows the deformation of the deck at different times and their maximum and minimum values during construction.

Table 5.6: Imposed strains, curvature and displacements to define the OSS at 10000 days taking creep into account for the modified structure.

Unknowns	**Value**
$\epsilon_{CL9'}$	-0.00406131
$\epsilon_{CL8'}$	-0.00284838
$\epsilon_{CL7'}$	-0.00329715
$\epsilon_{CL6'}$	-0.0024093
$\epsilon_{CL5'}$	-0.00514856
$\epsilon_{CL4'}$	-0.00642744
$\epsilon_{CL3'}$	-0.00645146
$\epsilon_{CL2'}$	-0.00606112
$\epsilon_{CL1'}$	-
ϵ_{CL1}	-
ϵ_{CL2}	-0.00691009
ϵ_{CL3}	-0.0072685
ϵ_{CL4}	-0.00661205
ϵ_{CL5}	-0.0060911
ϵ_{CL6}	-0.00313948
ϵ_{CL7}	-0.00583516
ϵ_{CL8}	-0.00543598
ϵ_{CL9}	-0.00628451

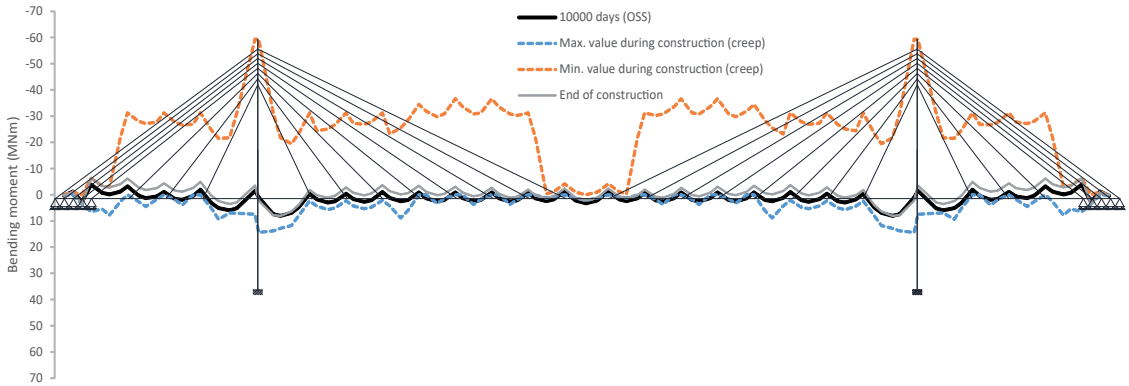

Figure 5.24: Bending moments at the deck. OSS achieved in 10000 days. Modified structure.

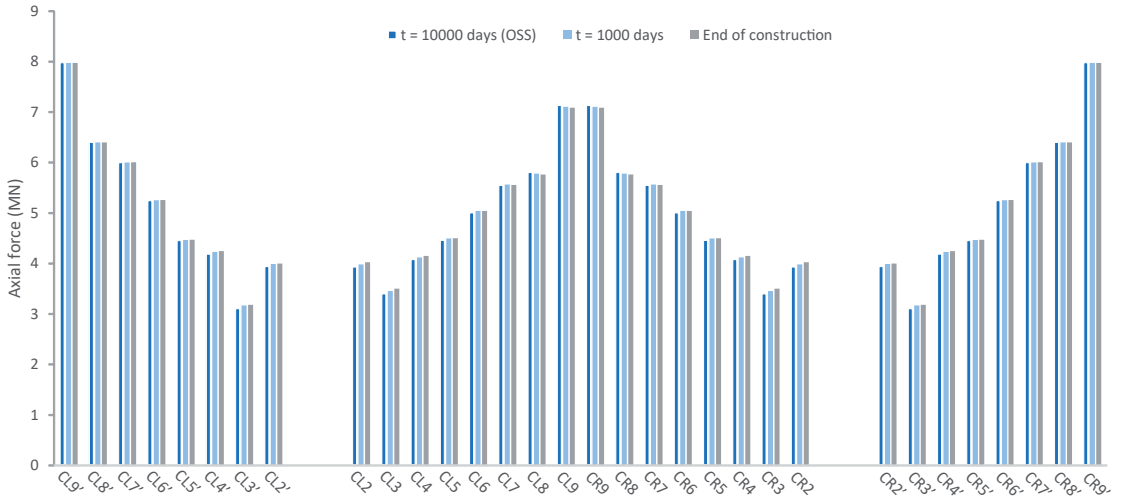

Figure 5.25: Stay forces at the end of cosntruction, at 1000 days and at 10000 days. OSS achieved in 10000 days. Modified structure.

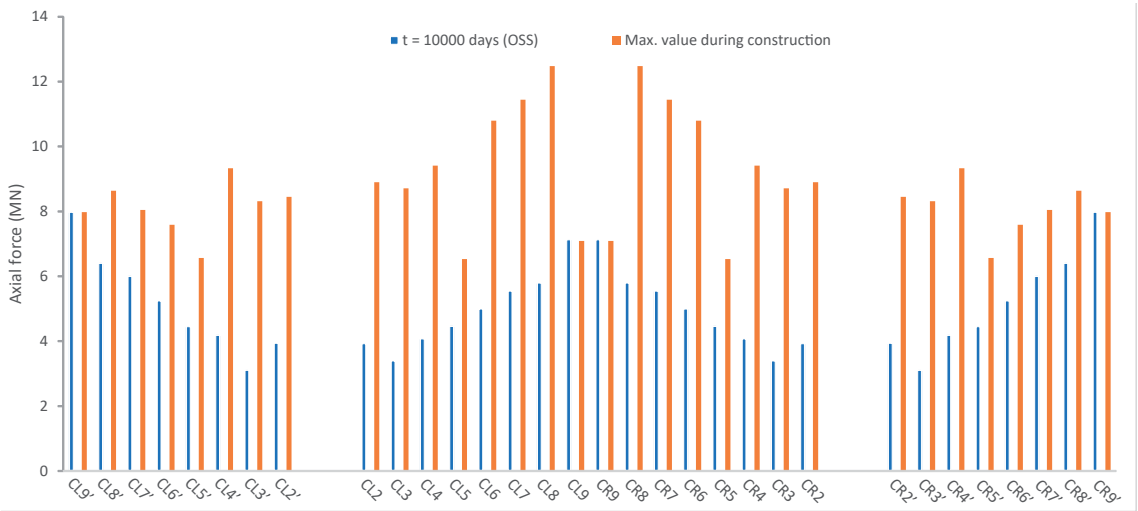

Figure 5.26: Maximum stay forces and stay forces at 10000 days. OSS achieved in 10000 days. Modified structure.

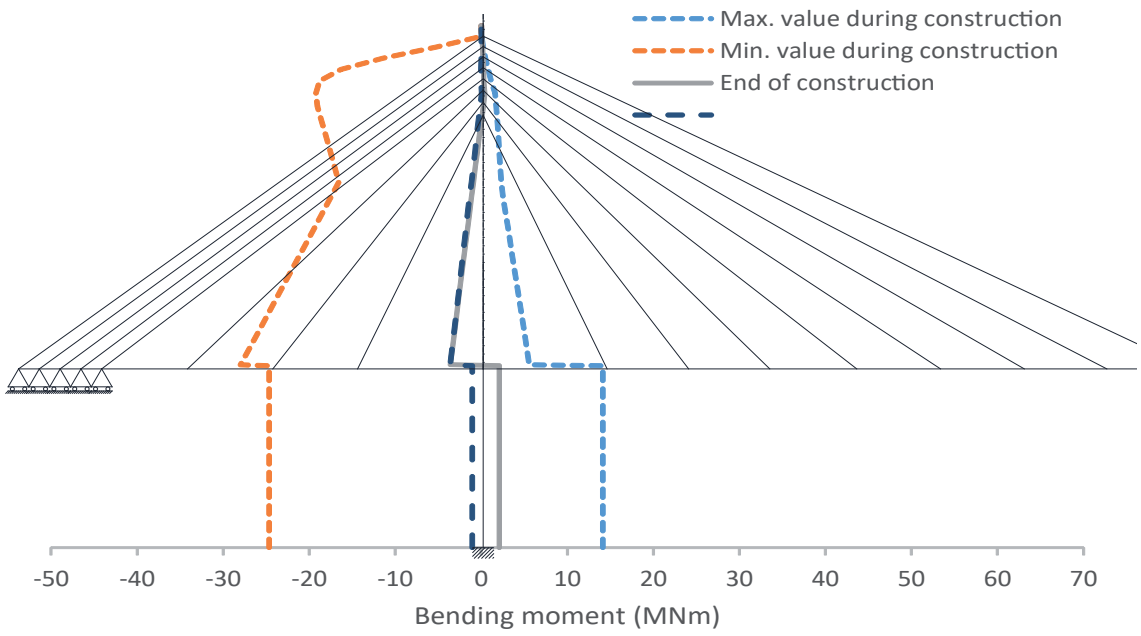

Figure 5.27: Bending moments at the pylon. OSS achieved in 10000 days. Modified structure.

From the results of the bending moments in the deck and pylon and the axial forces in cables some conclusions can be stated:

- The OSS at 10000 days is achieved with only one pretension operation using the imposed deformations of table 5.6. As we can see in the figures above the bridge has the behaviour of the equivalent continuous beam at time 10000 days. The distribution of bending moments along the deck is equal to the distribution that a continuous beam would have. Furthermore the bending moments at the pylons are close to zero when the OSS is achieved.

- The bending moments at the deck due to the creep are significantly lower in the modified structure (figure 5.24) than in the original (figure 5.21). The greater stiffness of the structural system during construction decreases the creep effects.

- The extreme values regarding the bending moments at the deck and pylon, and the axial stay forces are reached during the construction due to the derrick cranes and the greater flexibility of the structure while it is not completed as we can see in figures 5.24, 5.26 and 5.27. The axial forces during construction have twice the value of when the structure is finished. From the end of construction to 10000 days there are variations of the axial force from 0 % to 5 % in the stays. This difference is very small compared with the previous structure.

Chapter 6

Conclusions

6.1 Conclusions

In this thesis, two new criteria to define the Objective Service Stage have been presented for cable-stayed bridges constructed using the cantilever erection method. In these criteria, some conditions during construction, which have not been defined previously in the literature, have been considered. By including the construction process in the definition of the OSS, only one tensioning operation is necessary in each stay. As a result, the retensioning operations which usually are carried out are no longer needed in some cases and the cost of the structure is much cheaper.

Furthermore, an algorithm which takes the creep into account throughout the construction process and improves the Dischinger Hyphotesis has been validated with several patch tests.

The first new criteria which does not consider creep to define the OSS and the validated developed algorithm is applied in an adaptation of a real structure. As it can be seen in the results of the implementation on a full scale FEM model, the final objectives and the conditions imposed during the construction process are fulfilled when creep is not considered. An overall iterative process is not needed.

However, in CIP concrete bridges where the time dependent phenomena have great importance, the OSS is not achieved; as such, the criteria to define the OSS should consider not only the construction process but also the time dependent effects.

From the results of the study case, it can be concluded that the positive moments along the deck are increased significantly when creep is analyzed. In most cables, specifically those situated far from the pylon, the axial force is greater when creep is considered, however in certain cables, the axial force decreases. As a result, a retensioning process will be required at a certain point in the structure's lifetime to account for these differences caused by the creep.

Consequently, a new method has been proposed to achieve the OSS at a certain time. Unlike the previous method, the constructive process and creep effects are necessary

to be simulated. As regards the FEM model used the OSS can not be achieved with only one tensioning operation as some cables would be not be in tension during the construction so a retensioning operation would be advisable after the completion of the structure. The same structure with a rigid link between the pylon and the deck has been analyzed. Due to its greater stiffness during the construction the OSS is achieved at 10000 days taking creep and the constructive process into account with only one tensioning operation.

6.2 Future research

The two definitions of OSS presented for cable-stayed bridges allow to carry out only one tensioning operation. But, as it can be seen, when creep is considered the OSS is not achieved for some types of CIP concrete bridges. For this reason it would be recommendable to do further investigation on which types of bridges need more than one tensioning operation along their life span. Some ideas are given to improve the procedure to define the OSS and to improve the algorithm. There are also recommendations of which cases are suitable to be studied:

- Studying the shrinkage effects in concrete bridges built using the cantilever erection method.
- Definition of an OSS taking other time dependent phenomena into account such shrinkage or temperature changes for concrete bridges built using the cantilever erection method.
- Studying the effects of other phenomena, such as the sagging effect, in a full scale FEM model with longer spans and cables where these effects have greater importance.
- Implementing the simulation in other typologies of bridges, such as bridges with composite steel-concrete decks, bridges built with prefabricated concrete segments or extradosed bridges, which combine the characteristics of a pretensioned box girder bridge and a cable-stayed bridge.

Appendix A

FEM models characteristics

Table A.1: Node coordinates of the simple structure

Node	**X**	**Y**	**Node**	**X**	**Y**	**Node**	**X**	**Y**
1	-40.000	0.000	41	-44.000	10.000	81	-18.000	10.000
2	-40.000	2.000	42	-46.000	10.000	82	-16.000	10.000
3	-40.000	4.000	43	-48.000	10.000	83	-14.000	10.000
4	-40.000	6.000	44	-50.000	10.000	84	-12.000	10.000
5	-40.000	8.000	45	-52.000	10.000	85	-10.000	10.000
6	-40.000	10.000	46	-54.000	10.000	86	-8.000	10.000
7	-40.000	13.000	47	-56.000	10.000	87	-6.000	10.000
8	-40.000	16.000	48	-58.000	10.000	88	-4.000	10.000
9	-40.000	19.000	49	-60.000	10.000	89	-2.000	10.000
10	-40.000	22.000	50	40.001	10.000	90	-0.200	10.000
11	-40.000	25.000	51	38.000	10.000	91	18.000	10.000
12	-40.000	26.000	52	36.000	10.000	92	16.000	10.000
13	-40.000	27.000	53	34.000	10.000	93	14.000	10.000
14	-40.000	27.500	54	32.000	10.000	94	12.000	10.000
15	40.000	0.000	55	30.000	10.000	95	10.000	10.000
16	40.000	2.000	56	28.000	10.000	96	8.000	10.000
17	40.000	4.000	57	26.000	10.000	97	6.000	10.000
18	40.000	6.000	58	24.000	10.000	98	4.000	10.000
19	40.000	8.000	59	22.000	10.000	99	2.000	10.000
20	40.000	10.000	60	20.000	10.000	100	0.200	10.000
21	40.000	13.000	61	42.000	10.000			
22	40.000	16.000	62	44.000	10.000			
23	40.000	19.000	63	46.000	10.000			
24	40.000	22.000	64	48.000	10.000			
25	40.000	25.000	65	50.000	10.000			
26	40.000	26.000	66	52.000	10.000			
27	40.000	27.000	67	54.000	10.000			
28	40.000	27.500	68	56.000	10.000			
29	-40.001	10.000	69	58.000	10.000			
30	-38.000	10.000	70	60.000	10.000			
31	-36.000	10.000	71	-62.000	10.000			
32	-34.000	10.000	72	-64.000	10.000			
33	-32.000	10.000	73	-66.000	10.000			
34	-30.000	10.000	74	-68.000	10.000			
35	-28.000	10.000	75	-70.000	10.000			
36	-26.000	10.000	76	62.000	10.000			
37	-24.000	10.000	77	64.000	10.000			
38	-22.000	10.000	78	66.000	10.000			
39	-20.000	10.000	79	68.000	10.000			
40	-42.000	10.000	80	70.000	10.000			

Table A.2: Elements of the simple structure

El.	**N1**	**N2**	**Mat**	**El.**	**N1**	**N2**	**Mat**	**El.**	**N1**	**N2**	**Mat**
1	1	2	7	41	41	42	1	81	76	77	1
2	2	3	7	42	42	43	1	82	77	78	1
3	3	4	7	43	43	44	1	83	78	79	1
4	4	5	7	44	44	45	1	84	79	80	1
5	5	6	7	45	45	46	1	85	75	14	2
6	6	7	7	46	46	47	1	86	80	28	2
7	7	8	7	47	47	48	1	87	39	81	1
8	8	9	7	48	48	49	1	88	81	82	1
9	9	10	7	49	50	20	5	89	82	83	1
10	10	11	7	50	50	20	3	90	83	84	1
11	11	12	7	51	50	51	1	91	84	85	1
12	12	13	7	52	51	52	1	92	85	86	1
13	13	14	7	53	52	53	1	93	86	87	1
14	15	16	7	54	53	54	1	94	87	88	1
15	16	17	7	55	54	55	1	95	88	89	1
16	17	18	7	56	55	56	1	96	89	90	1
17	18	19	7	57	56	57	1	97	60	91	1
18	19	20	7	58	57	58	1	98	91	92	1
19	20	21	7	59	58	59	1	99	92	93	1
20	21	22	7	60	59	60	1	100	93	94	1
21	22	23	7	61	50	61	1	101	94	95	1
22	23	24	7	62	61	62	1	102	95	96	1
23	24	25	7	63	62	63	1	103	96	97	1
24	25	26	7	64	63	64	1	104	97	98	1
25	26	27	7	65	64	65	1	105	98	99	1
26	27	28	7	66	65	66	1	106	99	100	1
27	29	6	5	67	66	67	1	107	85	14	2
28	29	6	3	68	67	68	1	108	95	28	2
29	29	30	1	69	68	69	1	109	90	100	6
30	30	31	1	70	69	70	1				
31	31	32	1	71	34	11	2				
32	32	33	1	72	44	11	2				
33	33	34	1	73	55	25	2				
34	34	35	1	74	65	25	2				
35	35	36	1	75	49	71	1				
36	36	37	1	76	71	72	1				
37	37	38	1	77	72	73	1				
38	38	39	1	78	73	74	1				
39	29	40	1	79	74	75	1				
40	40	41	1	80	70	76	1				

Table A.3: Material characteristics of the simple structure

Material	**E** (kN/m^2)	ν	**Area** (m^2)	**Inertia** (m^4)
1	30900000	0.2	9.998	1.053
2	195000000	0.2	0.005942551	0
3	195000000	0.2	0	0
4	195000000	0.2	0	1.053
5	30900000	0.2	9.998	0
6	30900000	0.2	0	1.053
7	30900000	0.2	20	15

Table A.4: Node coordinates of the full scale FEM model

Node	**X**	**Y**	**Node**	**X**	**Y**	**Node**	**X**	**Y**
1	-91.000	0.000	41	91.000	50.250	81	-113.000	21.500
2	-91.000	5.375	42	91.000	51.900	82	-116.000	21.500
3	-91.000	10.750	43	91.000	53.450	83	-118.000	21.500
4	-91.000	16.125	44	91.000	54.900	84	-121.000	21.500
5	-91.000	21.500	45	91.000	56.270	85	-69.000	21.500
6	-91.000	25.800	46	91.000	57.600	86	-66.000	21.500
7	-91.000	30.100	47	91.000	58.900	87	-64.000	21.500
8	-91.000	34.400	48	91.000	60.150	88	-61.000	21.500
9	-91.000	37.300	49	91.000	61.400	89	113.000	21.500
10	-91.000	39.300	50	91.000	64.000	90	116.000	21.500
11	-91.000	41.150	51	-91.001	21.500	91	118.000	21.500
12	-91.000	43.000	52	-96.000	21.500	92	121.000	21.500
13	-91.000	44.850	53	-98.000	21.500	93	69.000	21.500
14	-91.000	46.700	54	-101.000	21.500	94	66.000	21.500
15	-91.000	48.500	55	-86.000	21.500	95	64.000	21.500
16	-91.000	50.250	56	-84.000	21.500	96	61.000	21.500
17	-91.000	51.900	57	-81.000	21.500	97	-123.000	21.500
18	-91.000	53.450	58	91.001	21.500	98	-126.000	21.500
19	-91.000	54.900	59	96.000	21.500	99	-128.000	21.500
20	-91.000	56.270	60	98.000	21.500	100	-131.000	21.500
21	-91.000	57.600	61	101.000	21.500	101	-59.000	21.500
22	-91.000	58.900	62	86.000	21.500	102	-56.000	21.500
23	-91.000	60.150	63	84.000	21.500	103	-54.000	21.500
24	-91.000	61.400	64	81.000	21.500	104	-51.000	21.500
25	-91.000	64.000	65	-103.000	21.500	105	123.000	21.500
26	91.000	0.000	66	-106.000	21.500	106	126.000	21.500
27	91.000	5.375	67	-108.000	21.500	107	128.000	21.500
28	91.000	10.750	68	-111.000	21.500	108	131.000	21.500
29	91.000	16.125	69	-79.000	21.500	109	59.000	21.500
30	91.000	21.500	70	-76.000	21.500	110	56.000	21.500
31	91.000	25.800	71	-74.000	21.500	111	54.000	21.500

Table A.4: Node coordinates of the full scale FEM model

Node	X	Y	Node	X	Y	Node	X	Y
32	91.000	30.100	72	-71.000	21.500	112	51.000	21.500
33	91.000	34.400	73	103.000	21.500	113	-133.000	21.500
34	91.000	37.300	74	106.000	21.500	114	-136.000	21.500
35	91.000	39.300	75	108.000	21.500	115	-49.000	21.500
36	91.000	41.150	76	111.000	21.500	116	-46.000	21.500
37	91.000	43.000	77	79.000	21.500	117	-44.000	21.500
38	91.000	44.850	78	76.000	21.500	118	-41.000	21.500
39	91.000	46.700	79	74.000	21.500	119	133.000	21.500
40	91.000	48.500	80	71.000	21.500	120	136.000	21.500
121	49.000	21.500	136	-29.000	21.500	151	19.000	21.500
122	46.000	21.500	137	-26.000	21.500	152	16.000	21.500
123	44.000	21.500	138	-24.000	21.500	153	14.000	21.500
124	41.000	21.500	139	-21.000	21.500	154	11.000	21.500
125	-138.500	21.500	140	141.000	21.500	155	-146.000	21.500
126	-39.000	21.500	141	29.000	21.500	156	-9.000	21.500
127	-36.000	21.500	142	26.000	21.500	157	-6.000	21.500
128	-34.000	21.500	143	24.000	21.500	158	-3.000	21.500
129	-31.000	21.500	144	21.000	21.500	159	-0.200	21.500
130	138.500	21.500	145	-143.500	21.500	160	146.000	21.500
131	39.000	21.500	146	-19.000	21.500	161	9.000	21.500
132	36.000	21.500	147	-16.000	21.500	162	6.000	21.500
133	34.000	21.500	148	-14.000	21.500	163	3.000	21.500
134	31.000	21.500	149	-11.000	21.500	164	0.200	21.500
135	-141.000	21.500	150	143.500	21.500			

Table A.5: Elements of the full scale FEM model

El.	N1	N2	Mat	El.	N1	N2	Mat	El.	N1	N2	Mat
1	1	1	2	41	42	43	18	81	64	77	1
2	2	2	3	42	43	44	19	82	77	78	1
3	3	3	4	43	44	45	20	83	78	79	1
4	4	4	5	44	45	46	21	84	79	80	1
5	5	5	6	45	46	47	22	85	66	17	29
6	6	6	7	46	47	48	23	86	70	17	29
7	7	7	8	47	48	49	24	87	74	42	29
8	8	8	9	48	49	50	25	88	78	42	29
9	9	9	10	49	51	5	26	89	68	81	1
10	10	10	11	50	51	5	27	90	81	82	1
11	11	11	12	51	51	52	1	91	82	83	1
12	12	12	13	52	52	53	1	92	83	84	1
13	13	13	14	53	53	54	1	93	72	85	1
14	14	14	15	54	51	55	1	94	85	86	1
15	15	15	16	55	55	56	1	95	86	87	1
16	16	16	17	56	56	57	1	96	87	88	1

Table A.5: Elements of the full scale FEM model

El.	**N1**	**N2**	**Mat**	**El.**	**N1**	**N2**	**Mat**	**El.**	**N1**	**N2**	**Mat**
17	17	17	18	57	58	30	26	97	76	89	1
18	18	18	19	58	58	30	27	98	89	90	1
19	19	19	20	59	58	59	1	99	90	91	1
20	20	20	21	60	59	60	1	100	91	92	1
21	21	21	22	61	60	61	1	101	80	93	1
22	22	22	23	62	58	62	1	102	93	94	1
23	23	23	24	63	62	63	1	103	94	95	1
24	24	24	25	64	63	64	1	104	95	96	1
25	26	26	2	65	52	16	28	105	82	18	30
26	27	27	3	66	55	16	28	106	86	18	30
27	28	28	4	67	59	41	28	107	90	43	30
28	29	29	5	68	62	41	28	108	94	43	30
29	30	30	6	69	54	65	1	109	84	97	1
30	31	31	7	70	65	66	1	110	97	98	1
31	32	32	8	71	66	67	1	111	98	99	1
32	33	33	9	72	67	68	1	112	99	100	1
33	34	34	10	73	57	69	1	113	88	101	1
34	35	35	11	74	69	70	1	114	101	102	1
35	36	36	12	75	70	71	1	115	102	103	1
36	37	37	13	76	71	72	1	116	103	104	1
37	38	38	14	77	61	73	1	117	92	105	1
38	39	39	15	78	73	74	1	118	105	106	1
39	40	40	16	79	74	75	1	119	106	107	1
40	41	41	17	80	75	76	1	120	107	108	1
121	121	109	1	151	124	131	1	181	152	153	1
122	122	110	1	152	131	132	1	182	153	154	1
123	123	111	1	153	132	133	1	183	145	23	35
124	124	112	1	154	133	134	1	184	147	23	35
125	125	19	31	155	125	21	33	185	150	48	35
126	126	19	31	156	127	21	33	186	152	48	35
127	127	44	31	157	130	46	33	187	145	155	1
128	128	44	31	158	132	46	33	188	149	156	1
129	129	113	1	159	125	135	1	189	156	157	1
130	130	114	1	160	129	136	1	190	157	158	1
131	131	115	1	161	136	137	1	191	158	159	1
132	132	116	1	162	137	138	1	192	150	160	1
133	133	117	1	163	138	139	1	193	154	161	1
134	134	118	1	164	130	140	1	194	161	162	1
135	135	119	1	165	134	141	1	195	162	163	1
136	136	120	1	166	141	142	1	196	163	164	1
137	137	121	1	167	142	143	1	197	155	24	36
138	138	122	1	168	143	144	1	198	157	24	36
139	139	123	1	169	135	22	34	199	160	49	36
140	140	124	1	170	137	22	34	200	162	49	36

Table A.5: Elements of the full scale FEM model

El.	**N1**	**N2**	**Mat**	**El.**	**N1**	**N2**	**Mat**	**El.**	**N1**	**N2**	**Mat**
141	141	20	32	171	140	47	34	201	159	164	37
142	142	20	32	172	142	47	34				
143	143	45	32	173	135	145	1				
144	144	45	32	174	139	146	1				
145	145	125	1	175	146	147	1				
146	146	126	1	176	147	148	1				
147	147	127	1	177	148	149	1				
148	148	128	1	178	140	150	1				
149	149	129	1	179	144	151	1				
150	150	130	1	180	151	152	1				

Table A.6: Material characteristics of the full scale FEM model

Material	**E** (kN/m^2)	ν	**Area** (m^2)	**Inertia** (m^4)
1	30900000	0.2	9.998	1.053
2	29800000	0.2	15.874	34.249
3	29800000	0.2	15.542	31.55
4	29800000	0.2	15.21	28.993
5	29800000	0.2	14.877	26.564
6	29800000	0.2	14.579	24.49
7	29800000	0.2	14.313	22.731
8	29800000	0.2	14.047	21.054
9	29800000	0.2	19.97	22.51
10	29800000	0.2	16.67	10.76
11	29800000	0.2	16.18	9.62
12	29800000	0.2	15.67	8.47
13	29800000	0.2	15.5	8.19
14	29800000	0.2	13.22	4.08
15	29800000	0.2	13.17	4.08
16	29800000	0.2	13.12	4.08
17	29800000	0.2	12.76	3.65
18	29800000	0.2	12.59	3.5
19	29800000	0.2	12.51	3.45
20	29800000	0.2	12.44	3.4
21	29800000	0.2	12.4	3.4
22	29800000	0.2	12.36	3.4
23	29800000	0.2	12.33	3.4
24	29800000	0.2	12.18	3.26
25	29800000	0.2	14.66	8.29
26	29800000	0.2	0	1.053
27	29800000	0.2	9.998	0
28	195000000	0.2	0.00594255	0
29	195000000	0.2	0.00865044	0
30	195000000	0.2	0.00977728	0

Table A.6: Material characteristics of the full scale FEM model

Material	**E** (kN/m^2)	ν	**Area** (m^2)	**Inertia** (m^4)
31	195000000	0.2	0.01102923	0
32	195000000	0.2	0.0119005	0
33	195000000	0.2	0.01291477	0
34	195000000	0.2	0.01315351	0
35	195000000	0.2	0.01625937	0
36	195000000	0.2	0.01234229	0
37	195000000	0.2	0	1.053
38	195000000	0.2	0	0

Appendix B

Patch Tests

The variables to take into account in the tests are: The length of the beam or pylon, L, the area of the concrete element, A_c, the inertia of the concrete element, I_c, the elasticity modulus of concrete, E_c, the area of the steel element, A_s, the inertia of the steel element, I_s, the elasticity modulus of steel, E_s, a concentrated load, P, a distributed load, q, the relative humidity, HR, the concrete strength, f_{cm}, the notional member size, h_0, and the age of the concrete at loading, t_0.

Patch test 1: Axial loading of a pylon.

The first patch test consists in the evaluation of the axial deformation of a concrete column when it is loaded by a concentrated force, P, at the upper part. The different variables used are gathered in table B.1.

The evolution of the deformation due to the creep can be seen in figure B.1. The displacement obtained by the algorithm is compared with the analytical solution which is expressed in equation B.0.1 where the total displacement, $\delta_{TOT}(t)$, is the sum of the elastic displacement, δ_E, and the displacement due to the creep, $\phi\delta_E$. The result is the same no matter how many elements are considered.

$$\delta_{TOT}(t) = \delta_E(1 + \phi(t)) \tag{B.0.1}$$

Table B.1: Characteristics patch test 1.

Characteristic	Value
L	5 m
A_c	1 m^2
I_c	0.083 m^4
E_c	31000 MPa
P	1000 kN
HR	70 %
f_{cm}	45 MPa
h_0	1784 mm
t_0	28 $days$

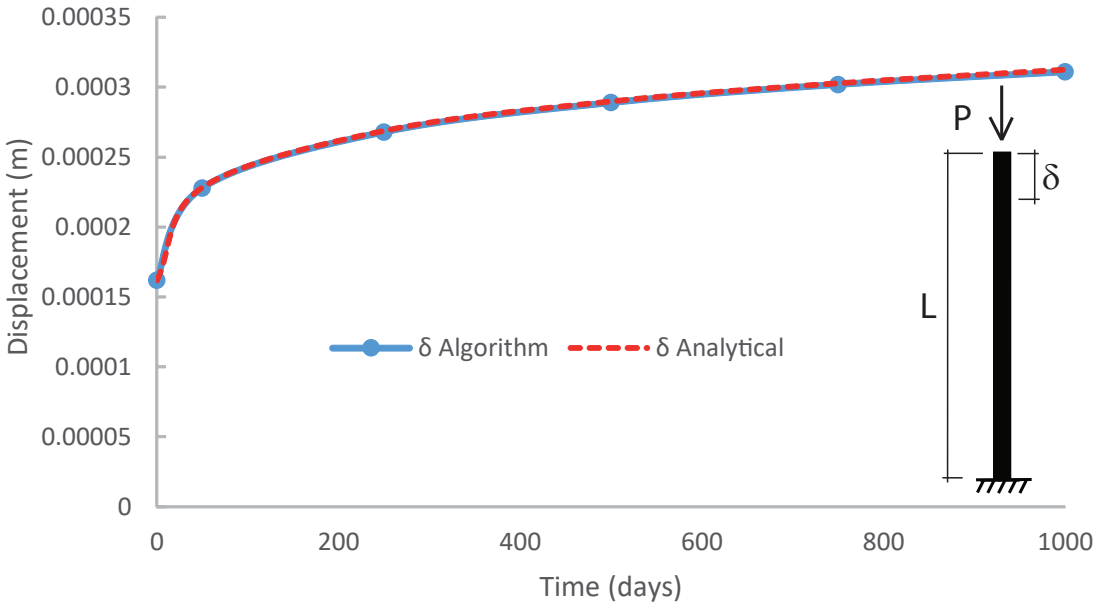

Figure B.1: Axial loading of a pylon.

Patch test 2: Axial loading of a pylon with change in boundary conditions.

In patch test 2 the same column as in patch test 1 is analyzed. A force P is applied and it produces an elastic displacement, δ_E, and a reaction, $R = P$, at the bottom fixed support. At the same day the boundary conditions are changed and a fixed support is installed at the upper part of the column.

The evolution of the reaction at the bottom fixed support throughout the time is studied after the change of boundary conditions and the result is compared to the analytical solution in figure B.2. The analytical reaction can be seen in equation B.0.2 and the variables used in B.2.

$$R(t) = Pe^{-\phi(t)} \tag{B.0.2}$$

Table B.2: Characteristics patch test 2.

Characteristic	Value
L	5 m
A_c	1 m^2
I_c	0.083 m^4
E_c	31000 MPa
P	1000 kN
HR	70 %
f_{cm}	45 MPa
h_0	1784 mm
t_0	28 $days$

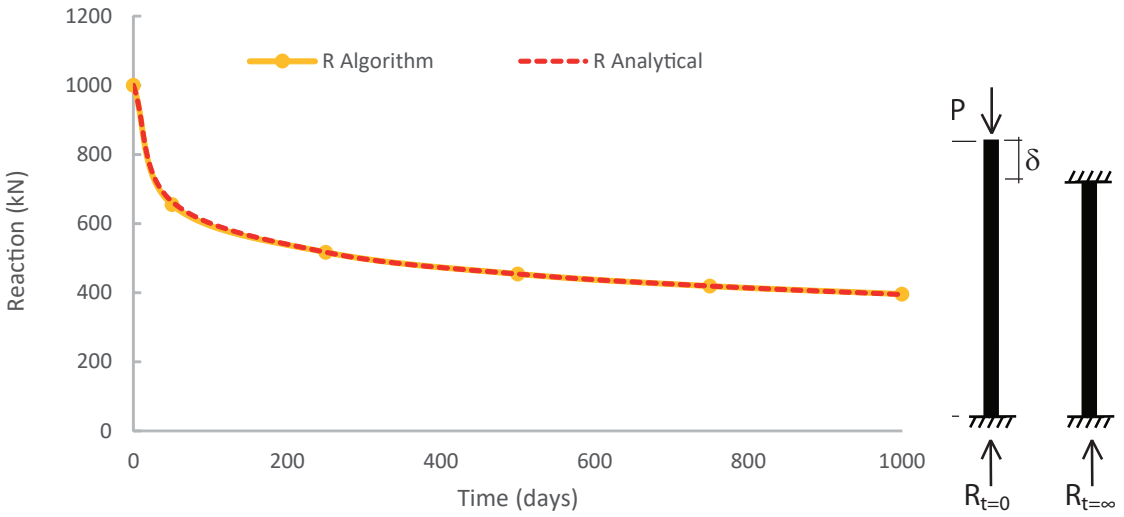

Figure B.2: Axial loading of a pylon with change in boundary conditions.

Patch test 3: Axial loading of a pylon in different ages.

The pylon used in patch tests 1 and 2 is loaded in two different times. The second force is applied 500 days after the first one. The evolution of the displacement throughout the time is evaluated for both cases. The characteristics of the test are gathered in table B.3.

The evolution of the displacement due to the second force depends on the consideration or not of the age of loading. In the algorithm the age of loading is considered. It can be appreciated in figure B.3 the difference between considering only the first age of loading, t_0, (Dischinger hypothesis) and considering all the age of loading.

In figure B.3 it can also be seen that the increment of displacement from the day 500 is the same for both cases as it states Dischinger in his simplification hypothesis.

Table B.3: Characteristics patch test 3.

Characteristic	**Value**
L	5 m
A_c	1 m^2
I_c	0.083 m^4
E_c	31000 MPa
$P_{t=0}$	1000 kN
$P_{t=500}$	1000 kN
HR	70 %
f_{cm}	45 MPa
h_0	1784 mm
t_0	28 $days$

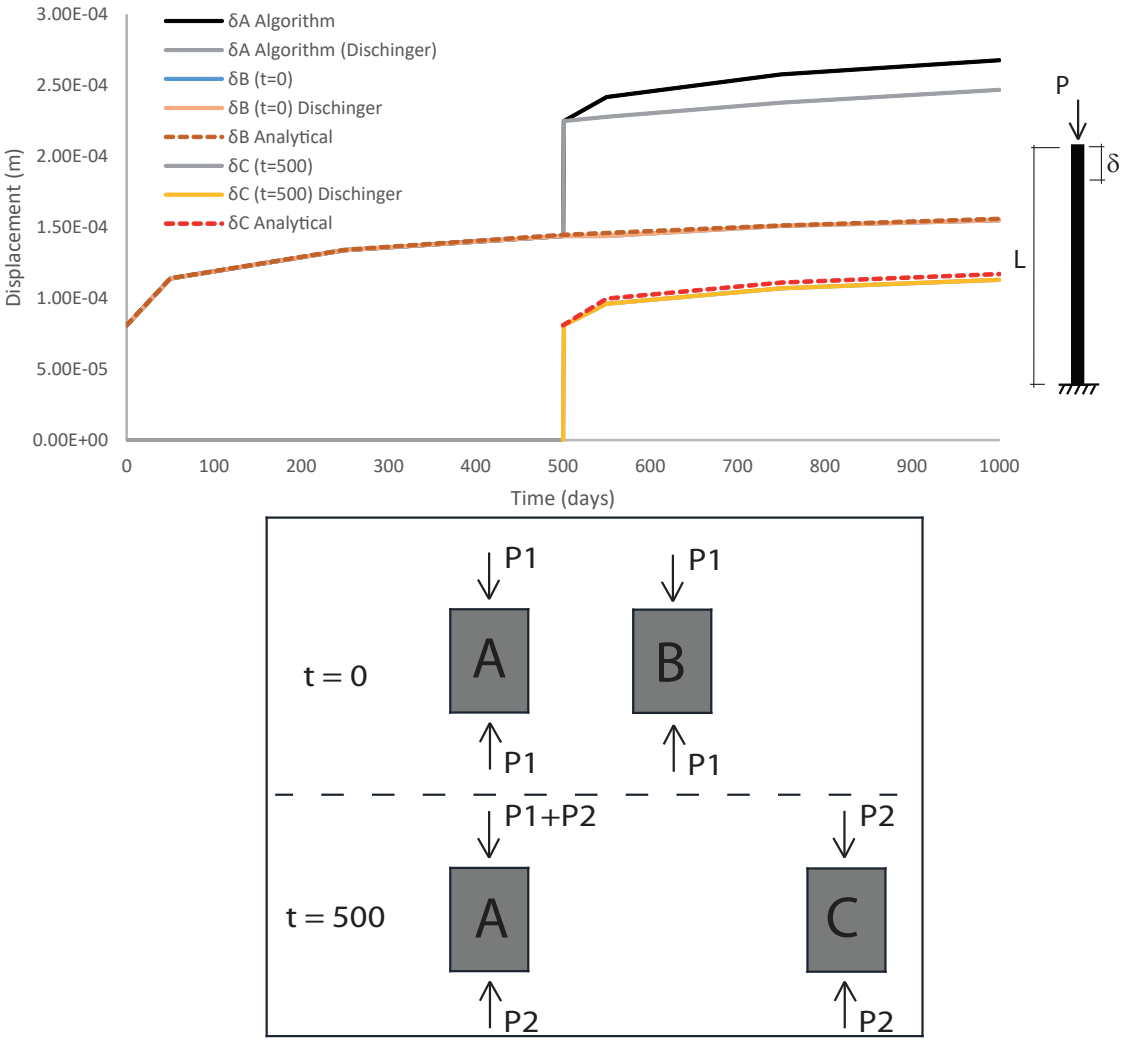

Figure B.3: Axial loading of a pylon in different ages.

Patch test 4: Distributed load in a cantilever beam.

In patch test 4 the evolution of the displacement throughout the time in a cantilever beam is studied. An uniform distributed load, q, is applied and the displacement is evaluated at the end of the beam. The data used for this test are gathered in table B.4.

The displacement obtained by the algorithm is compared with the analytical solution given by equation B.0.3. It can be seen that the results obtained are almost the same as the analytical ones. The number of elements of the beam considered don't affect the result.

$$\delta_{TOT}(t) = \delta_E(1 + \phi(t)) \tag{B.0.3}$$

Table B.4: Characteristics patch test 4.

Characteristic	Value
L	5 m
A_c	1 m^2
I_c	0.083 m^4
E_c	35500 MPa
q	100 kN/m
HR	70 %
f_{cm}	45 MPa
h_0	1784 mm
t_0	28 $days$

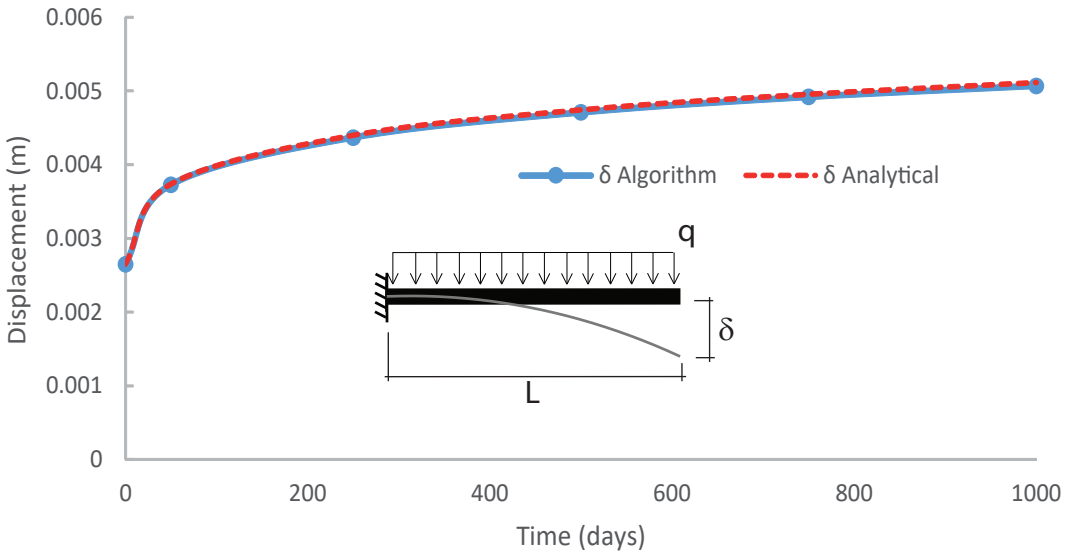

Figure B.4: Distributed load in a cantilever beam.

Patch test 5: Distributed load in a cantilever beam with change in boundary conditions.

In patch test 5 the same beam as in patch test 4 is analyzed. An uniform distributed force, q, is applied and it produces an elastic displacement, δ_E. Just after the deformation is produced, a pinned support is installed. Due to the creep effects a reaction, $R(t)$, at the support appears.

The evolution of the reaction at the pinned support throughout the time is studied after the change of boundary conditions and the result is compared to the analytical solution in figure B.6. The analytical reaction can be seen in equation B.0.4 and the variables used in B.5.

The analytical solution of equation B.0.4 is deduced by Manterola, J. [2] which takes into account the initial displacement, δ_0 and the displacement, δ_1 produced by an unitary concentrated force, $P = 1$, at the end of the beam. These displacements can be seen in figure B.5.

In this test the number of elements is an important issue. If one element is considered the solution in 1000 days differs from the analytical in 10 %. However we can obtain an enough accurate result (0,5%) if 10 elements are considered.

$$R(t) = \frac{\delta_0}{\delta_1}(1 - e^{\phi(t)}) \tag{B.0.4}$$

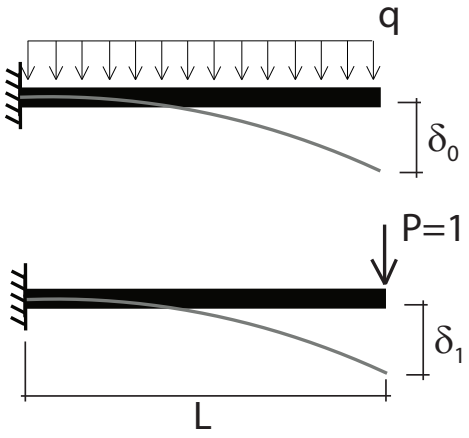

Figure B.5: Initial displacement and displacement produced by a concentrated force.

Table B.5: Characteristics patch test 5.

Characteristic	Value
L	$5\ m$
A_c	$1\ m^2$
I_c	$0.083\ m^4$
E_c	$35500\ MPa$
q	$100\ kN/m$
HR	$70\ \%$
f_{cm}	$45\ MPa$
h_0	$1784\ mm$
t_0	$28\ days$
δ_0	$2.65 \cdot 10^{-3}\ m$
δ_1	$1.41 \cdot 10^{-5}\ m$

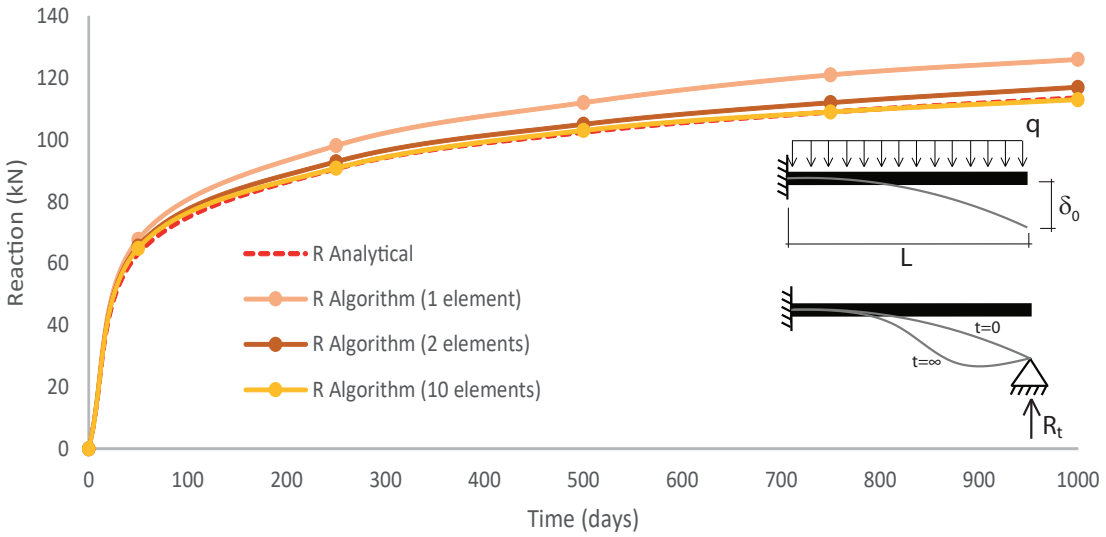

Figure B.6: Distributed load in a cantilever beam with change in boundary conditions.

Patch test 6: Distributed load in a cantilever beam. Load implemented in different ages.

The beam used in patch tests 4 and 5 is loaded in two different times. The second force is applied 500 days after the first one. The evolution of the displacement throughout the time is evaluated for both cases. The characteristics of the test are gathered in table B.6.

The evolution of the displacement due to the second force depends on the consideration or not of the age of loading. In the algorithm the age of loading is considered. It can be appreciated in figure B.7 the difference between considering only the first age of loading, t_0, (Dischinger hypothesis) and considering all the age of loading.

In figure B.7 it can also be seen that the increment of displacement from the day 500 is the same for both cases as it states Dischinger in his simplification hypothesis.

Table B.6: Characteristics patch test 6.

Characteristic	**Value**
L	5 m
A_c	1 m^2
I_c	0.083 m^4
E_c	35500 MPa
$q_{t=0}$	100 kN/m
$q_{t=500}$	100 kN/m
HR	70 %
f_{cm}	45 MPa
h_0	1784 mm
t_0	28 $days$

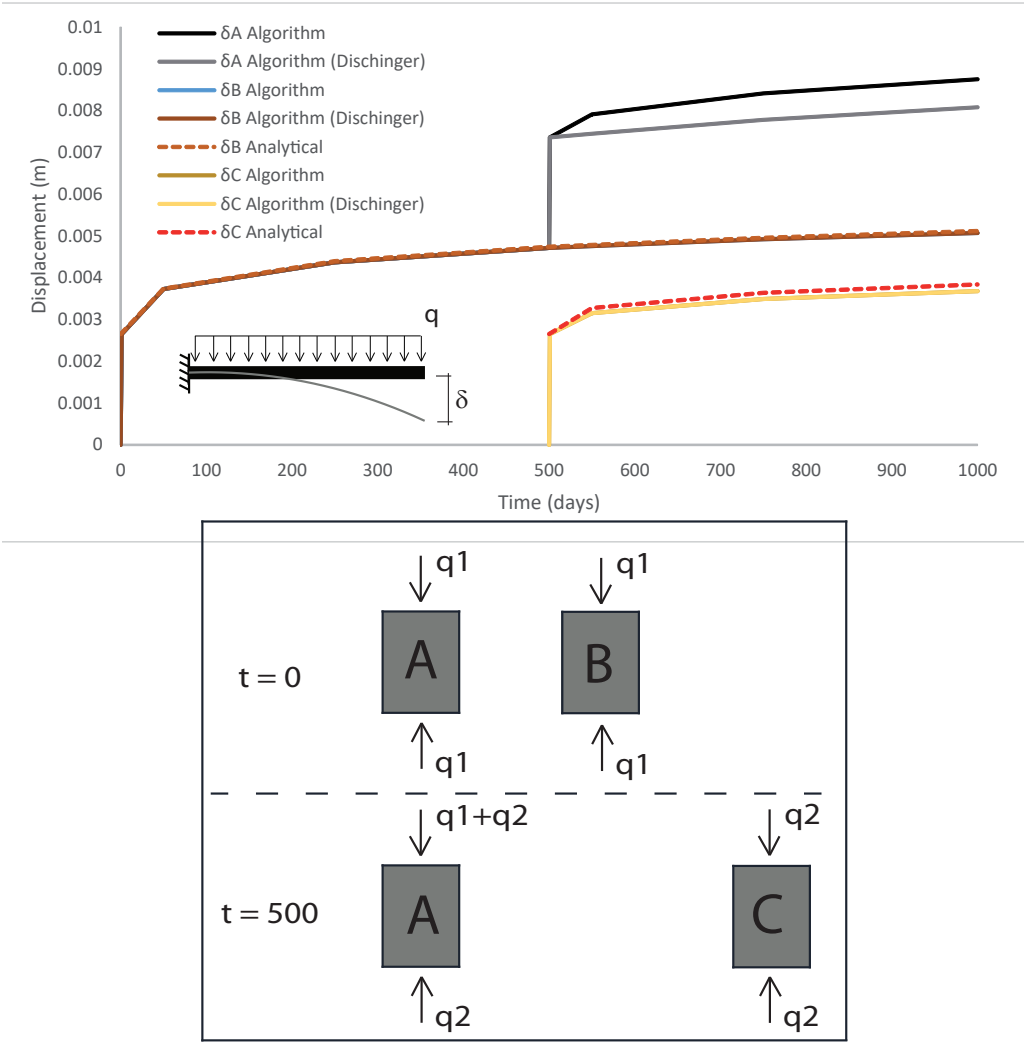

Figure B.7: Distributed load in a cantilever beam. Load implemented in different ages.

Patch test 7: System of two materials axial loaded.

In the patch test 7 a beam composed by two materials, concrete and steel, is analyzed. The beam is fixed at both ends. The different variables and material characteristics are gathered in table B.7.

In figure B.7 the response of the beam is studied. Firstly it is showed the evolution of the steel stay tension in two cases: pretension force = 0 and pretension force = P. Secondly the evolution of the displacement at the point that connects the steel stay with the concrete part is represented considering the same both cases. It has been also considered a case when the area of steel is bigger in order to appreciate better the difference of tension throughout the time. The bigger the steel area, the greater the difference of tension.

For the case when the pretension force is equal to the force applied to the concrete part it can be appreciated that the variation of tension and deformation to the creep is 0. In the algorithm it is considered that there is not creep when the concrete is in tension.

Table B.7: Characteristics patch test 7.

Characteristic	**Value**
L	5 m
A_c	1 m^2
I_c	0.083 m^4
E_c	35500 MPa
A_s	0.006 m^2
I_s	0 m^4
E_s	200000 MPa
P	1000 kN
HR	70 %
f_{cm}	45 MPa
h_0	1784 mm
t_0	28 $days$

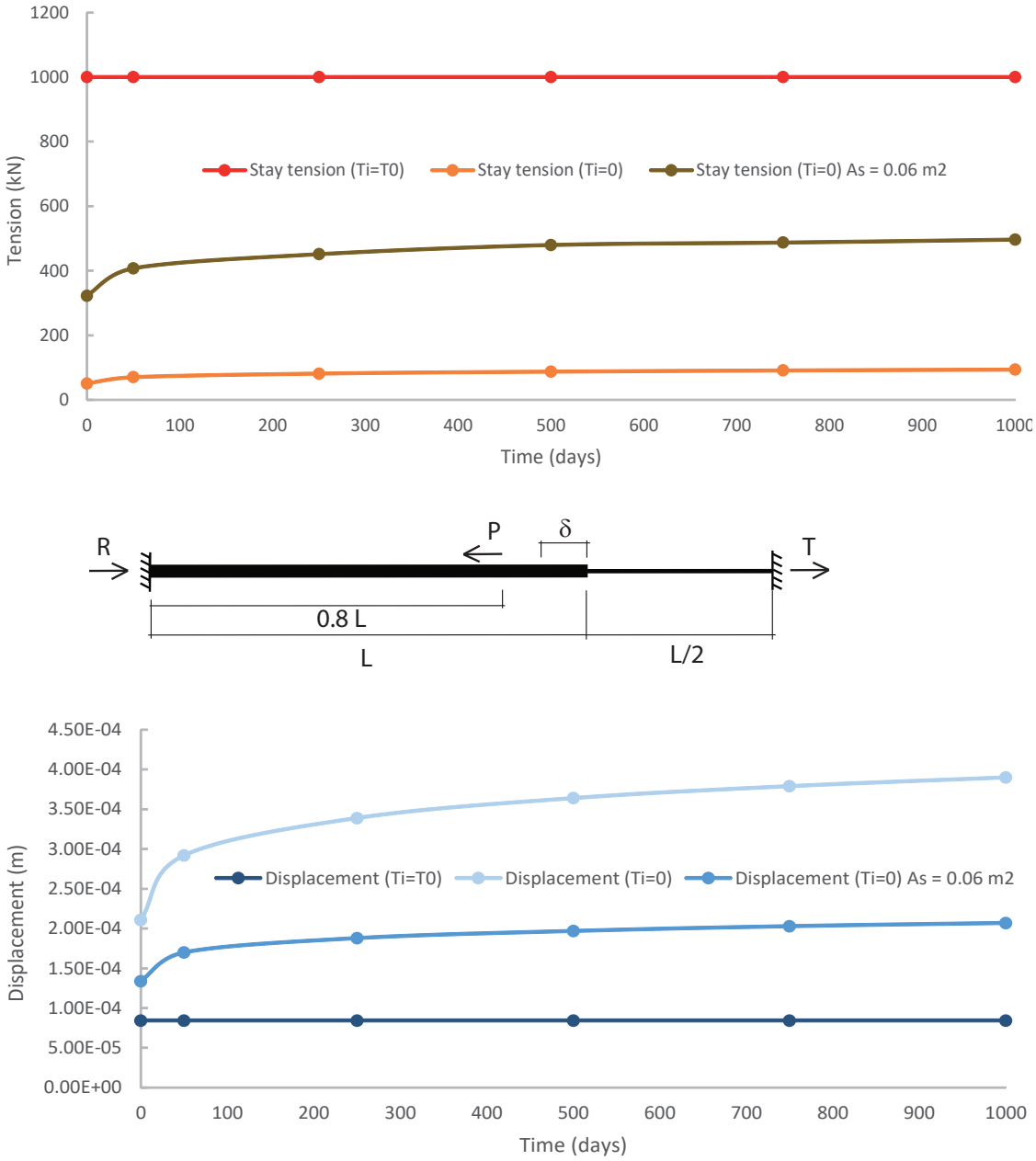

Figure B.8: System of two materials axial loaded.

Patch 8: System of one beam supported by one stay in the middle

For this patch test there are three cases. The first case is considering a steel stay. In the second a pretensioned stay is considered and in the third the stay is made of concrete. The characteristics used are gathered in table B.8

Table B.8: Characteristics patch test 8.

Characteristic	Value
L	5 m
A_c	1 m^2
I_c	0.083 m^4
E_c	35500 MPa
A_s	0.006 m^2
I_s	0 m^4
E_s	200000 MPa
q	100 kN/m
HR	70 %
f_{cm}	45 MPa
h_0	1784 mm
t_0	28 $days$

Patch test 8.1: System of one beam supported by one stay in the middle: Steel stay.

A uniformly distributed load is applied to the beam. The evolution of the reaction in the stay is analyzed and compared with the analytical solution B.0.5 where δ_T is the elongation of the stay under an unitary load, δ_0, is the elastic deflection of the beam and δ_v is the elastic deflection of the beam under an unitary load.

$$R(t) = R_0 \frac{1 - (1 - \alpha)e^{-\alpha\phi}}{\alpha} \tag{B.0.5}$$

$$\alpha = \frac{\delta_v}{\delta_v + \delta_T} \tag{B.0.6}$$

$$R_0 = \frac{\delta_0}{\delta_v + \delta_T} \tag{B.0.7}$$

The reaction tend to the line $R/R_0 = 1$ which corresponds to the case when the beam has a support at midspan.

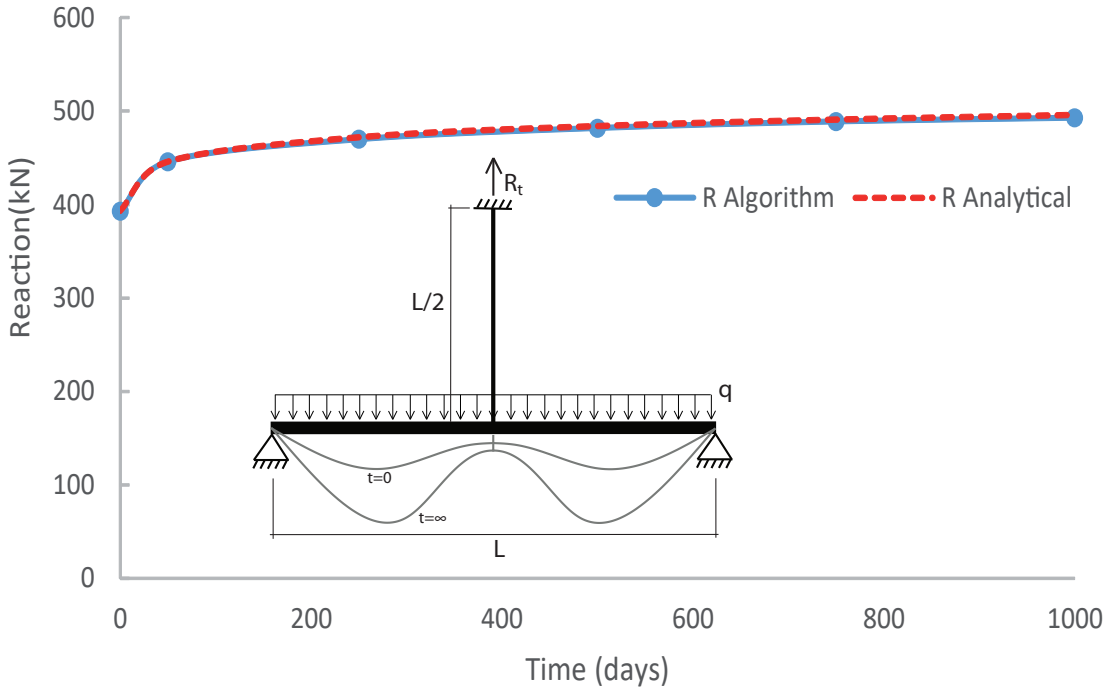

Figure B.9: System of one beam supported by one stay in the middle: Steel stay.

Patch test 8.2: System of one beam supported by one stay in the middle: Pretensioned stay.

An initial stress is given to the stay in order that the deflection of the beam is zero at the middle. As Manterola, J. [2] states the increment of R (equation B.0.8 is zero. Thus the the deflection of the beam changes but not the beam and the stay stresses. The evolution of the deformation at quarter span and the reaction can be seen in figure B.10.

$$\Delta R_i = \frac{1}{\delta_v + \delta_T}\left[0 - \sum_{i=1}^{j-1} \Delta R_i \delta_v [\phi(t_j, t_i) - \phi(t_{j-1}, t_i)]\right] \tag{B.0.8}$$

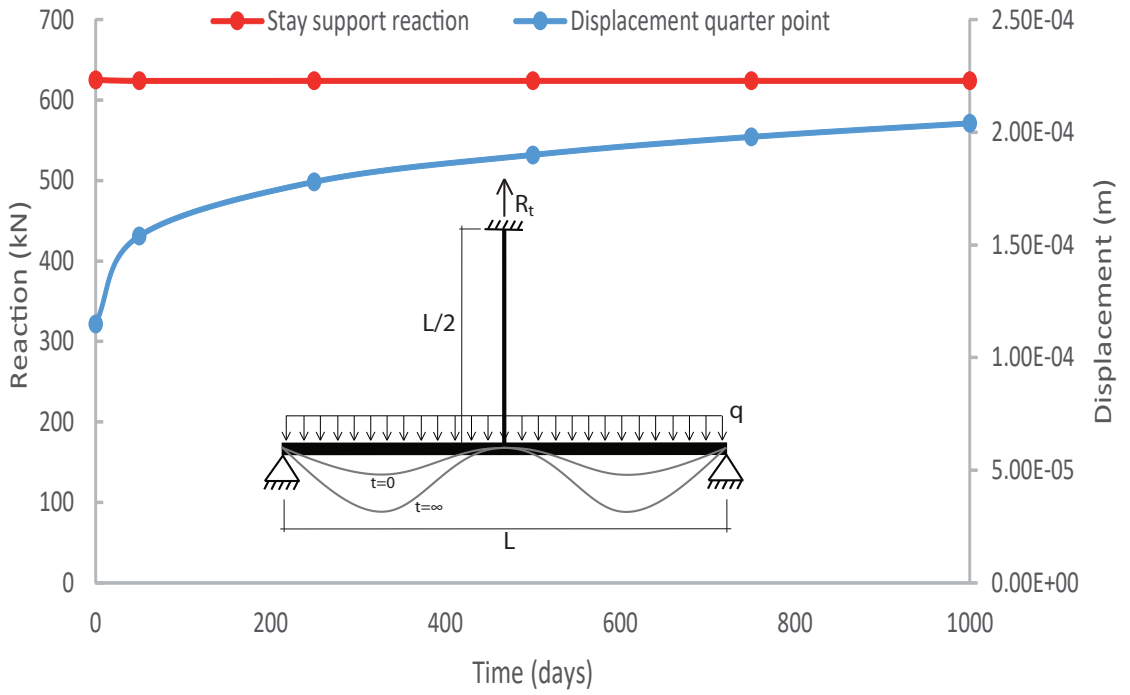

Figure B.10: System of one beam supported by one stay in the middle: Pretensioned stay.

Patch test 8.3: System of one beam supported by one stay in the middle: Concrete stay.

A concrete stay is equivalent to consider a support. If the creep conditions of the stay and the beam are the same the compatibility of movements is stated in equation B.0.9 and the increments of stresses are 0. In other words if the same conrete is used there will be increments of deflection due to the creep but the initial stresses in the beam and the stay will remain [2]. The evolution of the deformation at quarter span and the reaction can be seen in figure B.11.

$$\delta_0 - R_0\delta_v = R_0\delta_T \tag{B.0.9}$$

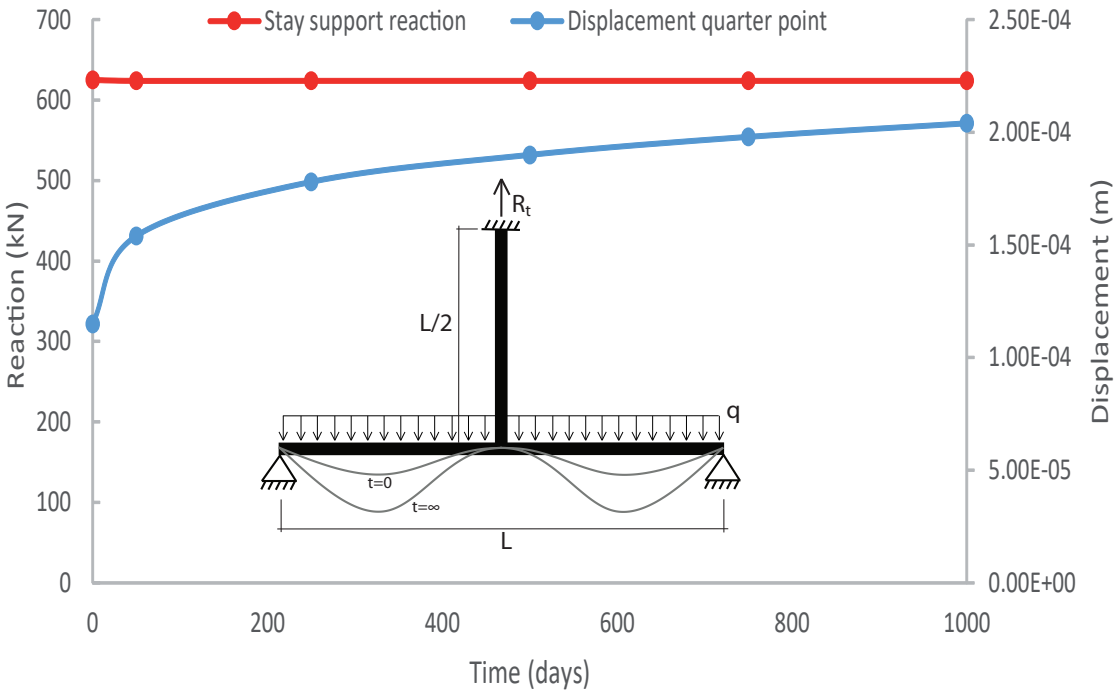

Figure B.11: System of one beam supported by one stay in the middle: Concrete stay.

Patch test 9: Beam built by the union of two cantilever beams.

In this test two cantilever beams are joined after an uniformly distributed load is applied. Due to the creep a bending moment appears at the point where the cantilever beams were joined.

he evolution of the bending moment can be seen in figure B.12. The solution is compared with the analytical solution in equation B.0.10 which takes into account the initial rotation, θ_0, and the rotation, θ_1, produced by an unitary applied moment, $M = 1$, at the end of the beam. The characteristics of this patch test are gathered in table B.9.

$$M(t) = \frac{\theta_0}{\theta_1}(1 - e^{\phi(t)}) \tag{B.0.10}$$

Table B.9: Characteristics patch test 9.

Characteristic	**Value**
L	5 m
A_c	1 m^2
I_c	0.083 m^4
E_c	35500 MPa
q	100 kN/m
HR	70 %
f_{cm}	45 MPa
h_0	1784 mm
t_0	28 $days$
θ_0	$7.07 \cdot 10^{-4}$ rad
θ_1	$1.70 \cdot 10^{-6}$ rad

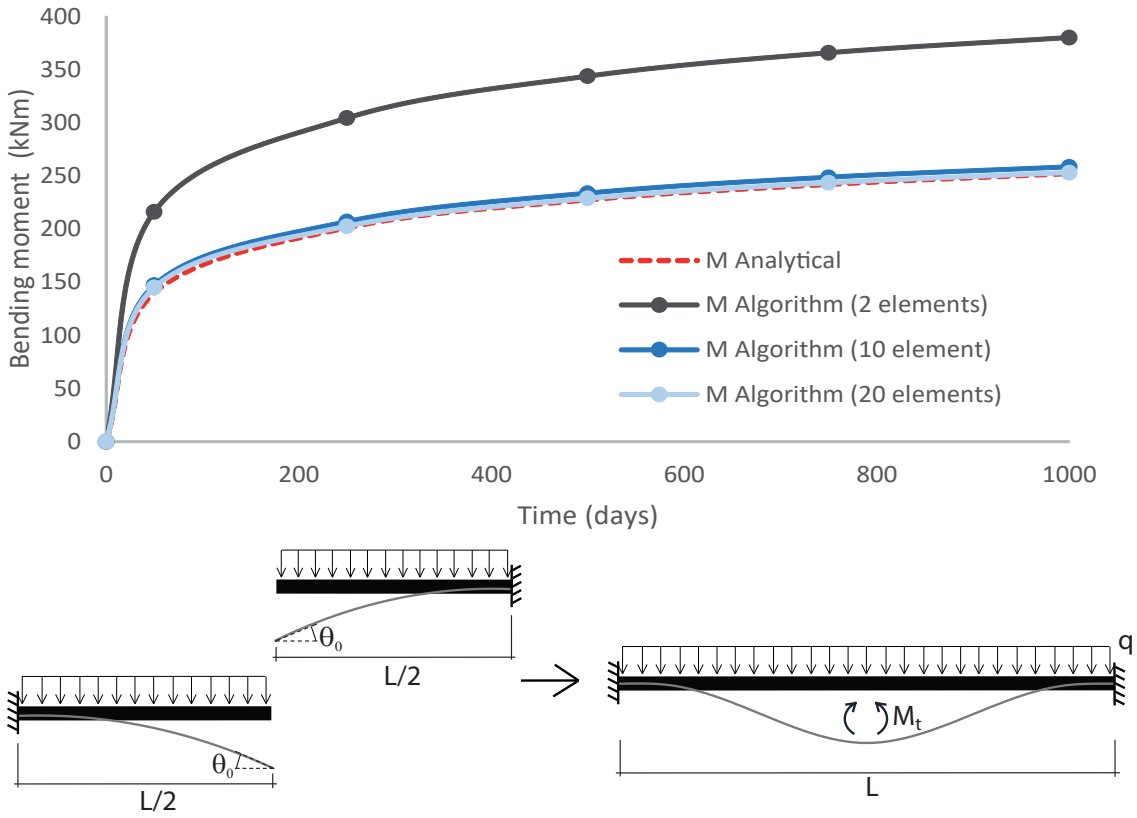

Figure B.12: Beam built by the union of two cantilever beams. Evolution of the moment at midspan.

Bibliography

[1] N.J. Gimsing. *Cable supported bridges, Concept and Design.* John Wiley and Sons, Chichester, 1997.

[2] J. Manterola, C. Siegrist, and M.A. Gil. *Puentes.* Escuela Tecnica Superior de Ingenieros de Caminos, Canales y Puertos de Madrid (In Spanish), Madrid, 2006.

[3] W. Podolny and J.B. Scalzi. *Construction and design of cable stayed bridge.* John Wiley and Sons, New York, 1986.

[4] J.J. Oliveira and A.J. Reis. Composite cable-stayed bridges: state of the art. *Bridge engineering*, 169:13–38, 2015.

[5] H. Wang, T. Tang, and H. Zheng. Analysis of cable-stayed bridges during construction by cantilever method. *Computers and Structures*, 82(4-5):329–346, 2004.

[6] J.A. Lozano-Galant. *Construction Control of Cable-Stayed Bridges.* PhD thesis, Universitat Politécnica de Catalunya, 2013.

[7] L. Carrillo. *Erection analysis of cable-stayed bridges.* PhD thesis, Escuela Tecnica Superior de Ingenieros de Caminos Canales y Puertos, Universidad Politecnica de Madrid, Madrid, Spain (in Spanish), 2015.

[8] Holger Svensson. *Cable-Stayed Bridges. 40 Years of Experience Worldwide.* Ernst Sohn, Zeuthen, Germany, 2012.

[9] F. Dischinger. Hängebrücken für schwerste verkehrslasten. *Bauingenieur (in German)*, 24:65–113, 1949.

[10] D. Janjic, M. Pircher, and H. Pircher. Optimization of cable tensioning in cable-stayed bridges. *Journal of Bridge Engineering*, 8(3):131–137, 2003.

[11] F. Leonhardt and W. Zellner. Comparative investigations between suspension bridges and cable-stayed bridges for spans exceeding 600 m. *The International Association for Bridge and Structural Engineering*, 32(1):127–165, 1972.

[12] M. Aschrafi. Comparative investigations of suspension bridges and cable-stayed bridges for spans exceeding 1000 m. *Long-Span and High-Rise Structures*, 24:447–452, 1998.

[13] M. Schlaich. Erection of cable-stayed bridges having composite decks with precast concrete slabs. *Journal of Bridge Engineering*, 6(5):333–339, 2001.

[14] Z. Behin and D. Murray. A substructure-frontal technique for cantilever erection analysis of cable-stayed bridges. *Computers and Structures*, 42(2):145–157, 1992.

[15] SETRA. *Recommandations de la Commission Interministírielle de la Precontrainte*. Service d'Etudes Techniques des Routes et Autoroutes, France, 2001.

[16] B.E. Lazar, M.S Troitsky, and M.C. Douglas. Load analysis balancing of cable stayed bridges. *ASCE Journal of Structural Engineering*, 92(8):1725–1740, 1972.

[17] D.W. Chen, F.T.K. Au, L.G. Tham, and P.K.K. Lee. Determination of initial cable forces in prestressed concrete cable-stayed bridge for given design deck profiles using the force equilibrium method. *Computers and Structures*, 74(1):1–9, 2000.

[18] G.H. Du. Optimal cable tension and construction tensioning of cable-stayed bridges. *Bridge Construct (in Chinese)*, 74:18–22, 1989.

[19] P.H. Wang, T.C. Tseng, and C.G. Yang. Initial shape of cable-stayed bridges. *Computers and Structures*, 46(6):1095–1106, 1993.

[20] J.H.O. Negrao and L.M.C. Simoes. Optimization of cable-stayed bridges with three dimensional modeling. *Computers and Structures*, 64(1-4):741–758, 1997.

[21] L.M.C. Simoes and J.H.J.O. Negrao. Optimization of cable-stayed bridges with box-girder decks. *Advances in Engineering Software*, 31:417–423, 2000.

[22] *MidaSoft Inc. Guide*. MIDASoft, 2004.

[23] H. Somja and V. Ville de Goyet. A new strategy for analysis of erection stages including an efficient method for creep analysis. *Engineering Structures*, 30(10):2871–2883, 2008.

[24] A.M.B. Martins, L.M.C Simoes, and J.H.J.O. Negrao. Time-dependent analysis and cable stretching force optimization of concrete cable-stayed bridges. In C. Pina H. Barros, R. Faria and C. Ferreira, editors, *International Conference on Recent Advantages in Nonlinears Models- Structural Concrete Application, CoRANh*, 2011.

[25] F.T.K. Au and X.T. Si. Accurate time-dependent analysis of concrete bridges considering concrete creep, concrete shrinkage and cable relaxation. *Engineering Structures*, 33(1):118–126, 2011.

[26] J.A Lozano-Galant and J. Turmo. Creep and shrinkage effects in service stresses of concrete cable-stayed bridges. *Computers and Concrete*, 13(4):483–499, 2014.

[27] J.A Lozano-Galant and J. Turmo. An algorithm for simulation of concrete cable-stayed bridges built on temprary supports and considering time dependent effects. *Engineering Structures*, 79(1):341–353, 2014.

[28] P. Reddy, J. Ghaboussi, and M. Hawkins. Simulation of construction of cable.stayed bridges. *Journal of Bridge Engineering*, 4(4):249–257, 1999.

[29] Z. Behin. *Erection analysis of cable-stayed bridges*. PhD thesis, Departament of Civil Engineering, University of Alberta, Edmonton, Canada, 1990.

[30] J.A. Lozano-Galant, I. Payá-Zaforteza, D. Xu, and J. Turmo. Analysis of the construction process of cable-stayed bridges built on temporary supports. *Engineering Structures*, 40:95–106, 2012.

[31] J.A. Lozano-Galant, Payá-Zaforteza I., D. Xu, and J. Turmo. Forward algorithm for the construction control of cable-stayed bridges built on temporary supports. *Engineering Structures*, 40(1):119–130, 2012.

[32] A. Pipinato, C. Pellegrino, and C. Modena. Structural analysis of the cantilever construction process in cable-stayed bridges. *Periodica Polytechnica. Civil Engineering*, 56(6):141–166, 2012.

[33] J.A. Lozano-Galant, I. Payá-Zaforteza, D. Xu, and J. Turmo. Direct simulation of the tensioning process of cable-stayed bridges. *Computers and Structures*, 121:64–75, 2013.

[34] N.C. Cluley and R. Shepherd. Analysis of concrete cable-stayed bridges for creep, shrinkage and relaxations effects. *Computers and Structures*, 58(2):337–350, 1996.

[35] M. Arici, M. F. Granata, P. Margiotta, and A. Recupero. Creep effects and stresss adjustments in cable-stayed bridges with concrete deck. *3rd fib International Congress, At Washington, USA*, January,2010.